

## 4.3 Nuclear Design

### 4.3.1 Design Bases

The GDC in 10 CFR 50, Appendix A provide the regulatory requirements for the nuclear design bases used to design the fuel and reactivity control systems. Specifically, the following GDC apply to Section 4.3:

- GDC 10 requires that acceptable fuel design limits be specified that are not to be exceeded during normal operation, including the effects of anticipated operational occurrences.
- GDC 11 requires that, in the power operating range, the prompt inherent nuclear feedback characteristics tend to compensate for a rapid increase in reactivity.
- GDC 12 requires that power oscillations that could result in conditions exceeding specified acceptable fuel design limits are not possible, or can be reliably and readily detected and suppressed.
- GDC 13 requires that instrumentation and controls (I&C) be provided to monitor variables and systems that can affect the fission process over anticipated ranges for normal operation, anticipated operational occurrences, and accident conditions, and maintain the variables and systems within prescribed operating ranges.
- GDC 20 requires automatic initiation of the reactivity control systems so acceptable fuel design limits are not exceeded as a result of anticipated operational occurrences, and requires automatic operation of systems and components important to safety under accident conditions.
- GDC 25 requires that no single malfunction of the reactivity control systems (this does not include rod ejection) causes violation of the acceptable fuel design limits.
- GDC 26 requires that two independent reactivity control systems of different design be provided, and that each system have the capability to control the rate of reactivity changes resulting from planned, normal power changes. One of the systems must be capable of reliably controlling anticipated operational occurrences. In addition, one of the systems must be capable of holding the reactor core subcritical under cold conditions.
- GDC 27 requires that the reactivity control systems have a combined capability, in conjunction with poison addition by the emergency core cooling system, of reliably controlling reactivity changes under postulated accident conditions, with appropriate margin for stuck rods.
- GDC 28 requires that the effects of postulated reactivity accidents neither result in damage to the reactor coolant pressure boundary greater than limited local yielding, nor cause sufficient damage to impair significantly the capability to cool the core.

Compliance with GDC 10, 11, 12, 25, 26, and 28 is addressed in this section. As noted in Section 3.1.2, the systems that demonstrate compliance with GDC 13 are described in Chapters 6, 7, 8, 9, 10, 11, and 12. As noted in Section 3.1.3, the protection system complies with GDC 20 and is described in Chapter 7. Also as noted in Section 3.1.3, the U.S. EPR complies with GDC 27 in that it is designed with means to make and hold the core subcritical under any anticipated conditions and with appropriate margin for contingencies.

The nuclear design bases address two distinct categories of plant operation that are defined by their anticipated frequency of occurrence and their risk to the public:

- Anticipated operational occurrences (AOOs) – Conditions of normal operation that are expected to occur one or more times during the life of the plant.
- Postulated accidents (PAs) – Events which are postulated, but are not expected to occur.

AOOs can happen frequently or regularly in the course of power operation, refueling, or maintenance. As such, they have a margin between any plant parameter and the value of that parameter that would require either automatic or manual protective action.

PAs are faults that are not expected to occur during the life of the plant, but are postulated because they have the potential to release significant amounts of radioactive material. They are the most drastic events which must be designed against, and they are the limiting plant design cases.

For AOOs, the core design power distribution limits required to maintain fuel integrity are met through conservative design and the actions of the control system. An adequate protection system that monitors reactor parameters is also used to mitigate the consequences of AOOs. The control and protection systems are described in Chapter 7, and the classification and consequences of AOOs and PAs are described in Chapter 15.

#### **4.3.1.1 Fuel Burnup**

Section 4.2 describes the fuel rod design basis. A limit on the initial excess reactivity or average discharge burnup is not required; however, there are limits set by other design bases, such as core negative reactivity feedback and shutdown margin.

Fuel burnup is a measure of fuel depletion that represents the integrated past energy output of the fuel, measured in Gigawatt-days per metric ton uranium (GWD/MTU), and is a convenient means for quantifying fuel exposure criteria. Peak fuel rod exposure will be no greater than 62.0 GWD/MTU as approved in COPERNIC Fuel Rod Design Computer Code (Reference 1).

The core design lifetime, or design discharge burnup, is achieved by loading sufficient initial excess reactivity in each fresh fuel region and by following a fuel replacement program that meets all safety-related criteria in each cycle of operation.

Initial excess reactivity loaded into the fresh fuel, although not a design basis, must be sufficient to maintain core criticality at full power operating conditions throughout the cycle life with equilibrium xenon, samarium, and other fission products present. The end of the cycle life is defined to occur when the chemical shim (boron) concentration is essentially zero with control rods inserted to the degree necessary for operational requirements. In terms of boron concentration, this represents approximately 10 ppm with all rods out (ARO).

The maximum assembly average burnup is chosen so that the peak rod burnup is within the limits in U.S. EPR Fuel Assembly Mechanical Design (Reference 2). This design basis, along with the design basis in Section 4.3.1.3, satisfies GDC 10.

#### **4.3.1.2 Negative Reactivity Feedbacks (Reactivity Coefficient)**

The moderator temperature coefficient of reactivity is less than or equal to 5 pcm/°F at hot zero power and less than or equal to 0 pcm/°F at or above 50% of rated thermal power for all times in the operating cycle. The fuel Doppler temperature reactivity coefficient is always negative. For rapid increases in reactivity from any power level, the fuel coefficient inherently compensates for the added reactivity and limits the resulting power excursion. The combination of a negative moderator temperature coefficient with the negative fuel temperature coefficient provides additional inherent control when operating at significant power levels. The negative reactivity feedback provided by the design satisfies GDC 11.

#### **4.3.1.3 Core Design Lifetime**

Core design lifetime is dictated by the energy output that is required. The lifetime of the core can be from 12 to 24 months depending on these energy requirements. End-of-life (EOL) is typically defined at the point in life where the fuel no longer contains sufficient reactivity to maintain 100% rated thermal power. To extend the core lifetime, temperature or power coastdowns or both might be necessary.

#### **4.3.1.4 Fuel Replacement Program**

At the completion of a cycle of operation some of the fuel assemblies are discharged. Fresh assemblies are inserted and some of the existing burned assemblies are repositioned. The placements of the fresh and burned assemblies are chosen so that the new cycle meets the design criteria. The U-235 enrichment and number of fresh assemblies required in the new cycle depends upon the anticipated energy requirements of the cycle.

The boron concentration during refueling is maintained at a sufficiently high level to provide sufficient shutdown margin during the entire refueling operation.

#### 4.3.1.5 Reactivity Coefficients

The reactivity coefficients include the fuel resonance absorption (Doppler) coefficient and the moderator temperature coefficient. Of these reactivity coefficients, the Doppler reactivity coefficient provides the most rapid reactivity compensation. The Doppler effects are associated with changes in fuel temperature and flux spectrum. Use of low-enriched uranium provides a negative Doppler reactivity coefficient. The first core is designed to also provide a negative moderator temperature coefficient for power operations. Therefore, changes in the average temperature or coolant void content provide additional, but slower, reactivity compensation. To reduce the amount of soluble boron in the coolant and maintain the required negative moderator temperature reactivity coefficient during power operations, the use of integral burnable absorbers is required.

Burnable absorbers of any type (discrete or integral) are only required in cycles where it may be necessary to reduce soluble boron concentrations to keep the moderator temperature coefficient negative for power operations or for power distribution control.

#### 4.3.1.6 Control of Power Distribution

The nuclear design basis is that, with at least a 95 percent confidence level:

- The fuel will not be operated at a peak linear power density (LPD) of greater than 13.56 kW/ft at 4590 MW<sub>t</sub> under normal operating conditions, including an allowance of 0.5 percent for calorimetric error and not including a power spike factor due to densification.
- Under abnormal conditions, including the maximum overpower condition, the fuel peak power will not cause melting, as defined in Section 4.4.1.
- The fuel will not operate with a power distribution that violates the departure from nucleate boiling (DNB) design basis (i.e., the measured departure from nucleate boiling ratio (DNBR) shall not be less than the DNBR design limit, as addressed in Section 4.4.1).
- Fuel management will produce values of fuel rod power and burnup consistent with the assumptions in the fuel rod mechanical integrity analysis in Reference 2.

The above design basis meets GDC 10.

Power shape calculations are performed with proven methods, as described in the Codes and Methods Applicability Report for the U.S. EPR (Reference 3). These codes and methods are verified by comparing measured data from operating reactors of

varying size and fuel assembly design to calculations. The codes and methods are then used to generate extreme power shapes which affect fuel design limits. The conditions under which limiting power shapes are assumed to occur are chosen conservatively with regard to any permissible operating state.

Nuclear peaking uncertainties are applied in the DNB and high linear power density (HLPD) analysis in Section 4.4.

#### **4.3.1.7 Maximum Controlled Reactivity Insertion Rate**

The maximum reactivity change rate for normal operations and a postulated accidental withdrawal of control banks (in sequence) are such that the peak heat generation rate and DNBR do not exceed the maximum allowable at over-power conditions. The reactor protection system is designed to protect the fuel design limits in the presence of any single malfunction of the reactivity control systems (GDC 25).

The maximum reactivity worth of control rods and the maximum rates of reactivity insertion employing control rods are limited. This precludes rupture of the coolant pressure boundary or disruption of the core internals to a degree that would impair core cooling capacity due to a rod withdrawal or ejection accident (refer to Section 15.4).

Following any postulated accident, such as a rod ejection or steam line break, the reactor can be brought to the shutdown condition and the core will maintain an acceptable heat-transfer geometry. This satisfies GDC 28.

Reactivity addition associated with an accidental withdrawal of a control bank (or banks) is limited by the maximum rod speed (or travel rate) and by the worth of the bank. The maximum control rod speed is described in Section 3.9.4.

The peak xenon burnout rate is significantly lower than the maximum reactivity addition rate for normal operation and for accidental withdrawal of control banks in overlap at hot zero power.

#### **4.3.1.8 Shutdown Margins**

Minimum shutdown margin as specified in the core operating limits report (COLR) is required for all modes of plant operation:

- Power operations.
- Startup.
- Hot standby.
- Hot shutdown.

- Cold shutdown.
- Refueling condition.

In analyses involving a reactor trip, the single highest-worth rod cluster control assembly (RCCA) is postulated to remain in the fully withdrawn position (stuck rod criterion).

The U.S. EPR has two independent reactivity control methods: the control rods and the soluble boron in the coolant. The control rod system can compensate for reactivity effects associated with the fuel and water temperature changes that accompany power level changes over the range from full-load to no-load. In addition, the control rod system provides the minimum shutdown margin under normal operating conditions and is capable of making the core subcritical rapidly enough to prevent exceeding acceptable fuel damage limits (very small number of rod failures), assuming that the highest worth control rod is stuck in the fully withdrawn position upon reactor trip.

The chemical and volume control system (CVCS) can compensate for all xenon burnout reactivity changes and will maintain the core reactivity within the shutdown requirements for the cold shutdown condition. Thus, two independent shutdown provisions are provided by a mechanical (control rod) and a chemical shim (soluble boron) control system, which satisfies GDC 26. Two phenomena that can occur in the core that have a potential to reduce the shutdown margin are crud buildup and boron deposition on the fuel rods. Both of these phenomena tend to deposit material on the surface of the fuel rod, which changes the neutronic characteristics of the rod. This buildup can cause the reactivity in the portion of rod where it occurs to decrease, causing a shift in power towards the bottom of the core. This redistribution adversely affects the worths of the rods, which are essential in maintaining sufficient shutdown margin. An indicator of severe crud deposition or boron deposition is the core axial offset. If the axial offset drifts more negative than the predicted values, then deposition of material on the fuel rods may be occurring.

#### **4.3.1.9 Stability**

The reactor I&C system detects and suppresses xenon-induced power distribution oscillations. Detection and suppression of xenon oscillations are addressed in Section 4.3.2. If not controlled, these power oscillations could result in conditions that exceed the specified acceptable fuel design limits. This satisfies GDC 12.

Oscillations of the total power output of the core, from whatever cause, are readily detected by the loop temperature sensors and by the fixed incore nuclear instrumentation. These systems protect the core and trip the reactor if power increases unacceptably, preserving the design margins to the fuel design limits. The stability of the turbine/steam generator/core systems and the reactor control system preclude total core power oscillations under normal operating conditions. The

redundancy of the protection circuits provides an extremely low probability of exceeding design power levels.

Prohibited motion of individual control rods can excite convergent azimuthal power oscillations. These azimuthal power oscillations are self-damping, due to reactivity feedback effects designed into the core. In addition, such oscillations are readily detected by the fixed incore detector system. Any resultant power distributions are evaluated against the requirements of the low DNBR and HLPD trip setpoints. Confidence that fuel design limits are not exceeded is provided by the reactor DNBR and HLPD trip setpoints. Incore thermocouples and loop temperature measurements also provide continuous indications of power fluctuations. The aeroball system (described in Section 4.4.6) can be activated to provide even more detailed core power distribution information.

## 4.3.2 Description

### 4.3.2.1 Nuclear Design Description

The reactor core consists of a specified number of fuel rods that are held in bundles by spacer grids and top and bottom fittings. The fuel rods are constructed of M5™ cylindrical tubes containing UO<sub>2</sub> or UO<sub>2</sub>+Gd<sub>2</sub>O<sub>3</sub> fuel pellets. The bundles, known as fuel assemblies, are arranged in a pattern which approximates a right circular cylinder.

An important design feature of the U.S. EPR is the heavy reflector, a large steel structure that replaces the thin baffle plates used in existing reactors (see Figure 3.9.5-3—Reactor Pressure Vessel Heavy Reflector). This reflector reduces fast neutron leakage and flattens the core power distribution. The reflector resides between the fuel and the core barrel and above the lower core support plate. To avoid any welded or bolted connections close to the core, the reflector consists of stacked forged slabs (rings) positioned one above the other (see slabs I-XII in Figure 3.9.5-3). Keys are used to align the slabs, and they are axially restrained by tie rods bolted to the lower core support plate. The heavy reflector is cooled by water flowing through cooling channels running axially through each slab.

The heavy reflector reduces the fast flux on the pressure vessel and improves the neutron economy in the active core. With a volume ratio of approximately 95 percent metal to 5 percent water, the heavy reflector efficiently reflects fast neutrons back to the fuel. In addition, the thermal neutron flux drops off immediately outside the core because there is only a small amount of water present (in the reflector cooling holes) and 4-8 in of steel separating the core from the water outside the reflector.

Each fuel assembly consists of a 17 x 17 rod array composed of 265 fuel rods and 24 guide tubes for inserting control rods or incore instrumentation. Figure 4.3-1—Cross

Section of the U.S. EPR High Thermal Performance Fuel Assembly shows the location of the fuel rods and the 24 guide tubes.

As illustrated later in this section, 89 of the 241 fuel assemblies contain control rods, called rod cluster control assemblies (RCCAs). For those assemblies, all 24 guide tubes are occupied by control rods, thus those assemblies do not have incore instrumentation. Section 4.2 provides details of the fuel assembly design.

The nuclear design description is based on an 18 month Cycle 1 core design, and Table 4.3-1—Core Design Criteria presents the neutronics design criteria. Table 4.3-2—Plant Operating Modes shows the reactor operating modes, along with their respective reactivity, thermal power, and reactor coolant temperatures. This information yields the detailed reactor core description, summarized in Table 4.3-3—Reactor Core Description. Figure 4.3-2—U.S. EPR Rod Group Insertion Limits versus Thermal Power show control rod bank power-dependent insertion limits (PDIL), which are defined as a function of rated thermal power. The 18 month Cycle 1 core design should be considered typical of a Cycle 1 design, and is presented for illustration purposes only.

In the initial core loading, the fuel rods within a given assembly have the same uranium enrichment in the radial plane. The exception to this is the loading of  $\text{UO}_2+\text{Gd}_2\text{O}_3$  rods used for power peaking and core reactivity control. The axial design of the fuel includes blanket regions at the top and of the fuel rods that contains  $\text{UO}_2$  pellets at reduced uranium enrichments. The axial design of the  $\text{UO}_2+\text{Gd}_2\text{O}_3$  rods includes cutback regions between the central gadolinia section of the rod and the blanket regions. The uranium enrichment in these cutback regions is the same as the uranium enrichment in the central zones of the non-gadolinia-bearing rods in the assembly.

Seven different fuel assembly designs with up to three rod types are used in the initial core loading. Each fuel assembly design for the initial core employs a uniform distribution of uranium and gadolinia bearing fuel rods. Figure 4.3-3—Typical Initial Core Loading Map shows the fuel loading pattern as used in the representative initial core design. The core is loaded by placing the lowest enriched fuel on the core periphery to enhance neutron economy, while distributing the remainder of the fuel in the core interior to establish a favorable radial power distribution. Table 4.3-4—Fuel Assembly Summary provides additional information on the seven types of fuel assemblies.

A core operating for 18 months between refueling will typically accumulate between 18 and 22 GWD/MTU per cycle. The exact reloading pattern, initial and final positions of assemblies, and the number of fresh assemblies and their placement depend on the energy requirement for the next cycle and the burnup and power histories of the fuel assemblies from the previous cycles.



The core average enrichment is set by the cycle length and energy requirements. During reactor operation, depletion of the fuel in the assemblies happens when the U-235 atoms absorb neutrons and fission. The fission process also forms fission products, some of which have high absorption cross sections that cause a core neutron flux reduction. The effect on the core flux from the depletion of the U-235 and the buildup of parasitic fission products is partially offset by the buildup of fissionable plutonium, formed through neutron absorption by U-238 atoms. Figure 4.3-4—Uranium Consumption and Plutonium Production versus Burnup shows the uranium consumption and plutonium buildup for a typical 17 x 17 fuel assembly.

To compensate for these effects, the core design for each cycle must have an initial fuel loading with sufficient excess reactivity to compensate for the depletion of the fissile material and the neutron absorption properties of the fission products. Neutron absorbing control rods in selected fuel assemblies and soluble boron in the reactor coolant compensate for this excess reactivity. The soluble boron is a neutron poison, and the concentration in the coolant can be adjusted as the excess reactivity of the core decreases. This compensates for the reactivity changes because of fuel burnup, the buildup of neutron absorbing fission products (including xenon and samarium), the depletion of the integral gadolinia burnable absorbers, and the change in temperature from cold to operating conditions. The CVCS is designed to add or remove soluble boron from the reactor coolant system (RCS) as a means of reactivity control. The CVCS is capable of changes in boron concentration that compensates for uranium depletion and peak xenon burnout and decay, along with the cold shutdown boration requirements. Section 9.3.4 describes the capability of the CVCS to counteract xenon decay. The requirements for rapid transient reactivity and safe shutdown are met with control rods.

As the boron concentration is increased, the moderator temperature coefficient becomes less negative. The use of a soluble absorber alone would result in a positive moderator coefficient at beginning-of-life (BOL) in the initial core. Therefore, integral burnable absorbers in the fuel are used in the first core to reduce the soluble boron concentration so that the moderator temperature coefficient is negative for power operating conditions. During operation, the poison content in these rods is depleted, thus adding positive reactivity to offset some of the negative reactivity from fuel depletion and fission product buildup. The depletion rate of the burnable absorber rods is not critical, since chemical shim is always available and is flexible enough to cover any possible deviations in the expected burnable absorber depletion rate. Figure 4.3-5—Boron Concentration Versus Burnup for a First Core provides a typical boron letdown curve for an initial operating cycle.

In addition to providing reactivity control, the integral gadolinia burnable absorbers are strategically located to provide a favorable radial power distribution. Figures 4.3-6—Fuel Assembly Designs A1 and A2 through 4.3-9—Fuel Assembly Design C3 show the location of the gadolinia bearing fuel rods within the seven different fuel

assembly types used in the initial core design. The figures also show the axial distribution of uranium enrichments within each fuel rod type. These radial and axial gadolinia assembly distributions are typical of that required to hold down reactivity, minimize power peaking within the assembly, and provide favorable core radial power distributions. The locations of these fuel types in the initial core are shown in Figure 4.3-3. Note in these figures that no gadolinia-bearing fuel rods are located adjacent to the guide tube locations for incore instrumentation.

Table 4.3-5—Nuclear Design Parameters contains a summary of the reactor core design parameters, including reactivity coefficients and delayed neutron fractions and lifetimes. These data are typical of an initial core design and do not necessarily reflect the conservative values used in the Chapter 15 analyses.

#### 4.3.2.2 Power Distribution

The power distribution within the U.S. EPR core has been calculated over a broad range of conditions, and the accuracy of the power distribution calculations has been verified for several reactor types. Details of the verification for reactor cores of 157 assemblies, 177 assemblies, and 193 assemblies are provided in Reference 3 and in Section 4.3.2.2.7.

##### 4.3.2.2.1 Definitions

Power distributions can be quantified in terms of hot channel factors. These factors are a measure of the peak fuel pellet power within the reactor core and the total energy produced in a coolant channel, relative to the total reactor power output. These factors are expressed in terms of fundamental nuclear or thermal design quantities, including:

- Power density is the thermal power produced per unit volume of the core (kW/liter or W/cm<sup>3</sup>).
- Linear power density is the thermal power produced per unit length of active fuel (kW/ft). Since fuel assembly geometry is standardized, this is the unit of power density most commonly used. For all practical purposes, it differs from kW/L by a constant factor that includes geometry and the fraction of the total thermal power generated in the fuel rod.
- Average linear power density is the total thermal power produced in the fuel rods divided by the total active fuel length of all rods in the core.
- Local heat flux is the heat flux at the surface of the cladding (Btu-ft<sup>-2</sup>-hr<sup>-1</sup>). For nominal rod parameters, this differs from linear power density by a constant factor.
- Rod power (or rod integral power) is the length-integrated linear power in one rod (kW).

- Core average rod power is the total thermal power produced in the fuel rods divided by the number of fuel rods (assuming all rods have equal length).

The hot channel factors used in the review of power distributions in this section are defined as follows:

- $F_Q$ , heat flux hot channel factor, is defined as the maximum local heat flux divided by the average fuel rod heat flux, allowing for manufacturing tolerances on fuel pellets and rods and measurement uncertainty.
- $F_Q^N$ , nuclear heat flux hot channel factor, is defined as the maximum local fuel rod linear power density divided by the average fuel rod linear power density, assuming nominal fuel pellet and rod parameters.
- $F_E$ , engineering heat flux hot channel factor, is the allowance on heat flux required for manufacturing tolerances. The engineering factor allows for local variations in enrichment, pellet density and diameter, surface area of the fuel rod, and eccentricity of the gap between the pellet and cladding.
- $F_M$ , measurement uncertainty is the uncertainty associated with calculation of  $F_Q^N$  from a full core flux map.
- $F_{\Delta H}^N$ , nuclear enthalpy rise hot channel factor, is defined as the ratio of the highest integrated rod power to the average rod power.

Manufacturing tolerances, hot channel power distribution, and surrounding channel power distributions are treated explicitly in the calculation of the DNBR described in Section 4.4.

It is convenient to define sub-factors of  $F_Q$ . However, design limits are set in terms of the total peaking factor.

$F_Q$  = Total peaking factor or heat flux hot channel factor

$$= \frac{\text{Maximum } kW / ft}{\text{Average } kW / ft}$$

without densification effects,

$$F_Q = F_Q^N \times F_E \times F_M$$

To include the allowances made for densification effects, which are height dependent, the following quantity is defined:

$S(Z)$  = the allowance made for densification effects at height  $Z$  in the core. See Section 4.3.2.2.5.

Then,

$$F_Q^T = \text{Total peaking factor including densification allowance}$$

$$F_Q^T = \max(F_Q^N \times S(Z) \times F_E \times F_M)$$

#### 4.3.2.2.2 Radial Power Distributions

The core radial power distribution at full power is a function of the fuel assembly loading pattern, control rod pattern and insertion, and fuel burnup distribution. Power level, xenon and samarium concentrations, and moderator density also have an effect on the radial power distribution, but these factors are quite small, as is the effect of a non-uniform flow distribution. Figures 4.3-10—Quarter Core Relative Assembly Radial Power Distribution (HFP Near BOL, ARO, No Xenon) through 4.3-16—Quarter Core Relative Assembly Radial Power Distribution (HFP Near EOL, Bank D at PDIL, Equilibrium Xenon Power Distribution) show typical one-quarter core radial power distributions for representative hot full power (HFP) operating conditions at beginning-, middle-, and end-of-life (BOL, MOL and EOL). Other variables in the figures are xenon concentration (none or equilibrium) and control rod position (rods withdrawn or Bank D rods inserted to the PDIL). The conditions represented in the figures are as follows:

- Figure 4.3-10: BOL—Control Rods Withdrawn—No Xenon
- Figure 4.3-11: BOL—Control Rods Withdrawn—Equilibrium Xenon
- Figure 4.3-12: BOL—Control Rods Inserted—Equilibrium Xenon

- Figure 4.3-13: MOL—Control Rods Withdrawn—Equilibrium Xenon
- Figure 4.3-14: MOL—Control Rods Inserted—Equilibrium Xenon
- Figure 4.3-15: EOL—Control Rods Withdrawn—Equilibrium Xenon
- Figure 4.3-16: EOL—Control Rods Inserted—Equilibrium Xenon

Since the position of the hot channel can vary, a single reference design radial power distribution is not selected for DNB calculations. Rather, a set of limiting power distributions are required to verify the DNB limiting condition for operation (LCO) setpoints. The selected power distributions are representative of both the pre- and post-transient conditions.

#### 4.3.2.2.3 Assembly Power Distributions

For comparison, Figures 4.3-17—Fuel Assembly (1/2 Assembly Symmetry) Power Distribution (HFP Near BOL, ARO, Equilibrium Xenon) and 4.3-18—Fuel Assembly (1/2 Assembly Symmetry) Power Distribution (HFP Near EOL, ARO, Equilibrium Xenon) show the fuel assembly power distribution for BOL and EOL (control rods withdrawn and equilibrium xenon).

Since the detailed power distribution surrounding the hot channel varies from time to time, the DNB analysis (as described in Section 4.4) assumes a conservatively flat assembly power distribution. In this analysis, the limiting DNB assembly power is artificially raised to meet the requirements of the DNB LCO used in the verification of the DNB setpoints.

#### 4.3.2.2.4 Axial Power Distributions

The shape of the power profile in the axial (vertical) direction is largely under the control of the operator through the manual movement of the control rods, or through the automatic motion of the rods in response to changes in the core average power level or core average moderator temperature. Nuclear effects that cause variations in the axial power shape include moderator density, the Doppler effect on resonance absorption, and the spatial distributions of xenon and fuel burnup. Automatically controlled variations in total power output and full length rod motion are also important in determining the axial power shape at any time in the cycle. Signals are available to the operator from the fixed incore self powered neutron detectors (SPNDs), which are located in twelve radial locations in the reactor vessel and run parallel to the core axis. Each location has six axially spaced SPNDs. The difference between the core power in the top half and the bottom half is displayed on the control panel, and is called the axial offset (AO).

$$AO = \frac{\phi_t - \phi_b}{\phi_t + \phi_b}$$

Where  $\phi_t$  is the average integrated detector response in the top of the core, and

$\phi_b$  is the average integrated detector response in the bottom of the core.

Representative axial power shapes for BOL, MOL, and EOL conditions are shown in Figures 4.3-19—Typical Axial Power Shape at Beginning of Life through 4.3-21—Typical Axial Power Shape at End of Life. These figures cover a wide range of axial offset, including values not permitted at full power.

The radial power distribution shown in Figure 4.3-12 includes the partial insertion of control rods. These partially rodded configurations are treated explicitly via three-dimensional analyses. Figure 4.3-22—Comparison of Typical Fuel Assembly Axial Power Distributions with a Core Average Axial Power Distribution and Bank D Slightly Inserted compares the axial power distribution for several assemblies at different distances from inserted control rods, with the core average axial distribution. The most significant difference observed in comparing these power shapes to the core average shape is seen in the low power peripheral assemblies.

#### 4.3.2.2.5 Local Power Peaking

Fuel densification, which has been observed to occur under irradiation in several operating reactors, causes the fuel pellets to shrink both axially and radially. As a result, gaps can occur in the fuel column if a pellet becomes wedged against the cladding and the pellets below settle in the fuel rod. The gaps, which are random and vary in length and location, result in decreased neutron absorption in the vicinity of the gap. This produces power peaking in the adjacent fuel rods, resulting in an increased power peaking factor for the core. A quantitative measure of this local power peaking is given by the power spike factor,  $S(Z)$ , where  $Z$  is the axial location in the core.

Fuel manufacturing practices for modern nuclear fuel designs have largely eliminated the potential for significant fuel densification and gap formation during reactor operation. Therefore, it is appropriate to use a power spike factor of 1.0 for the U.S. EPR fuel. Justification for a spike factor of 1.0 is contained in Core Operating Limit Methods for Westinghouse-Designed PWRs (Reference 4).

#### 4.3.2.2.6 Limiting Power Distributions

As described above and in Chapter 15, AOs are those occurrences that are expected frequently or regularly in the course of power operation, maintenance, or

maneuvering of the plant. As such, AOOs are accommodated by reserving margin through the use of Limiting Conditions for Operation (LCOs). The range of conditions that are possible during normal operation are considered in establishing the initial conditions used in analyzing the consequences of postulated accidents. Thus, the analysis of each accident condition is conservative (i.e., it is based on the most adverse set of conditions that can occur during normal operation).

Chapter 15 presents the list of steady state and shutdown conditions, permissible deviations, and operational transients. Implicit in the definition of normal operation is proper and timely action by the reactor operator. That is, the operator follows recommended operating procedures for maintaining appropriate power distributions and takes any necessary remedial actions when alerted to do so by the plant instrumentation. Thus, as stated above, the worst or limiting power distribution that can occur during normal operation is considered as the starting point for analysis of postulated accidents.

Improper procedural actions or errors for AOOs by the operator are assumed in the design. Some of the consequences which might result are presented in Chapter 15. Continuous monitoring of the incore spatial power distribution verifies that LCO limits for DNBR, AO, quadrant power tilt, and LPD, as specified in the COLR, are not violated at the initiation of an AOO.

In addition to the power distribution, the RCS pressure, temperature, and flow are continuously monitored and used to verify the COLR LCO limits on DNBR, LPD, quadrant tilt, and AO are not violated. Maintaining the hot channel factor ( $F_Q$ ) below the LOCA analytical limit depends on the definition of the LPD LCO. The AO LCO also protects against exceeding the maximum  $F_Q$ . The AO LCO bands as specified in the COLR provide operational guidelines that maintain the  $F_Q$  below the limit used in the LOCA analyses during Mode 1 operation. The AO bands are defined such that for a maneuver scenario, the  $F_Q$  remains below the LOCA limit when the reactor is at the rated thermal power condition.

The LPD and AO LCO limits protect the upper bound on the  $F_Q$  peaking factor required to support the LOCA analyses. Included are all of the nuclear effects that influence the radial and axial power distributions throughout core life for various operational conditions, including load follow, reduced power operation, and axial xenon transients.

Radial power distributions are calculated for the full power condition, and include fuel and moderator temperature feedback effects. The steady-state nuclear design calculations are done for normal flow, with the same mass flow in each channel and neglecting flow redistribution effects. The effect of flow redistribution is treated explicitly in verifying the DNB LCO and trip setpoints. The effect of xenon on radial

power distribution is small (compare Figures 4.3-10 and 4.3-11), but is included as part of the normal design process.

The core average axial power profile, however, can experience significant and rapid changes because of control rod motion and load changes, and slower changes because of changes in the xenon distribution. Since the properties of the nuclear design dictate what axial power shapes can occur, boundaries on the AO limits of interest can be set in terms of the parameters that are readily observed in the plant. Specifically, the nuclear design parameters that are important to the axial power distribution analysis are:

- Core power level.
- Core height.
- Axial geometry of the assembly.
- Coolant temperature and flow.
- Coolant temperature as a function of reactor power.
- Fuel cycle lifetimes.
- Rod bank worths.
- Rod bank overlap.

Normal operation of the plant assumes compliance with the following conditions:

- Control rods in a single bank move together with no individual rod insertion differing by more than 8 steps (indicated) from the bank demand position.
- Control banks are sequenced with overlapping banks.
- The full length control bank insertion limits are not violated.
- Axial offset and control bank position limits are adhered to, as specified in the COLR.

The reactor protection system setpoints are determined consistent with these four conditions.

The axial power distribution procedures referred to above are part of the required normal reactor operating procedures. Normal operations require control of the axial offset within a permissible range at power levels greater than 50 percent of rated thermal power. The limits on AO are given in the COLR. Operation within a set of AO limits minimizes xenon transient effects on the axial power distribution, as the xenon distribution is maintained in phase with the power distribution.



Calculations are performed for normal operation of the reactor throughout its cycle lifetime. The BOL and EOL conditions are evaluated, along with at least one additional mid-cycle exposure. The effects of different operational maneuvers are also evaluated. A set of maneuvers are studied to determine the general behavior of the local power density as the core returns to the rated thermal power condition.

These cases represent many possible reactor states during a fuel cycle, and they have been chosen to be a definitive representation of the cycle. The cases described above are necessary and sufficient to generate an AO LCO limit that prevents the upper limit on  $F_Q$  from being exceeded during normal operation. Calculated values of  $F_Q$  are increased by a design allowance and by the engineering factor  $F_E$ .

This upper limit on  $F_Q$  is verified for operation within an allowed LPD and AO operating space, as detailed in the Technical Specifications. The LPD and AO LCO limits are specified in the COLR. The LCO limits and  $F_Q$  are monitored using the fixed incore SPND detectors, supplemented by periodic full-core aeroball measurements. These systems generate computer-based alarms if there are deviations from the allowed LCO operating space.

Figure 4.3-23—Maximum  $F_Q$  as a Function of Core Height represents an upper limit on  $F_Q$  versus core height. This envelope provides a conservative representation of the limiting values of local power density.

Allowing for fuel gamma energy transport to non-fuel regions (.974), the average linear power is 5.08 kW/ft at 4590 MW<sub>t</sub>. The conservative upper limit design value of the normalized local power density, reduced by uncertainty allowances, and the engineering factor is 2.40, corresponding to a peak linear power density of 12.19 kW/ft.

The limiting operating conditions are addressed by generating axial shapes at various power levels and rod configurations, combined with unrealistically severe axial xenon distributions. These adverse xenon distributions are applied to rodded and unrodded core configurations at different power levels. This provides axial power distributions that are more limiting than those that are reasonably achievable.

Events are assumed to start from typical normal operating situations, which include normal xenon transients. The final power distributions are represented using the conservative axial shapes that were generated. In determining the power distributions, it is further assumed that the total core power level would be limited by a reactor trip to below 116.7 percent of rated thermal power (see Table 15.0-7).

$F_Q$  increases with decreasing power. Likewise,  $F_{\Delta H}^N$  increases with decreasing power. Changes in the maximum powered rod because of power level changes or control rod

insertion are captured in the online verification of the DNBR and LPD LCO limits.

Verification of the hot full power  $F_{\Delta H}^N$  limit becomes a design basis criterion which is used for establishing acceptable control rod patterns and control bank sequencing. Likewise, fuel loading patterns for each cycle are selected with consideration of this

design criterion. The worst values of  $F_{\Delta H}^N$  for possible rodded configurations occurring in normal operation are used in verifying that this criterion is met. Typical radial factors and radial power distributions are shown in Figures 4.3-17 to 4.3-18. The worst values generally occur with the control rods at their insertion limits. Operation within the allowed AO LCO establishes rod positions which are at or above the allowed rod insertion limits.

During normal operations, if a situation arises that could result in local power densities that are a precondition for a hypothetical accident, but which would not itself cause fuel failure, administrative controls and alarms are provided for returning the core to a safe condition. These controls and alarms are described in detail in Section 7.7.

Crud deposition or boron buildup on the fuel rods can also affect power distribution. However, the continuous monitoring of the DNB, the LPD, and the AO against LCO limits would detect changes in power distribution caused by these phenomena.

#### 4.3.2.2.7 Experimental Verification of Power Distribution Analysis

The experimental verification of power distribution analysis is described in Reference 3 and is summarized below. A processing code is used to calculate the power distribution based on the incore instrumentation measurements. As required by Technical Specifications, a comparison of measured and calculated power distributions is performed periodically throughout each cycle lifetime.

The fixed incore instrumentation system provides continuous axial and radial monitoring of the core power distribution during normal and off-normal operation. These axial and radial power distributions are used in the LCO verification of the COLR limits on DNBR and LPD, along with the trip functions based on DNBR and HLPD limits. The fixed incore instrumentation system continuously monitors the core AO and verifies that operation is within the AO LCO limits. The fixed incore instruments also continuously monitor the  $F_Q$  to verify it meets the requirements of the LOCA analyses. The aeroball system (see below) is required to verify the  $F_{\Delta H}$  limit, as required by Technical Specifications.

The aeroball system is a movable incore measurement system used to monitor the detailed power distribution in the core and to calibrate the fixed incore instrumentation at a frequency required by Technical Specifications. Measurements made with the fixed incore detector and aeroball systems, described in Section 4.4.6, require consideration of the following three uncertainties:

1. Reproducibility of the measured signal.
2. Errors in the calculated relationship between detector current and local flux.
3. Errors in the calculated relationship between detector flux and peak rod power or peak local power some distance from the measurement thimble.

For the fixed incore detectors, these uncertainties are addressed by calibration with the aeroball system, as noted above. For the aeroball system, item 1 is addressed through the comparison of signals from symmetric channels. Separate detectors are used to determine the activity of the aeroballs activated in core symmetric locations, and the signals are compared for consistency. Items 2 and 3 are addressed using the uncertainty that is applied to the local peaking factors. Local power distribution predictions are verified in critical experiments (described below) on arrays of rods with simulated guide thimbles, control rods, and burnable poisons. These critical experiments provide quantification of errors in items 2 and 3 above.

Reference 3 describes the critical experiments performed to determine the local peaking uncertainty. The standard deviation of the relative uncertainty was determined by comparing calculated pin-by-pin fission rate distributions with the critical experiment measurements. These data, in combination with the power distribution measurement uncertainty evaluation, are used to determine the uncertainties on the integrated and the local hot channel peaking. The total uncertainty on the integrated rod power is 4.1 percent and the total uncertainty on the hot channel factor is 5.1 percent. The total uncertainty for the integrated rod power and the hot channel factor are not used in the verification of the DNBR and LPD LCO limits or trip setpoints. Treatment of the uncertainties for these functions is described in Incore Trip Setpoint and Transient Methodology for U.S. EPR Topical Report (Reference 5).

In comparing measured power distributions (or detector currents) with calculations for the same operating conditions, it is not possible to isolate out the detector reproducibility. Comparisons between measured and predicted signals are provided in References 3 and 6. These comparisons between measured and predicted power distributions confirm the adequacy of both the integrated rod power uncertainty allowance and the hot spot channel factor uncertainty allowance.

The integrated rod power uncertainty is statistically combined to verify the DNB LCO and trip limits, and the hot spot channel uncertainty is statistically combined to verify the LPD LCO and trip limits.

There are two types of accumulated data on power distributions in actual operation:

- Data obtained in steady state operation at constant power in the normal operating configuration.

- Data with unusual values of axial offset obtained as part of the excore detector calibration exercise required by Technical Specifications.

These data are presented in detail in Reference 3. Figure 4.3-24—Measured Values of  $F_Q$  for Steady State Full Power Rod Configurations contains a summary of measured values of  $F_Q$  as a function of axial offset for the plants from the above report.

#### 4.3.2.2.8 Testing

An extensive series of physics tests will be performed on the first core. These tests and the criteria for satisfactory results are described in the initial test program in Section 14.2. Since not all limiting situations can be created at BOL, the main purpose of the tests is to provide a check on the calculational methods used for predicting the test conditions. Tests performed at the beginning of each reload cycle verify the selected safety-related parameters of the reload design.

#### 4.3.2.2.9 Monitoring Instrumentation

The adequacy of instrument numbers, spatial deployment, required correlations between readings and power peaking, calibration, and errors are described in Reference 5. The relevant conclusions are summarized in Sections 4.3.2.2.7 and 4.4.6.

Provided the limitations given in Section 4.3.2.2.6 on rod insertion and axial offset are observed, the fixed incore detector system provides adequate online monitoring of power distributions. Details of the specific limits on the rod positions and axial offset are given in the COLR.

Limits for alarms and reactor trips are also given in Technical Specifications and descriptions of the systems are in Section 7.7.

#### 4.3.2.3 Reactivity Coefficients

The kinetic characteristics of the reactor core determine how the core responds to changing plant conditions and to operator adjustments made during normal operation, as well as during abnormal or accidental transients. These kinetic characteristics are quantified in the reactivity coefficients. The reactivity coefficients reflect the changes in the neutron multiplication because of varying plant conditions, such as power, moderator or fuel temperatures, or pressure or void conditions (although the latter are relatively unimportant in the U.S. EPR). Since the reactivity coefficients change during the life of the core, ranges of coefficients are employed in the transient analyses used to determine the response of the plant throughout life. The analytical methods and calculational models used in calculating the reactivity coefficients are given in Section 4.3.3.

The results of such simulations and the reactivity coefficients used are presented in Chapter 15. The reactivity coefficients are calculated on a core-wide basis by three-

dimensional nodal diffusion theory methods. The effect of radial and axial power distribution on core average reactivity coefficients is implicit in those calculations, and is not significant under normal operating conditions. However, the spatial effects are included in these analyses and are particularly important in some transient conditions. These include a postulated rupture of the main steam line break and a rod ejection accident, as described in Sections 15.1.5 and 15.4.8, respectively.

Quantitative information for calculated reactivity coefficients—including the fuel Doppler coefficient, moderator coefficients (density, temperature, pressure, and void), and power coefficient—is given in the following sections.

#### **4.3.2.3.1 Fuel Temperature (Doppler) Coefficient**

The fuel temperature or Doppler coefficient is defined as the change in reactivity per degree change in effective fuel temperature, and is primarily a measure of the Doppler broadening of U-238 and Pu-240 resonance absorption peaks. Doppler broadening of other isotopes is also considered, but their contribution to the Doppler effect is small. An increase in fuel temperature increases the effective resonance absorption cross sections of the fuel and produces a corresponding reduction in reactivity.

The fuel temperature coefficient is calculated by performing two-group, three-dimensional calculations, using the PRISM code, with the moderator temperature held constant and the fuel temperature varied. The spatial variation of fuel temperature is taken into account by calculating the effective fuel temperature as a function of power density, as addressed in Section 4.3.3.

A typical Doppler temperature coefficient as a function of core burnup is shown in Figure 4.3-25—Typical Doppler Temperature Coefficient. A typical Doppler-only contribution to the power coefficient, defined later, is shown in Figure 4.3-26—Typical Doppler-Only Power Coefficient at BOL and EOL as a function of relative core power. The integral of the differential curve on Figure 4.3-26 is the Doppler contribution to the power defect and is shown in Figure 4.3-27—Typical Doppler-Only Power Defects at BOL and EOL as a function of relative power. The Doppler coefficient becomes more negative as a function of life as the Pu-240 content increases, thus increasing the Pu-240 resonance absorption, but the overall value becomes more negative since the fuel temperature changes with burnup, as described in Section 4.3.3. The upper and lower limits of the Doppler coefficient used in accident analyses are given in Section 15.0.0.

#### **4.3.2.3.2 Moderator Coefficients**

The moderator coefficient is a measure of the change in reactivity due to changes in reactor coolant parameters, such as temperature (moderator density), pressure, or void. The coefficients related to these coolant parameters are moderator density, pressure, and void coefficients.

The moderator temperature (density) coefficient is defined as the change in reactivity per degree change in the moderator temperature. Generally, the effects of the changes in moderator density and temperature are considered together. The soluble boron used in the reactor as a means of reactivity control also affects the moderator density coefficient, since both the soluble boron poison density and the water density decrease when the coolant temperature rises. An increase in the soluble poison density introduces a positive component in the moderator coefficient. If the concentration of soluble poison is large enough, the net value of the coefficient may be positive, but this is precluded by design criteria. The effect of control rods is to make the moderator coefficient more negative since the thermal neutron mean free path, and hence the volume affected by the control rods, increases with an increase in temperature.

With burnup, the moderator temperature coefficient becomes more negative, primarily as a result of boric acid dilution, but also to a significant extent from the effects of the buildup of plutonium and fission products.

The moderator temperature coefficient is calculated for a range of plant conditions by performing two-group calculations, in which the moderator temperature (and density) is varied by about  $\pm 10^{\circ}\text{F}$  about each of the mean temperatures. The moderator coefficient is shown as a function of core temperature and boron concentration for a typical core in Figures 4.3-28—Typical Zero Power Moderator Temperature Coefficient at BOL through 4.3-30—Typical Zero Power Moderator Temperature Coefficient at EOL. The temperature range covered is from cold ( $38^{\circ}\text{F}$ ) to nominal hot zero power inlet temperatures. The contribution of the Doppler coefficient (due to the change in moderator temperature) is not included in these results. Figure 4.3-31—Typical Hot Full Power Moderator Temperature Coefficient shows the hot, full-power moderator temperature coefficient for a typical core plotted as a function of first cycle lifetime for the just-critical boron concentration condition based on the design boron letdown condition.

The moderator temperature coefficients presented are for a core-wide basis, since they are used to describe the core behavior when the moderator temperature changes can be considered to affect the entire core.

The moderator pressure coefficient relates the change in moderator density, resulting from reactor coolant pressure changes, to the corresponding effect on neutron production. This coefficient is opposite in sign and considerably smaller than the moderator temperature coefficient. A typical range of pressure coefficients over the range of moderator temperatures at zero power is  $-0.2$  to  $+0.4$  pcm/psi, but is always positive at operating conditions and becomes more positive during life, typically  $+0.1$  to  $+0.5$  pcm/psi.

The occurrence of small amounts of local subcooled boiling in the reactor during full power operation may result in small steam bubbles, called voids. The average void

fraction is the fraction (by volume) of the moderator that is void, and is substantially less than one percent at normal operating conditions. The void coefficient is the change in reactivity associated with these voids in the moderator. Voiding is a local effect and the void coefficient increases from -50 pcm/percent void early in life to +250 pcm/percent void at EOL.

#### **4.3.2.3.3 Power Coefficient**

The combined effect of moderator temperature and fuel temperature change as the core power level changes is called the total power coefficient, and is expressed as reactivity change per percent power change. A typical power coefficient at BOL and EOL conditions is shown in Figure 4.3-32—Typical Total Power Coefficient at BOL and EOL.

The power coefficient becomes more negative with burnup, reflecting the combined effect of the changes in moderator and fuel temperature coefficients with burnup. The power defect (the integral of the reactivity coefficient) at BOL and EOL is shown in Figure 4.3-33—Typical Total Power Defect at BOL and EOL.

#### **4.3.2.3.4 Comparison of Calculated and Experimental Reactivity Coefficients**

The calculated reactivity coefficients will be verified by experiments performed during the startup tests, as described in Section 14.2 (see tests #190, #191, #192, #207, and #218).

Section 4.3.3 describes the comparison of calculated and experimental reactivity coefficients, and the results are presented in Reference 3.

#### **4.3.2.3.5 Reactivity Coefficients Used in Transient Analysis**

Table 4.3-5 summarizes the range of values for the reactivity coefficients, while the best estimate values as a function of various parameters are shown in Figures 4.3-25 through 4.3-33. The exact values of the coefficient used in the transient analysis depend on whether the transient of interest is examined at BOL or EOL, whether the most negative or the most positive coefficients are appropriate, and whether spatial non-uniformity must be considered in the analysis. Conservative values of coefficients, considering these various aspects of the analysis, are used in the Chapter 15 transient analyses.

#### **4.3.2.4 Control Requirements**

To provide the shutdown margin stated in the COLR under conditions where a cooldown to ambient temperature is required, concentrated soluble boron is added to the coolant. Boron concentrations (natural B-10 abundance) for several core conditions are listed in Table 4.3-5. For all core conditions including refueling, the boron concentration is well below the solubility limit. The rod cluster control

assemblies are employed to bring the reactor to the hot shutdown condition. The minimum required shutdown margin is given in the COLR.

The shutdown margin (SDM) for hot conditions is presented in Table 4.3-6—Reactivity Requirements for Rod Cluster Control Assemblies (First Cycle). The SDM is determined by comparing the difference between the rod cluster control assembly reactivity available with an allowance for the most reactivity rod stuck out of the core, with the reactivity required for control and protection purposes. The total rod worth in the SDM includes an allowance of 10 percent for uncertainties (see Section 4.3.3).

The control rods are required to provide sufficient reactivity to account for the power defect from full power to zero power, and to provide the required shutdown margin. The reactivity addition resulting from power reduction consists of contributions from the Doppler effect, moderator temperature, flux redistribution, and reduction in void content, as presented below.

#### **4.3.2.4.1 Doppler Effect**

The Doppler effect arises from the broadening of U-238 and Pu-240 resonance cross sections with an increase in effective pellet temperature. This effect occurs over the range of zero power to full power due to the large fuel pellet temperature increase with power generation.

#### **4.3.2.4.2 Average Moderator Temperature**

At power, the control rod motion is used to automatically control both the average moderator temperature and the power. At the same time, RCS boron concentration is automatically adjusted through boron addition and dilution by the CVCS system so that the control rods can reach their preferred positions subsequent to average temperature-driven rod movements. Automatic temperature control starts at 25% power. The nominal core average temperature program as a function of power is presented in Section 4.4.3. When the core is shut down to the hot zero power condition, the average moderator temperature is the equilibrium no-load value, which is based on the steam generator shell-side design pressure.

The average temperature values used in the Chapter 15 safety analyses are presented in the event-specific sections.

Since the moderator coefficient is negative, reactivity increases with a decrease in power. The moderator coefficient becomes more negative as the fuel depletes because of the change in the fuel composition.



#### 4.3.2.4.3 Redistribution

During full power operation, the coolant density decreases with core height, and this, together with partial insertion of control rods, results in less fuel depletion near the top of the core. Thus, under steady state conditions, the relative power distribution is slightly asymmetric toward the bottom of the core. Conversely, at hot zero power conditions the coolant density is uniform over the core height, and there is no flattening due to the Doppler effect. The result is a flux distribution which, at zero power, can be skewed toward the top of the core. The reactivity insertion due to the skewed distribution is calculated with an allowance for the effect of xenon distribution.

#### 4.3.2.4.4 Void Content

Nucleate boiling at full power produces a small void content in the core. The voids collapse with power reduction and this causes a small reactivity contribution.

#### 4.3.2.4.5 Rod Insertion Allowance

At full power, the control bank is operated within a prescribed band of travel to compensate for small changes in boron concentration, changes in moderator temperature, and the very small changes in the xenon concentration not compensated for by the changes in boron concentration. When the control bank reaches either limit of this band, a change in boron concentration is required to compensate for any additional reactivity changes.

#### 4.3.2.4.6 Burnup

The excess reactivity in the fresh fuel is sufficient to maintain core criticality at full power operating conditions throughout the cycle life with xenon, samarium, and other fission products present. This excess reactivity depletes with fuel burnup, but early in the cycle it is controlled by the addition of soluble boron to the coolant and burnable absorber to the fuel. The soluble boron concentration and the unit boron worth are given in Tables 4.3-1 and 4.3-5, respectively. Since the excess reactivity is controlled by soluble boron and burnable absorber, compensation for the excess reactivity is not included in the control rod requirements.

#### 4.3.2.4.7 Xenon and Samarium Poisoning

Changes in xenon and samarium concentrations in the core occur at a sufficiently slow rate, even following rapid power level changes, that the resulting reactivity change can be controlled by changing the soluble boron concentration. Changes in soluble boron concentrations are also addressed in Section 4.3.2.4.16.

#### 4.3.2.4.8 pH Effects

Control of the coolant pH is accomplished through the addition of lithium. The neutron absorption by lithium is small compared to that of boron, and the coolant lithium concentration is much lower than the coolant boron concentration. Therefore, the change in reactivity due to a change in coolant pH is negligible and occurs slowly enough to be controlled by the boron system.

#### 4.3.2.4.9 Experimental Confirmation

Section 4.3.3 describes the nuclear design calculational methods and compares calculated and experimental data. Results are detailed in Reference 3.

#### 4.3.2.4.10 Control

Core reactivity is controlled by means of a chemical absorber dissolved in the coolant, rod cluster control assemblies, and integral burnable absorbers, as described below.

#### 4.3.2.4.11 Chemical Absorber

The concentration of boron in solution as boric acid is used to control the relatively slow reactivity changes associated with:

- The moderator temperature defect in going from cold shutdown at ambient temperature to the hot operating temperature at zero power.
- The transient xenon and samarium poisoning that occurs following power changes or changes in rod cluster control assembly position.
- The reactivity effects of fissile inventory depletion and buildup of long-life fission products.
- The integral burnable absorber depletion.

Boron concentrations for various core conditions are presented in Table 4.3-5.

#### 4.3.2.4.12 Rod Cluster Control Assemblies

The number and design of the RCCAs is shown in Table 4.3-7—RCCA and Integral Burnable Absorber Description. The RCCAs are used for shutdown and control purposes to offset the fast reactivity changes associated with:

- The required shutdown margin in the hot zero power all rods inserted condition with the most reactive rod stuck out.
- The reactivity compensation as a result of an increase in power above hot zero power (power defect, including Doppler, and moderator reactivity changes).

- Unplanned fluctuations in boron concentration, coolant temperature, or xenon concentration (with rods not exceeding the allowable rod insertion limits).
- Reactivity ramp rates resulting from load changes.

The allowed control bank reactivity insertion is limited at full power to maintain shutdown capability. As the power level is reduced, control rod reactivity requirements are also reduced, and more rod insertion is allowed. The control bank position is monitored and the operator is notified by an alarm if the limit is approached. The determination of the insertion limit uses conservative xenon distributions and axial power shapes. In addition, the RCCA withdrawal pattern determined from these analyses is used to determine power distribution factors, and the maximum worth of an inserted RCCA ejection accident. For further information, refer to the COLR on rod insertion limits.

The power distribution, rod ejection, and rod misalignment analyses are based on the arrangement of the shutdown and control banks of the RCCAs, as shown in Figure 4.3-34—Rod Cluster Control Assembly Pattern. All shutdown rod cluster control assemblies are withdrawn before withdrawal of the control banks is initiated. In going from zero to 100 percent power, control Banks A, B, C, and D are withdrawn sequentially in overlap. The limits of rod positions are provided in the COLR.

#### **4.3.2.4.13 Integral Burnable Absorber Rods**

The integral burnable absorber rods provide partial control of the excess core reactivity. In doing so, these rods make the moderator temperature coefficient less positive at normal operating conditions. They perform this function by reducing the requirement for soluble poison in the moderator at the beginning of the fuel cycle, though they lose their effectiveness as the absorber is depleted. Figure 4.3-3 illustrates a typical pattern showing the location of the fuel assemblies containing integral burnable absorber rods, together with the number of absorber rods per assembly. The specific arrangements of absorber rods within the assemblies are shown in Figures 4.3-6 through 4.3-9.

#### **4.3.2.4.14 Peak Xenon Startup**

The boron control system compensates for the peak xenon buildup. Startup from the peak xenon condition is accomplished with a combination of control rod motion and boron dilution. The boron dilution may be made at any time, including during the shutdown period, provided the shutdown margin is maintained.

#### **4.3.2.4.15 Load Follow Control and Xenon Control**

During load follow maneuvers, power changes are accomplished using control rod motion and either boron dilution or additions, as required. Control rod motion is limited by the control rod insertion limits as provided in the COLR and summarized in

Section 4.3.2.4.12. The power distribution is maintained within acceptable limits through the relative locations of rod banks. Reactivity changes due to the changing xenon concentration can be controlled by rod motion or changes in the soluble boron concentration.

#### **4.3.2.4.16 Burnup**

Control of the excess reactivity for burnup is accomplished, using soluble boron and integral burnable absorbers. The boron concentration must be limited during operating conditions so that the moderator temperature coefficient is not positive at power conditions. Sufficient integral burnable absorber is installed at the beginning of a cycle to give the desired cycle lifetime, without exceeding the minimum boron concentration requirement. The practical minimum boron concentration is in the range of 0 to 10 ppm.

#### **4.3.2.5 Control Rod Patterns and Reactivity Worths**

The rod cluster control assemblies (see Figure 4.3-34) are designated by function as the control groups and the shutdown groups. (The terms group and bank are used synonymously to describe a particular arrangement of control assemblies.) The control banks are labeled A, B, C, and D and the shutdown banks are labeled SA, SB, and SC. The axial position of the RCCAs may be controlled manually or automatically, and all are dropped into the core upon a reactor trip signal.

Two criteria have been employed for selecting the control groups. First, the total reactivity worth must be adequate to meet the typical BOL and EOL requirements specified in Table 4.3-6. Second, in view of the fact that these rods may be partially inserted at power operation, the power peaking should be low enough so that the power capability requirements are met.

The position of control banks for criticality under any reactor condition is determined by the concentration of boron in the coolant. On an approach to criticality, boron is adjusted so that criticality is achieved with control rods above the insertion limit set by shutdown and other considerations (see the COLR). If required, a set withdrawal limit at low power may be used early in the cycle to maintain the moderator temperature coefficient within the limit specified in the COLR.

Rod ejection is addressed Section 15.4.8.

Allowable deviations due to misaligned control rods are addressed in Technical Specifications.

A representative calculation for two banks of control rods withdrawn in overlap (rod withdrawal accident) is given in Figure 4.3-35—Differential Bank Worth with Two Banks in Overlap.

Calculation of control rod reactivity worth versus time following reactor trip involves both control rod velocity and differential reactivity worth. The rod position versus time of travel after rod release is given in Figure 4.3-36—Rod Position versus Time of Travel after Rod Release. For nuclear design purposes, the reactivity worth versus rod position is calculated by a series of steady state calculations at various control rod positions. These calculations assume the rods are initially at the power dependent insertion limit in order to minimize the initial reactivity insertion rate. A typical result of these calculations is shown on Figure 4.3-37—Reactivity Worth versus Rod Position.

The shutdown groups provide additional negative reactivity to provide an adequate shutdown margin. Shutdown margin is defined as the amount by which the core would be subcritical at hot shutdown if all RCCAs are tripped, but assuming that the highest worth rod cluster control assembly remains fully withdrawn and no changes in xenon or boron concentration take place. The loss of control rod worth due to the material irradiation is negligible, since only Bank D can be partially inserted into the core under normal operating conditions (near full power).

The values given in Table 4.3-6 show that the available reactivity in withdrawn RCCAs provides the design basis minimum shutdown margin, allowing for the highest worth RCCA to be at its fully withdrawn position. An allowance for the uncertainty in the calculated worth of N-1 rods is made before determining the shutdown margin. The values in Table 4.3-6 are calculated from a nominal design model. These values may vary cycle-to-cycle due to loading pattern changes, and may also change during the cycle based upon actual plant operation or reanalysis to remove conservatisms.

#### **4.3.2.6 Criticality of Reactor During Refueling**

The basis for maintaining the reactor subcritical during refueling is presented in Section 4.3.1.4, and a summary of how control requirements are met is given in Sections 4.3.2.4 and 4.3.2.5.

Criticality of fuel assemblies outside the reactor is precluded by the design of the fuel transfer and fuel storage facilities and by administrative control procedures. Section 9.1 addresses fuel handling and storage.

#### **4.3.2.7 Stability**

##### **4.3.2.7.1 Introduction**

Pressurized water reactors with negative overall power coefficients are inherently resistant to power oscillations, therefore this review is limited to xenon-induced power distribution oscillations.

Xenon-induced oscillations occur as a result of rapid perturbations to the power distribution that causes the xenon and iodine fission product concentrations to be out of phase with the perturbed power distribution. This results in a shift in the iodine and xenon distribution that causes the power distribution to change in an opposite direction from the initial perturbation, which initiates oscillations. The magnitude of the power distribution oscillation can either increase or decrease with time. Thus, the core can be considered to be either unstable or stable with respect to these oscillations.

Xenon oscillation modes can be classified into three general types: azimuthal, radial, and axial. Xenon stability analyses indicate that any azimuthal xenon oscillations induced in the core would be damped. Axial and radial xenon oscillations, however, could exhibit instabilities in the absence of appropriate control action. Before presenting the methods of analysis and control, it is appropriate to reiterate several important aspects of the xenon oscillation phenomenon.

- The time scale for the oscillations is long and any induced oscillation typically exhibits a period of about one day.
- Xenon oscillations are readily detectable, as described below.
- As long as the initial power peak associated with the perturbation that initiates the oscillation is within acceptable limits, the operator has time (on the order of hours to days) to take appropriate remedial action before the allowable peaking factors are exceeded.

#### 4.3.2.7.2 Stability Index

The stability of a xenon oscillation may be described by the following equation:

$$|\Delta P_{\text{peak}}(t)| = A \exp(Bt)$$

Where:

- $|\Delta P_{\text{peak}}(t)|$  is the absolute value difference in indicated relative power (Axial Offset, assembly power) from the peak to the equilibrium value.
- A is the inferred maximum  $\Delta P_{\text{peak}}$  at  $t=0$ .
- B is the stability index.

The stability of a reactor can be characterized by a stability index or a damping factor, which is defined as the natural exponent that describes the growing or decaying amplitude of the oscillation. A positive stability index (B) indicates an unstable core. A zero or a negative value indicates stability for the oscillatory mode being investigated. The stability index is generally expressed in units of inverse hours, so that a value of -0.01/hr would mean that the amplitude of each subsequent oscillation cycle decreases by about 25 percent for a period of about 30 hours for each cycle.

#### 4.3.2.7.3 Azimuthal Stability

An azimuthal oscillation consists of an X-Y power shift from one side of the reactor core to the other. The U.S. EPR is stable with respect to azimuthal oscillations because azimuthally symmetric operation and design practices preclude such instabilities.

#### 4.3.2.7.4 Radial Stability

A radial xenon oscillation consists of a power shift inward and outward from the center of the core to the periphery. The core may exhibit radial instability in conjunction with axial instability should rod motion induce a xenon transient. When the transient is damped by rod motion, the radial oscillation is damped with the axial oscillation. Thus, addressing radial oscillation stability is inherent in addressing axial stability.

#### 4.3.2.7.5 Axial Stability

Axial xenon oscillations consist of a power shift between the top and bottom of the reactor core. This type of oscillation could be unstable, and RCCA actions may be required to limit the oscillation magnitude. Power distributions, both radial and axial, are monitored so that the operator can move the RCCAs to control any axial oscillation.

#### 4.3.2.7.6 Stability Control and Protection

The protection system described in Section 7.2 prevents exceeding acceptable fuel design limits and limits the consequences of postulated accidents. Since the reactor is predicted to be stable with respect to azimuthal xenon oscillations, no special protective system features are needed to accommodate azimuthal mode oscillations.

Axial oscillations during a power maneuver are controlled by RCCA movement and adjustments to the soluble boron concentration. A typical controlled xenon oscillation is illustrated in Figure 4.3-38—Typical Damped Xenon Oscillation. Certain periods of core life may be prone to xenon-induced axial power oscillation, however these oscillations are very slow acting and allow adequate time for damping control strategies to be identified and implemented.

#### 4.3.2.8 Vessel Irradiation

Section 5.3.1 describes the pressure vessel irradiation and surveillance program that addresses the issue of radiation damage to the reactor vessel. Summarized below are the methods and analyses used in that program to determine the neutron and gamma ray flux attenuation between the core and the pressure vessel.

The materials surrounding the core serve to protect the vessel from radiation damage by attenuating neutrons originating in the core, and gamma rays originating from both

the core and structural components. These materials include the heavy reflector, core barrel, and the associated water annuli, all of which are within the region between the core and the pressure vessel.

In general, few-group neutron diffusion theory codes are used to determine fission power density distributions within the active core, and the accuracy of these analyses is verified by incore measurements on operating reactors. Region and rodwise power-sharing information from the core calculations is then used as source information in two-dimensional  $S_n$  transport calculations that compute the flux distributions throughout the reactor.

The neutron flux distribution and spectrum in the various structural components varies significantly from the core to the pressure vessel. Representative values of the neutron flux distribution and spectrum are presented in Table 4.3-8—Typical Neutron Flux Levels in the Reactor Core and Reactor Pressure Vessel. The values listed are based on time-averaged equilibrium cycle reactor core parameters and power distributions, and are suitable for long-term nvt projections and for correlation with radiation damage estimates. Flux and radiation damage estimates are verified through the analysis of actual test samples from the irradiation surveillance program, as described in Section 5.3.1.

### 4.3.3 Analytical Methods

This section describes the analytical methods used in nuclear design, including those used for predicting criticality, reactivity coefficients, burnup, and stability. The analytical methods are validated by comparison with measured data.

#### 4.3.3.1 Analytical Methodology Summary

The base analytical methodology is presented in Reactor Analysis Systems for PWRs – Volume 1 - Methodology Description (Reference 6), with additional details in Codes and Methods Topical Report (Reference 3). Modifications to the methodology used in the latter reference include:

- Use of a 0.625 eV cutoff for thermal neutrons is used in Reference 3 (1.855 eV is used in Reference 6).
- Inclusion of the U. S. EPR heavy reflector model.
- Introduction of a new inferred power distribution reconstruction methodology.

The base analytical methodology uses CASMO-3 to generate cross sections and PRISM to determine core reactivity and power distributions. PRISM evaluates number densities and burnup of key isotopes on a nodal basis using microscopic cross sections. The nodal expansion method (NEM) is used to solve the two-group diffusion theory



representation of the reactor core. Pin power distributions are generated by PRISM using a pin power reconstruction technique.

The reactor kinetics methodology is presented in NEMO-K – A Kinetic Solution in Nemo (Reference 7). The reactor kinetics methodology uses CASMO-3 to generate cross sections and NEMO-K to perform three-dimensional space-time reactor kinetics calculations. NEMO-K incorporates time-dependent solutions for neutronics, fuel temperature, and coolant properties into the steady-state NEMO code. NEMO-K has been demonstrated to accurately predict reactivity, power distribution, and rod worths during fast (rod ejection type) core transients as well as slower (rod drop type) events. NEMO-K is used to perform U. S. EPR rod ejection analyses.

#### **4.3.3.1.1 Cross Section Generator Methodology**

The cross section generator methodology is summarized in Table 4.3-9—Cross Section Generation Methodology.

#### **4.3.3.1.2 Reactor Core Simulator Methodology**

The reactor core simulator methodology is summarized in the Table 4.3-10—Reactor Core Simulator Methodology.

#### **4.3.3.1.3 Treatment of U. S. EPR Heavy Radial Reflector**

The U.S. EPR reflector (see Figure 3.9.5-3) consists of a large steel structure, varying in thickness from 4 to 8 in, with flow channels for cooling. There is a thin water region between the core and reflector, as shown in Figure 4.3-39—Typical Layout of the Reflector. This configuration minimizes the thermalization of neutrons leaving the core while reflecting more fast neutrons back into the core than is possible with standard reflector geometries.

The neutronic treatment of the heavy reflector is similar to that used for standard reflectors, in that transport theory calculations are performed to generate a set of equivalent reflector cross sections. The heavy reflector has seven different sectional geometries (see Figure 4.3-40—Reflector Geometry) which are represented by seven one-dimensional slab geometries in the neutronic model. In the model, fuel nodes are placed to the west of the reflector nodes, with reflective boundary conditions applied to the north, south and west boundaries, and a vacuum boundary condition applied to the east boundary. The flux solutions from the corresponding eigenvalue problems for these spectral geometries provide the heterogeneous reflector response matrix at the fuel-to-reflector interface.

The corresponding homogeneous (diffusion theory based) reflector response matrix at this interface is determined by solving for a number of consistent boundary value problems, so that the matrix elements depend analytically on the cross sections of the

homogeneous reflector node. The requirement that the heterogeneous and homogeneous response functions be equal sets up a series of non-linear equations for the equivalent cross sections. Solving this set of equations produces cross section libraries for the seven radial reflector node geometries.

Since no measured data exist for a core with a heavy reflector, the reflector cross sections generated as described above were qualified by comparing two-dimensional fresh core MCNP calculations to equivalent two-dimensional, two-group PRISM calculations. These comparisons include two first core loadings with moderator temperature variations from 68°F–644°F and boron concentrations variations from 0 ppm–1500 ppm. Details are provided in Reference 3.

#### 4.3.3.1.4 **MEDIAN Power Distribution Reconstruction Methodology**

During plant operation, a three-dimensional core power distribution is periodically derived from a combination of measured and calculated data. It is called the inferred power distribution to differentiate it from the specific measured and calculated data utilized by the reconstruction methodology. The aeroball system, described in Section 4.4.6, is the source of the measured data.

The analytical methodology described in the preceding subsections provides the calculated theoretical three-dimensional power, burnup and neutron flux distributions and detector signals. These calculations are based on a physical core model that is continuously updated online to account for the actual reactor operating parameters, such as thermal reactor power, control rod bank configurations, and coolant inlet temperature.

The inferred power distribution is generated by the PRISM module MEDIAN (measured dependent interpolation algorithm using NEM), which is a calculation module only used for reconstructing the inferred relative power distribution using the aeroball system measured data. Because it is a module in PRISM, it uses the PRISM-calculated theoretical solution. MEDIAN performs the following steps:

- Adapts the group-wise neutron fluxes at the measured nodes to achieve optimal consistency between theoretical results and measurements.
- Extrapolates the instrumented location group-wise fluxes to the non-instrumented locations using the nodal balance equation.

The three-dimensional inferred power distribution in the instrumented nodes includes the flux depression effect due to the presence of grid spacers, since the measured activation distributions include this effect. For the three-dimensional inferred power distributions in the non-instrumented nodes, the cross sections and coupling coefficients of the PRISM-calculated theoretical solution do not include this flux depression effect. In order to capture the flux depression effect due to the presence of

grid spacers, spacer grid form functions (SGFF) are applied to the axial power distributions in non-instrumented locations. The SGFF are generated using SCALE Version 4.4a. Details are provided in Reference 5.

#### **4.3.3.2 Validation**

The base analytical design methodology described in Section 4.3.3.1 uses a cross section generator code system and a reactor core simulator code (PRISM). In order to demonstrate the capability and accuracy of the analytical design methodology, data calculated using this methodology are compared to measured data obtained from critical experiments, reactor startup physics tests, and core-follow data obtained from commercial reactors. The validation criteria are based on the ANSI/ANS-19.6.1 standard (Reference 8).

##### **4.3.3.2.1 Critical Experiment Reactivity Measurements**

Critical experiment reactivity comparisons with calculated results from the cross section generation portion of the methodology are presented in Table 4.3-11—Critical Experiment Reactivity Measurements taken from Reactor Analysis Systems for PWRs, Volume 2—Benchmarking Results (Reference 9).

Examples of critical experiments for which data are available are the Strawbridge-Barry room temperature critical experiments (Reference 10), the KRITZ increased temperature critical experiments (Reference 11), and the Babcock and Wilcox room temperature critical experiments (Reference 12). The measured data from these experiments include reactivity for a variety of lattice configurations, enrichments, burnable absorber loadings, boron concentrations, and temperatures. Pin-by-pin fission rate distribution data are also available for various lattice configurations, enrichments, and burnable absorber loadings.

The calculations presented in Table 4.3-11 were performed by Studsvik using MICBURN-3/CASMO-3 with the Studsvik G-library. The current code system uses the Studsvik K-library modified to include self-shielding in the resonance region (4 eV–9118 eV) for the gadolinia isotopes Gd-155 through Gd-158. Use of the modified K-library would yield comparable results, thus satisfying the specified criterion.

##### **4.3.3.2.2 Validation with Commercial Reactor Measurements**

Reference 3 presents detailed benchmarking results using the following plant and fuel types:

- Westinghouse 157 assembly, 17x17 array (2 plants).
- Siemens KONVOI 193 assembly, 18x18 array (1 plant).
- Siemens KONVOI 177 assembly, 15x15 array (1 plant).

Tables 4.3-12—Summary of Startup Physics Test Measurements and 4.3-13—Summary of Core Follow Measurements, taken from Reference 3, summarize the startup physics and core follow benchmarks.

#### 4.3.3.2.3 Inferred Relative Power Distribution Uncertainties

Uncertainties associated with the inferred relative power distribution are provided in Section 4.3.2.2.7.

#### 4.3.3.2.4 NEMO Validation

The steady-state NEMO methodology has been benchmarked against the PRISM methodology for several proposed U.S. EPR core designs. Comparisons include calculations of  $F_{\Delta H}$ ,  $F_Q$ , control rod worth, ejected rod worth, and moderator temperature coefficient values. The two methodologies provide similar results, as presented in U.S. EPR Rod Ejection Accident Methodology Topical Report (Reference 13).

#### 4.3.4 Changes

The U.S. EPR is an evolutionary PWR with a rated thermal power of 4590 MW<sub>t</sub>. The nuclear design is similar to those of currently operating PWRs. There are, however, some changes from currently operating PWRs:

- Heavy reflector: The reactor vessel heavy reflector is a stainless steel structure and fills the space between the multi-cornered radial periphery of the reactor core and the cylindrical core barrel. The heavy reflector is described in Sections 4.3.2.1 and 4.3.3.1.3. The purpose of the heavy reflector is to reduce fast neutron leakage, reduce the neutron fluence on the reactor vessel, and flatten the power distribution. The heavy reflector affects the leakage of neutrons from the core, which reduces the fast fluence incident upon the vessel. Additionally since more neutrons are reflected back into the core, the efficiency of the core design is improved.
- Analytical methods: The analytical methods to be used with the U.S. EPR are presented in Reference 3. All of the methods described in this reference have previously been approved by the NRC.
- Aeroball measurement system (AMS): The aeroball detectors in the U.S. EPR are based on a pneumatic system that inserts vanadium-doped steel balls into the 40 detector locations in the core. The balls are inserted into all 40 locations at the same time and then, using the same pneumatic system, withdrawn and counted with scintillation detectors to determine the activation. The activation is proportional to the power, from which a detailed axial and radial power distribution can be inferred. The advantage of the aeroball measurement system is the reduced time required to take a core flux map, compared to other moveable incore detector systems. With the AMS, a flux map requires minutes rather than hours. The aeroball system is described in Section 4.4.6.

- Incore-based protection system: Part of the protection system in the U.S. EPR is based on a set of Co-59 self-powered neutron detectors (SPNDs). There are twelve SPND strings with six detectors per string situated to provide maximum coverage of the core. The SPNDs are described in Chapter 4.4.6. The advantage of the Co-59 SPNDs is their rapid response time and the three-dimensional representation they provide for monitoring DNB and LPD. The fixed incore detector and aeroball systems are described in Section 4.4.6.
- Annular control rods: The U.S. EPR uses a control rod design with an annular absorber. This design provides a lighter control rod with less absorber material, yet does not compromise the control rod design requirements. These lighter rods meet the rod drop time requirements and have sufficient worth so that sufficient shutdown margin exists when they are fully inserted. The control rods are described in Sections 4.2.1.6, 4.2.2.9, and 4.3.2.6.

### 4.3.5

#### References

1. BAW-10231P-A, Revision 1, "COPERNIC Fuel Rod Design Computer Code," FRAMATOME ANP, January 2004.
2. Letter, Ronnie L. Gardner (AREVA NP Inc.) to Document Control Desk (NRC), Request for Review and Approval of ANP-10285P, Revision 0, "U.S. EPR Fuel Assembly Mechanical Design Topical Report," NRC:07:051, October 2, 2007.
3. ANP-10263P-A, Revision 0, "Codes and Methods Applicability Report for the U.S. EPR," AREVA NP, Inc., August 2007.
4. BAW-10163P-A, "Core Operating Limit Methodology for Westinghouse-Designed PWRs," B&W Fuel Company, June 1989.
5. Letter, Ronnie L. Gardner (AREVA NP Inc.) to Document Control Desk, NRC, Request for Review and Approval of ANP-10287P, Revision 0, "Incore Trip Setpoint and Transient Methodology for U.S. EPR Topical Report," November 2007.
6. EMF-96-029(P)(A), "Reactor Analysis Systems for PWRs – Volume 1 - Methodology Description," Siemens Power Corporation, January 1997.
7. BAW-10221P-A, "NEMO-K – A Kinetics Solution in Nemo," FRAMATOME COGEMA FUELS, September 1998.
8. ANSI/ANS 19.6.1-2005, "Reload Startup Physics Tests for Pressurized Water Reactors," American Nuclear Society, 2005.
9. EMF-96-029(P)(A), "Reactor Analysis Systems for PWRs – Volume 2 - Benchmarking Results," Siemens Power Corporation, January 1997.
10. L. E. Strawbridge and R. F. Barry, "Criticality Calculations for Uniform Water-Moderated Lattices," Nuclear Science and Engineering, Vol. 23, pp. 58-73, 1965.

11. R. Persson, E. Blomsjo, and M. Edenius, "High-temperature critical experiments with H<sub>2</sub>O-moderated fuel assemblies in KRITZ," Technical Meeting No. 2/11, NUCLEX 72, 1972.
12. L. W. Newman, "Urania–Gadolinia: Nuclear Model Development and Critical Experiment Benchmark," BAW-1810, Babcock and Wilcox Company, DOE/ET/34212-41, April, 1984
13. Letter, Ronnie L. Gardner (AREVA NP Inc.) to Document Control Desk, NRC, Request for Review and Approval of ANP-10286P, Revision 0, "U.S. EPR Rod Ejection Accident Methodology Topical Report," November, 2007.

**Table 4.3-1—Core Design Criteria  
Sheet 1 of 3**

PARAMETER	DESIGN CRITERIA
<b>Coastdown Operation</b>	
$T_{AVG}$ Coast	
Reduction	Operation at 100% Power, 1°F ( $T_{AVG}$ ) per EFPD
Duration <sup>1</sup>	10°F reduction (10 EFPD)
Power Coast <sup>2</sup>	
Reduction	1.0% power per EFPD
Duration	35.7 days
Duration	30.02 EFPD
Total Coast	
Duration	45.7 days
Duration	40.0 EFPD
<b>Cycle Energies</b>	
Cycle Length	547.5 days <sup>3</sup>
Nominal CF	100.0%
Lower window CF	92.0%
EOFPC	547.5 EFPD
EOFPC	10.0 ppm
Coastdown	40.0 EFPD
EOC	
Lower window	503.7 EFPD
Nominal	547.5 EFPD
Upper window	587.5 EFPD
<b>Bundle Design Requirements</b>	
Max Gd rods per bundle	28
Gd <sub>2</sub> O <sub>3</sub> concentration	2, 4, 6, or 8 wt% Gd <sub>2</sub> O <sub>3</sub>
<b>Bundle Design Flexibility</b>	Radially symmetric enrichment variations allowed
<b>Gd<sub>2</sub>O<sub>3</sub> Pin Placement Flexibility</b>	1. None adjacent to an instrument tube.
	2. None adjacent to other Gd <sub>2</sub> O <sub>3</sub> rods.
	3. None on the assembly edge.
	4. Minimize the number adjacent to a guide tube.
	5. No asymmetric loading of Gd <sub>2</sub> O <sub>3</sub> rods radially within an assembly.

**Table 4.3-1—Core Design Criteria  
Sheet 2 of 3**

PARAMETER			DESIGN CRITERIA		
<b>Control Rods</b>			Absorber composed of annular slugs consisting of silver (80%), indium (15%), and cadmium (5%).		
<b>Power Independent Insertion Limits (PDIL)</b>			See Figure 4.3-2		
HFP					
HZP					
<b>Depletion Requirements</b>			Design depletions are done with ARO		
<b>Operating Conditions</b>					
Rated thermal power			4590 MW		
Coolant average temperature (linear behavior between defined points)			Power (%)	T <sub>AVG</sub> (°F)	T <sub>IN</sub> (°F)
			0	578	578
			25	587	579
			35	587	576
			60	594	575
			100	594	563
			120	594	558
Bypass flow			3.64%		
Core flow			498,936 gpm		
System pressure			2250 psia		
<b>Peak Pin Exposure</b>			62.0 GWD/MTU for UO <sub>2</sub> rods		
			55.0 GWD/MTU for Gd <sub>2</sub> O <sub>3</sub> rods		
<b>F<sub>ΔH</sub> Limit for LOCA</b>					
TS limit (HFP)			1.70 at 100% power		
<b>F<sub>Q</sub> Limits for LOCA</b>					
TS limit			2.6		
<b>Boron Bias/k<sub>eff</sub> Target</b>			Target k <sub>eff</sub> of 1.0 without bias, based on benchmark results of other units		
<b>Moderator Temperature Coefficient</b>					
			TS Limit (pcm/°F)		
BOC	HZP	ARO	≤5		
BOC	50%P	ARO	≤0		
BOC	HFP	ARO	≤0		
EOFP	HFP	ARO	≥-50		
EOC	~80%P	ARO	≥-50		



**Table 4.3-1—Core Design Criteria  
Sheet 3 of 3**

PARAMETER	DESIGN CRITERIA
<b>Shutdown Margin, Modes 1 &amp; 2</b>	3000 pcm (Note: shutdown margin calculation should be made at BOC, EOC, and most reactive point in cycle)
<b>Refueling Boron Concentration</b>  Maintains 5% shutdown with ARI-MRR	2400 ppm (natural B <sup>10</sup> abundance)
<b>Modes States Table</b>	See Table 4.3-2
<b>Minimum Temperature for Criticality</b>	568°F
<b>Minimum RCS Temperature</b>	38°F

**Notes:**

1. A temperature of 10°F is considered a maximum T<sub>AVG</sub> coast for licensing purposes and does not include uncertainties or potential hardware (e.g., turbine) limitations that may further limit a T<sub>AVG</sub> reduction.
2. Power coast duration is selected such that a final power level of 70% is reached.
3. Refueling outage is not considered in determining the design cycle energy.

Table 4.3-2—Plant Operating Modes

MODE	TITLE	REACTIVITY CONDITION ( $k_{eff}$ )	RATED THERMAL POWER <sup>1</sup>	REACTOR COOLANT TEMPERATURE
1	Power Operation	$\geq 0.99$	$> 5\%$	NA
2	Startup	$\geq 0.99$	$\leq 5\%$	NA
3	Hot Standby	$< 0.99$	NA	$\geq 350^{\circ}\text{F}$
4	Hot Shutdown <sup>2</sup>	$< 0.99$	NA	$350^{\circ}\text{F} > T_{avg} > 200^{\circ}\text{F}$
5	Cold Shutdown <sup>2</sup>	$< 0.99$	NA	$\leq 200^{\circ}\text{F}$
6	Refueling <sup>3</sup>	NA	NA	NA

**Notes:**

1. Excluding decay heat. For nuclear design, minimum shutdown margin is 3000 pcm for Mode 2 through 5, and 5000 pcm for Mode 6.
2. All reactor vessel head closure bolts fully tensioned. For nuclear design, all control rods in, minus the most reactive RCCA.
3. One or more reactor vessel head closure bolts less than fully tensioned.

**Table 4.3-3—Reactor Core Description  
Sheet 1 of 2**

<b>Active Core</b>	
<b>Equivalent Diameter</b>	148.3 in
<b>Active Fuel Height First Core (cold)</b>	165.354 in
<b>Height-to-Diameter Ratio</b>	1.115
<b>Total Cross Section Area</b>	119.95 ft <sup>2</sup>
<b>H<sub>2</sub>O/U Molecular Ratio, Lattice (cold)</b>	2.78
<b>Reflector Thickness and Composition used in Neutronic Design</b>	
Top – water plus steel	11.81 in
Bottom – water plus steel	11.81 in
Side – water plus steel	~4 in minimum; ~8 in maximum
<b>Fuel Assemblies</b>	
Number	241
Rod array	17X17
Rods per assembly	265
Rod pitch	0.496 in
Overall transverse dimensions	8.426 x 8.426 in
Nominal fuel weight (per assembly)	536.086 kg U
M5 weight in core	75,447 lb
Number of grids per assembly	10
Composition of grids	Alloy 718 (top and bottom grids) M5 (intermediate mixing grids)
Diameter of guide thimbles Upper region above dashpot	0.451 in ID 0.490 in OD
Diameter of guide thimbles Lower (dashpot) region	0.397 in ID 0.490 in OD
<b>Fuel Rods</b>	
Number	63,865
Outside diameter	0.3740 in
Diametral gap $[(ID_{cladding} - OD_{pellet}) / 2]$	0.0033 in
Cladding thickness	0.0225 in
Cladding material	M5

**Table 4.3-3—Reactor Core Description  
Sheet 2 of 2**

<b>Active Core</b>	
<b>Fuel Pellets</b>	
Material	UO <sub>2</sub> (sintered)
Diameter	0.3225 in
Length	0.531 in (enriched UO <sub>2</sub> )
	0.531 in (UO <sub>2</sub> +Gd <sub>2</sub> O <sub>3</sub> )
	0.531 in (blanket UO <sub>2</sub> )
<b>Mass of UO<sub>2</sub> per foot of fuel rod</b>	0.324 lb/ft

**Table 4.3-4—Fuel Assembly Summary**

<b>Fuel Assembly Type</b>	<b>Number of Assemblies</b>	<b>Average Enrichment wt % <sup>235</sup>U</b>	<b>Density</b>	<b>For Detailed Fuel Assembly Design, See Listed Figure.</b>
A1	64	2.23	96%	See Figure 4.3-6. Fuel stack height (cold) is 165.354 in.
A2	12	2.23	96%	
B1	32	2.62	96%	See Figure 4.3-7. Fuel stack height (cold) is 165.354 in.
B2	56	2.61	96%	
C1	24	3.14	96%	See Figure 4.3-8. Fuel stack height (cold) is 165.354 in.
C2	21	3.13	96%	
C3	32	3.12	96%	

**Table 4.3-5—Nuclear Design Parameters (First Cycle)**  
Sheet 1 of 2

<b>Core Average Linear Power (includes gamma energy deposition)</b>	5.22 kW/ft	
<b>Total Heat Flux Hot Channel Factor, <math>F_Q</math></b>	2.60	
<b>Nuclear Enthalpy Rise Hot Channel Factor, <math>F_{\Delta H}^N</math></b>	1.70	
<b>Reactivity Coefficients</b>		
Doppler-only power coefficient (upper limit) <sup>1</sup>	-19.3 to -10.9 pcm/%power	
Doppler-only power coefficient (lower limit) <sup>1</sup>	-8.8 to -7.9 pcm/%power	
Doppler temperature coefficient <sup>1</sup>	-1.8 to -1.3 pcm/°F	
Moderator temperature coefficient <sup>1</sup>	-33.4 to 2.9 pcm/°F	
Boron coefficient <sup>1</sup>	-9.5 to -7.9 pcm/ppm	
<b>Delayed Neutron Fraction and Lifetime</b>		
$\beta_{\text{eff}}$ , BOL	0.0074	
$\beta_{\text{eff}}$ , EOL	0.0052	
$l'$ , BOL ( $\mu\text{s}$ )	21.75	
$l'$ , EOL ( $\mu\text{s}$ )	23.22	
<b>Control Rods</b>		
Rod requirements	See Tables 4.3-1, 4.3-6, and 4.3-7	
Maximum ejected rod worth	See Section 15.4	
<b>Bank Worth, HZP no overlap<sup>1</sup></b>	BOL pcm	EOL pcm
Control Bank D	816	1083
Control Bank C	1063	1000
Control Bank B	1138	1283
Control Bank A	578	573
Shutdown Bank A	2089	1997
Shutdown Bank B	919	1214
Shutdown Bank C	1026	1216
<b>Boron Concentrations (natural boron)</b>		
Zero power, $k_{\text{eff}} = 0.99$ , cold <sup>2</sup> , RCCAs out	1593 ppm	
Zero power, $k_{\text{eff}} = 0.99$ , hot <sup>3</sup> , RCCAs out	1600 ppm	
Design basis refueling boron concentration	2400 ppm	
Zero power, $k_{\text{eff}} = 0.95$ , cold <sup>2</sup> , RCCAs in	1215 ppm	

**Table 4.3-5—Nuclear Design Parameters (First Cycle)  
Sheet 2 of 2**

Zero power, $k_{\text{eff}}=1.00$ , hot <sup>3</sup> , RCCAs out	1485 ppm
Full power, $k_{\text{eff}}=1.00$ , hot <sup>3</sup> , RCCAs out, no xenon	1383 ppm
Full power, $k_{\text{eff}}=1.00$ , hot <sup>3</sup> , RCCAs out, equilibrium xenon	1069 ppm
Reduction with fuel burnup <sup>4</sup>	-100 ppm/(GWD/ MTU)

**Notes:**

1.  $1 \text{ pcm} = 10^{-5} \Delta\rho$ , Where  $\Delta\rho$  is calculated from two statepoint values of  $k_{\text{eff}}$  by  $(k_2 - k_1)/(k_2 \times k_1)$ .
2. Cold is defined as 38°F, 1 atm.
3. Hot is defined as  $T_{\text{in}} = 578^\circ\text{F}$  (zero power) and  $T_{\text{in}} = 563.42^\circ\text{F}$  (full power), 2250 psia.
4. Use of Gd alters slope of boron letdown requirements. Reported value is representative of MOL to EOL.

**Table 4.3-6—Reactivity Requirements for Rod Cluster Control Assemblies  
(First Cycle)**

<b>Reactivity Effects</b>		
<b>1. Estimated RCCA Worth (89 rods)</b>	BOL	EOL
a All RCCAs inserted	10,942 pcm	11,697 pcm
b Most reactive RCCA	2425 pcm	1756 pcm
c At power dependent insertion limit	162 pcm	346 pcm
d Total available RCCA worth, with adjustment to accommodate uncertainties (0.90 x (item a - item b - item c))	7520 pcm	8636 pcm
<b>2. Control Requirements</b>		
a Total power defect	991 pcm	1822 pcm
b Axial flux redistribution	174 pcm	284 pcm
c Coolant void effects	50 pcm	50 pcm
d Total positive reactivity insertion	1215 pcm	2156 pcm
<b>3. Shutdown Margin Available (item 1d - item 2d)</b>	6305 pcm	6480 pcm
<b>4. Required Shutdown Margin</b>	3000 pcm	3000 pcm
<b>5. Excess Shutdown Margin</b>	3305 pcm	3480 pcm



**Table 4.3-7—RCCA and Integral Burnable Absorber Description**

<b>Rod Cluster Control Assembly</b>	
Neutron absorber	Ag-In-Cd
Absorber ID	0.174 in
Absorber OD	0.341 in
Density	10.17 g/cm <sup>3</sup>
Cladding material	ANSI 316L cold worked
Cladding thickness	0.0185 in
Number of clusters, full length	89
Number of absorber rods per cluster	24
<b>Integral Burnable Absorber Rods (First Core)</b>	
Number	2284
Material	Gadolinia (Gd <sub>2</sub> O <sub>3</sub> ) integral to fuel
Pellet diameter	0.3225 in
Pellet length	0.531 in
Cladding outside diameter	0.3740 in
Diametral gap	0.0033 in
Cladding thickness	0.0225 in
Cladding material	M5
Poison loading	2, 4, 6, and 8 wt % Gd <sub>2</sub> O <sub>3</sub> (see Figures 4.3-6 thru 4.3-9 for loading)

**Table 4.3-8—Typical Neutron Flux Levels in the Reactor Core and Reactor Pressure Vessel**

<b>Location</b>	<b>Total<sup>1</sup></b>	<b>E ≥ 1.0 MeV<sup>1</sup></b>	<b>E ≥ 0.1 MeV<sup>1</sup></b>	<b>E ≤ 0.414 eV<sup>1</sup></b>
Core center	4.43x10 <sup>14</sup>	1.11x10 <sup>14</sup>	2.34x10 <sup>14</sup>	3.84x10 <sup>13</sup>
Core outer radius at mid-height	4.96x10 <sup>13</sup>	6.03x10 <sup>12</sup>	2.54x10 <sup>13</sup>	7.36x10 <sup>11</sup>
Core top	3.33x10 <sup>13</sup>	6.10x10 <sup>12</sup>	1.32x10 <sup>13</sup>	6.88x10 <sup>12</sup>
Core bottom	8.91x10 <sup>13</sup>	1.85x10 <sup>13</sup>	3.86x10 <sup>13</sup>	1.76x10 <sup>13</sup>
Pressure vessel wetted ID azimuthal peak	7.64x10 <sup>10</sup>	7.74x10 <sup>9</sup>	1.89x10 <sup>10</sup>	3.92x10 <sup>10</sup>

**Notes:**

1. All values have units of n/cm<sup>2</sup>-sec.

**Table 4.3-9—Cross Section Generation Methodology**

<b>Nuclear Data Library or Computer Code</b>	<b>Description</b>	<b>Additional Information</b>
Studsvik 40 energy group (10 group gamma) nuclear data library	This data library (denoted K) is condensed from the Studsvik 70 energy group library. The data in this library primarily consist of ENDF/B-4 data.	Reference 3
CASLIB	Reformats the library data as needed for MICBURN-3 and CASMO-3	Reference 3
MICBURN-3	Calculates microscopic burnup in burnable absorber rods (in particular for gadolinia-bearing fuel rods) and generates the burnable absorber cross section data required by CASMO-3	Reference 3
CASMO-3	Performs fuel assembly calculations and generates the cross section data required by the reactor core simulator methodology	Reference 3

**Table 4.3-10—Reactor Core Simulator Methodology**

<b>Computer Code</b>	<b>Description</b>	<b>Additional Information</b>
PRISM	Performs reactor core calculations	Reference 3
NEMO-K	Performs reactor core kinetics calculations (rod ejection analyses)	Reference 7

**Table 4.3-11—Critical Experiment Reactivity Measurements**

Description	Results	Criteria	Comments
Number of critical experiment $k_{eff}$ calculations	37	$\geq 25$	All 37 calculations performed by Studsvik using the 70 energy group Studsvik library
Range of the $k_{eff}$ mean plus or minus one standard deviation	0.99932–1.00146	Must be within the range 0.98 to 1.02	$k_{eff}$ calculated as 1.00039 $\pm$ 0.00107
Calculations include a variety of lattice configurations, enrichments, burnable absorber loadings, and boron concentrations	No significant trends observed	No significant trends	

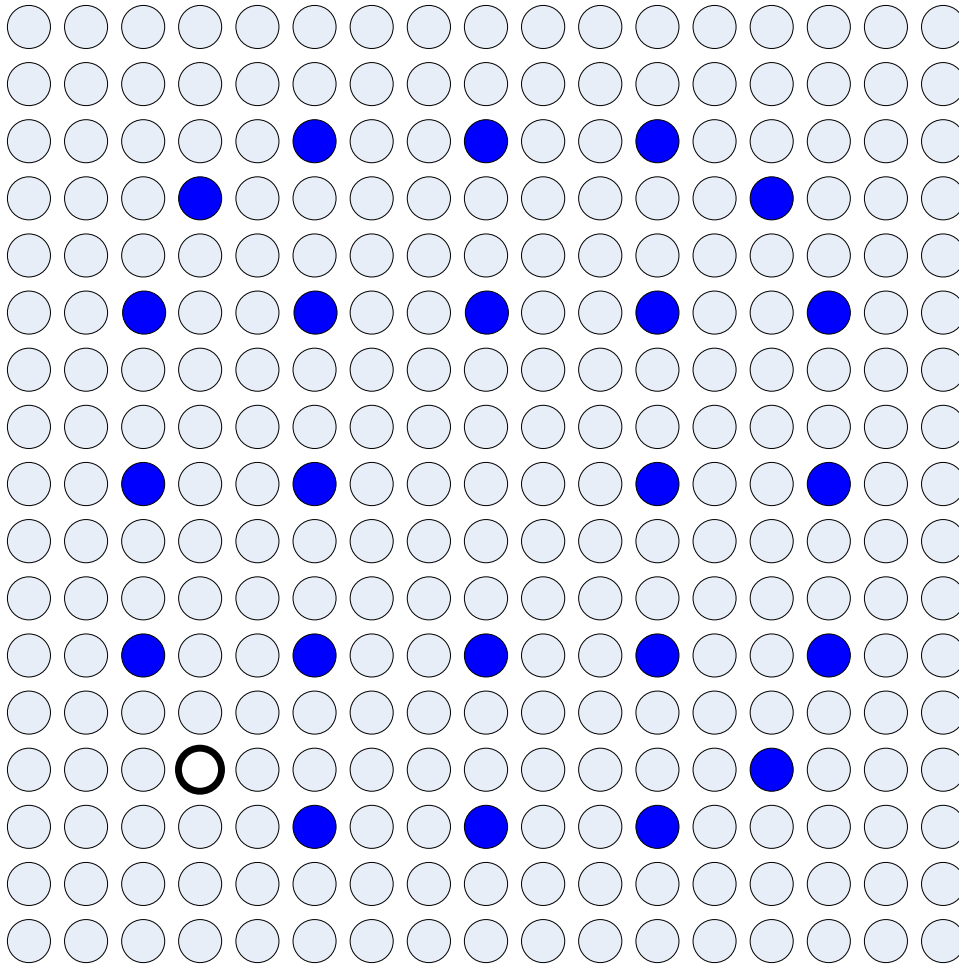
**Table 4.3-12—Summary of Startup Physics Test Measurements**

<b>Description</b>	<b>Results</b>	<b>Criteria</b>	<b>Comments</b>
Plant/fuel types	4	>3	Plants A, B, G1 and G2
Number of Westinghouse plant types	2	>1	Plants A and B
Number of Siemens - KONVOI plant types	2	>1	Plants G1 and G2
Number of evaluated cycles per plant type	14 cycles for 2 Westinghouse reactors with 157 assemblies, 5 cycles for Siemens - KONVOI reactor with 193 assemblies, 5 cycles for Siemens reactor with 177 assemblies	>3	13 cycles for Plant A 1 cycle for Plant B 5 cycles for Plant G2 5 cycles for Plant G1
Total number of evaluated cycles	24	>9	
ARO HZP critical boron concentrations	Maximum absolute difference: 48 ppm	Maximum absolute difference <50 ppm	
Individual HZP Control Bank Worth	Maximum absolute difference: 12.06%	Maximum absolute difference <15% or 100 pcm, whichever is larger	
Total HZP control Bank worth	Maximum absolute difference: 8.49%	Maximum absolute difference <10%	
ARO HZP isothermal temperature Coefficient	Maximum absolute difference: 0.990 pcm/°F	Maximum absolute difference <2.0 pcm/°F	

**Table 4.3-13—Summary of Core Follow Measurements**

Description	Results	Criteria	Comments
Plant/fuel types	4	>3	Plants A, B, G1, and G2
Number of Westinghouse plant types	2	>1	Plants A and B
Number of Siemens - KONVOI plant types	2	>1	Plants G1 and G2
Number of evaluated cycles per plant type	13 cycles for 2 Westinghouse reactors with 157 assemblies, 5 cycles for Siemens - KONVOI reactor with 193 assemblies, 5 cycles for Siemens reactor with 177 assemblies	>3	12 cycles for Plant A 1 cycles for Plant B 5 cycles for Plant G2 5 cycles for Plant G1
Total number of evaluated cycles	23	>9	
HFP critical boron concentrations	Minimum of one measured datum point per 30 EFPD for U.S. plants; as available for European plants	Minimum of one measured datum point per 30 EFPD	
	Maximum absolute difference between trend of measured data and calculated data < 50 ppm	Maximum absolute difference <50 ppm	
Assembly average power distributions	Maximum RMS difference: 0.027	RMS difference <0.05	$RMS = \sqrt{\frac{\sum_{i=1}^N (\Delta X)_i^2}{N}}$
Core average axial power distributions	Maximum RMS difference: 0.047	RMS difference <0.05	

**Figure 4.3-1—Cross Section of the U.S. EPR High Thermal Performance Fuel Assembly**



Rod Type	# of Rods	Rod Description
	265	Fuel Rod
	23	Guide Tube
	1	Guide Tube – This tube represents the four symmetric locations in the assembly that may contain incore instrumentation. There is a maximum of two instrumentation guide tubes per assembly.

EPR2125 T2

Figure 4.3-2—U.S. EPR Rod Group Insertion Limits Versus Thermal Power

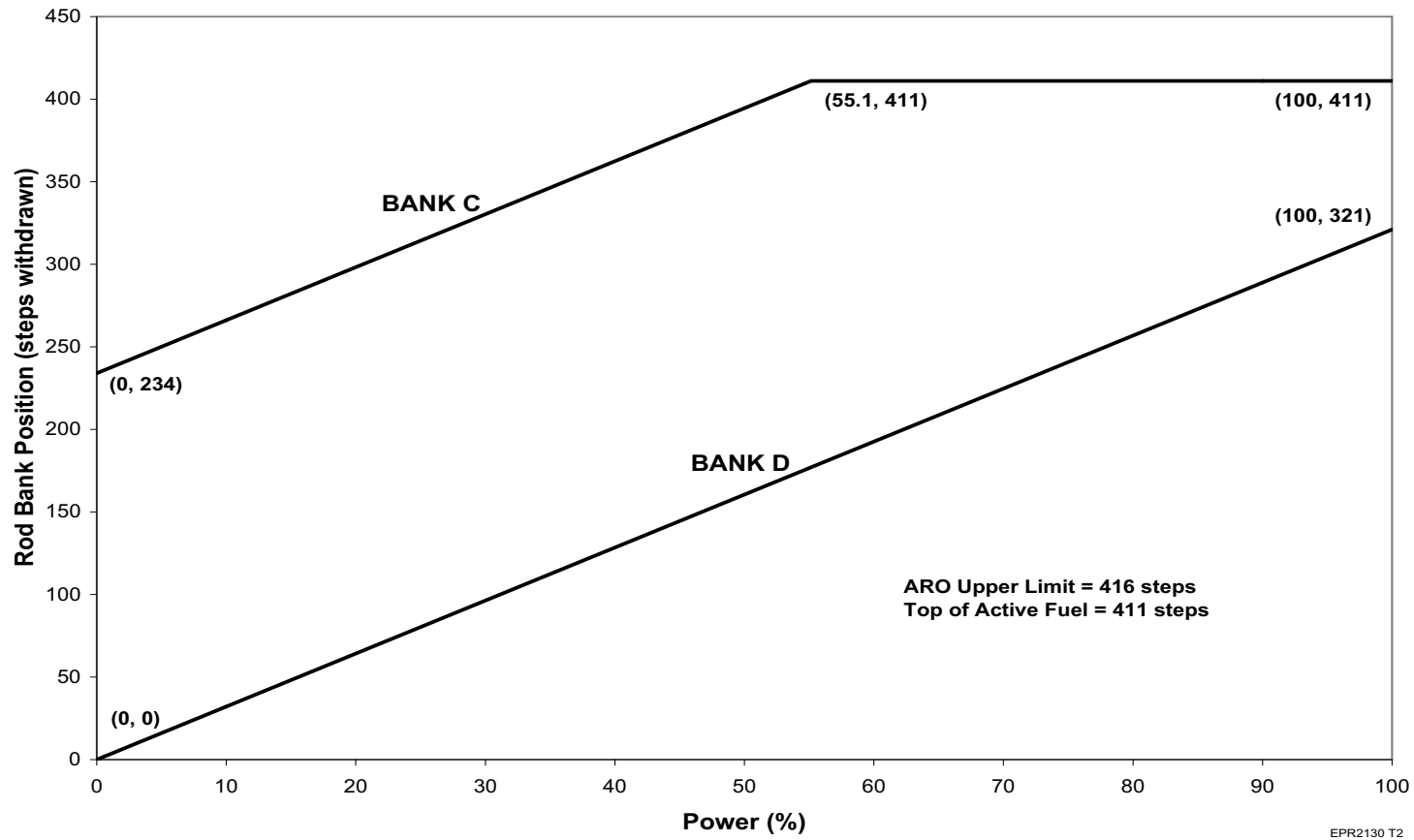
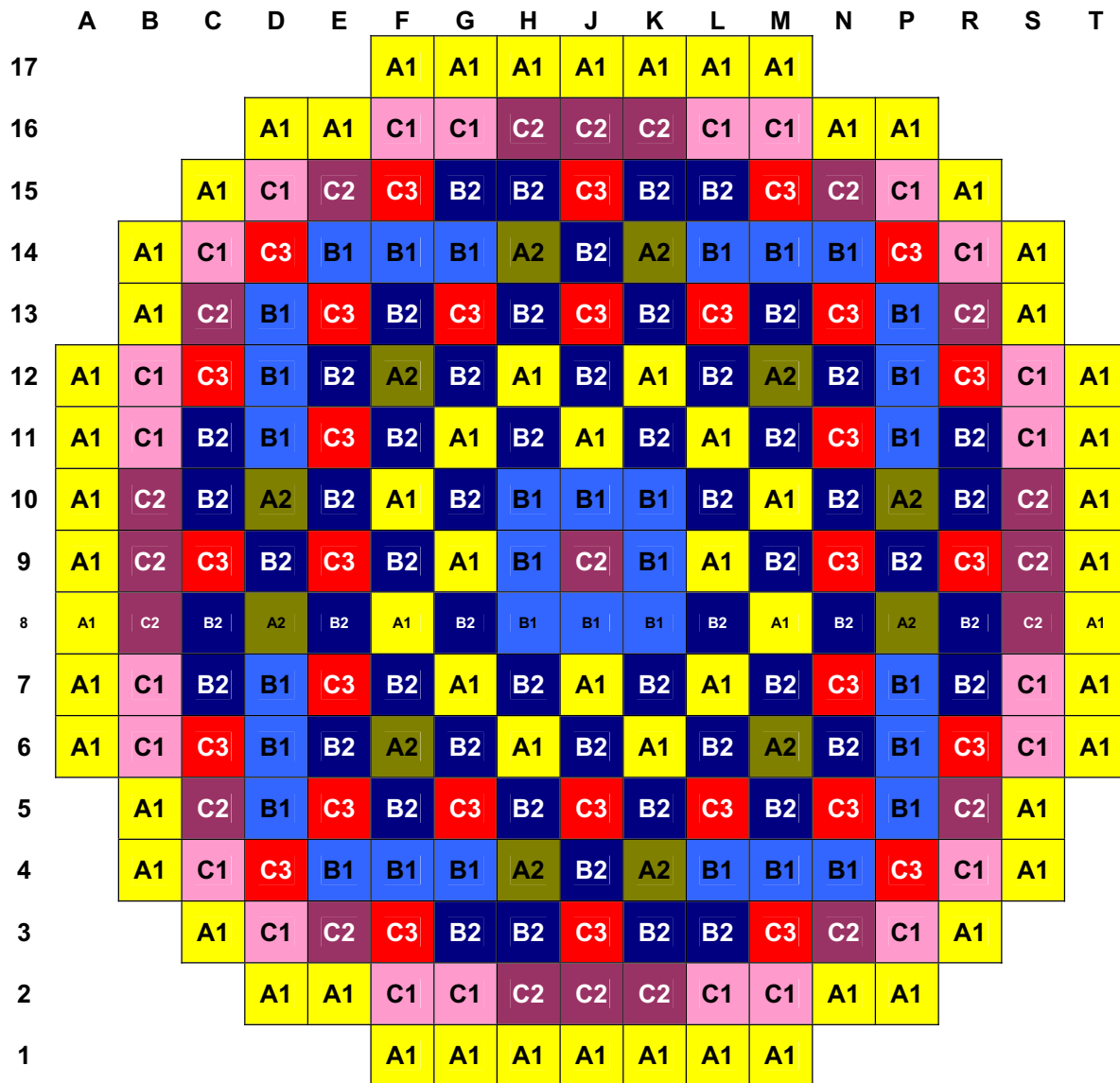




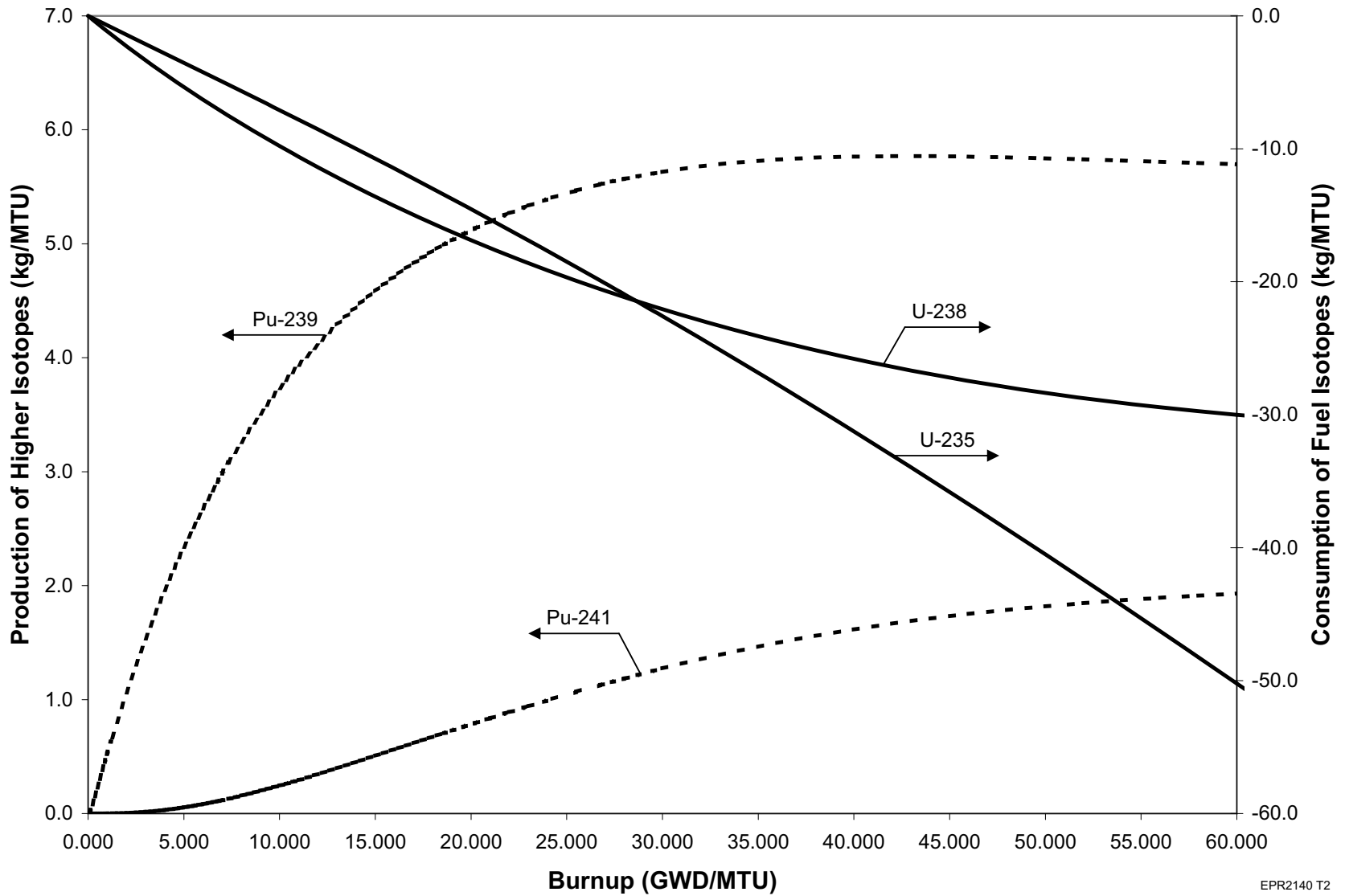
Figure 4.3-3—Typical Initial Core Loading Map



Fuel Type	Description
A1	2.25 wt% central zone enrichment (CZE) with no gadolinia
A2	2.25 wt% CZE with 4 rods at 4 wt% gadolinia
B1	2.70 wt% CZE with 8 rods at 8 wt% and 4 rods at 4 wt% gadolinia
B2	2.70 wt% CZE with 12 rods at 8 wt% and 4 rods at 2 wt% gadolinia
C1	3.25 wt% CZE with 4 rods at 6 wt% and 4 rods at 2 wt% gadolinia
C2	3.25 wt% CZE with 8 rods at 6 wt% and 4 rods at 2 wt% gadolinia
C3	3.25 wt% CZE with 12 rods at 8 wt% and 4 rods at 2 wt% gadolinia

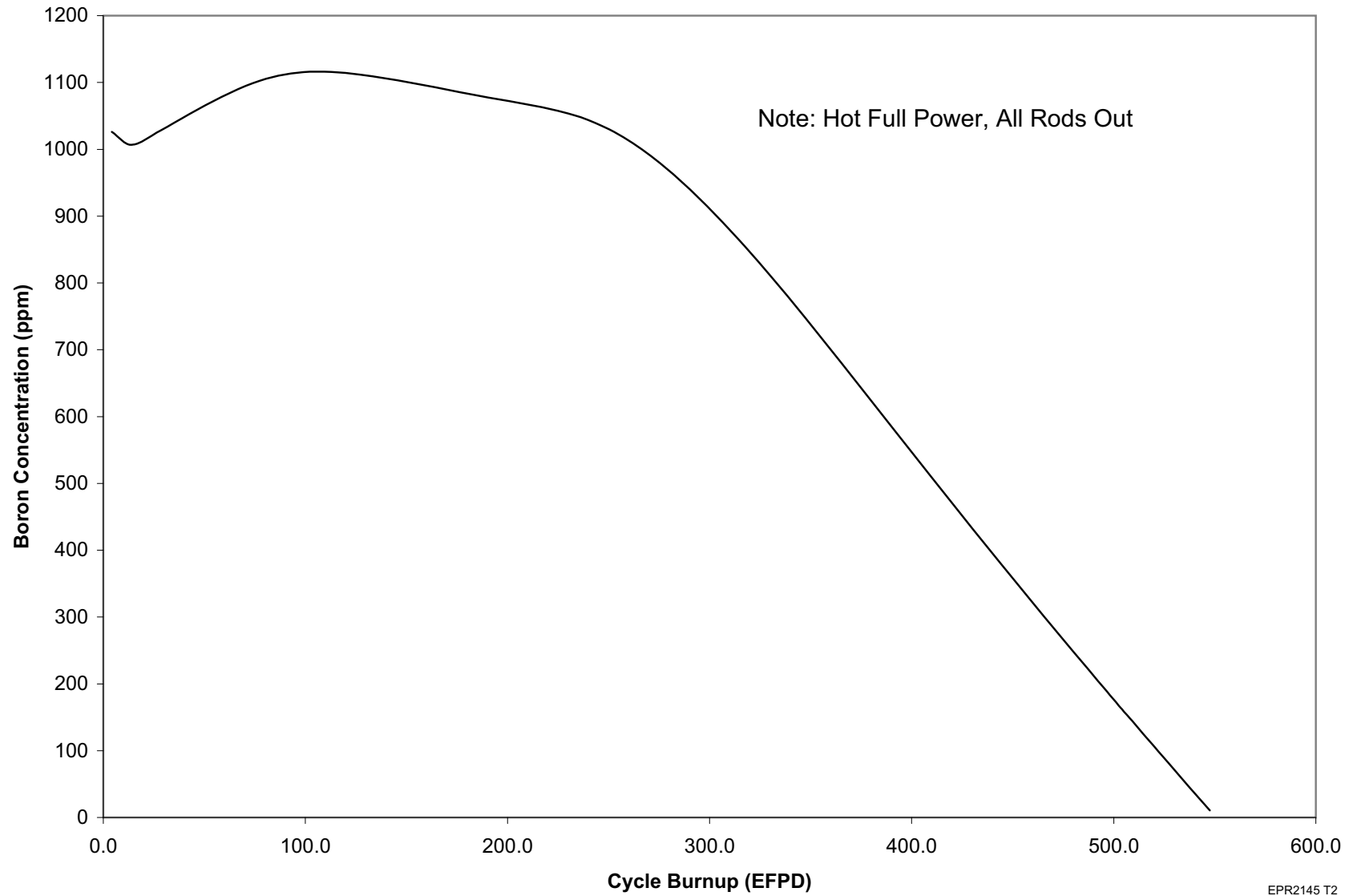
EPR2135 T2

Figure 4.3-4—Uranium Consumption and Plutonium Production Versus Burnup



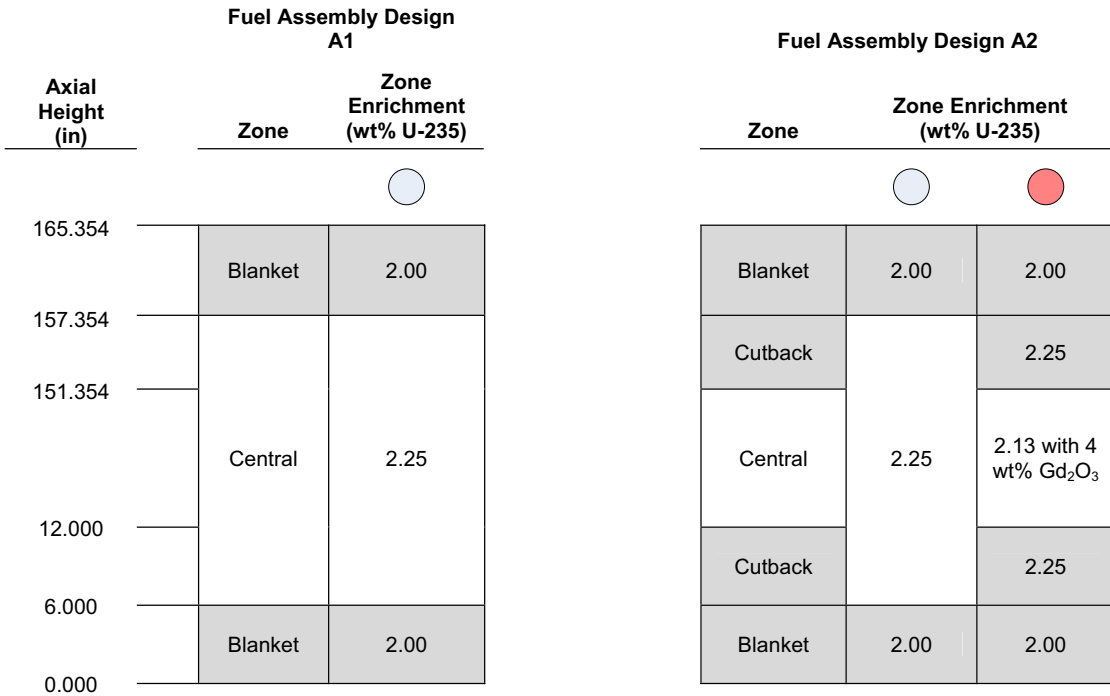
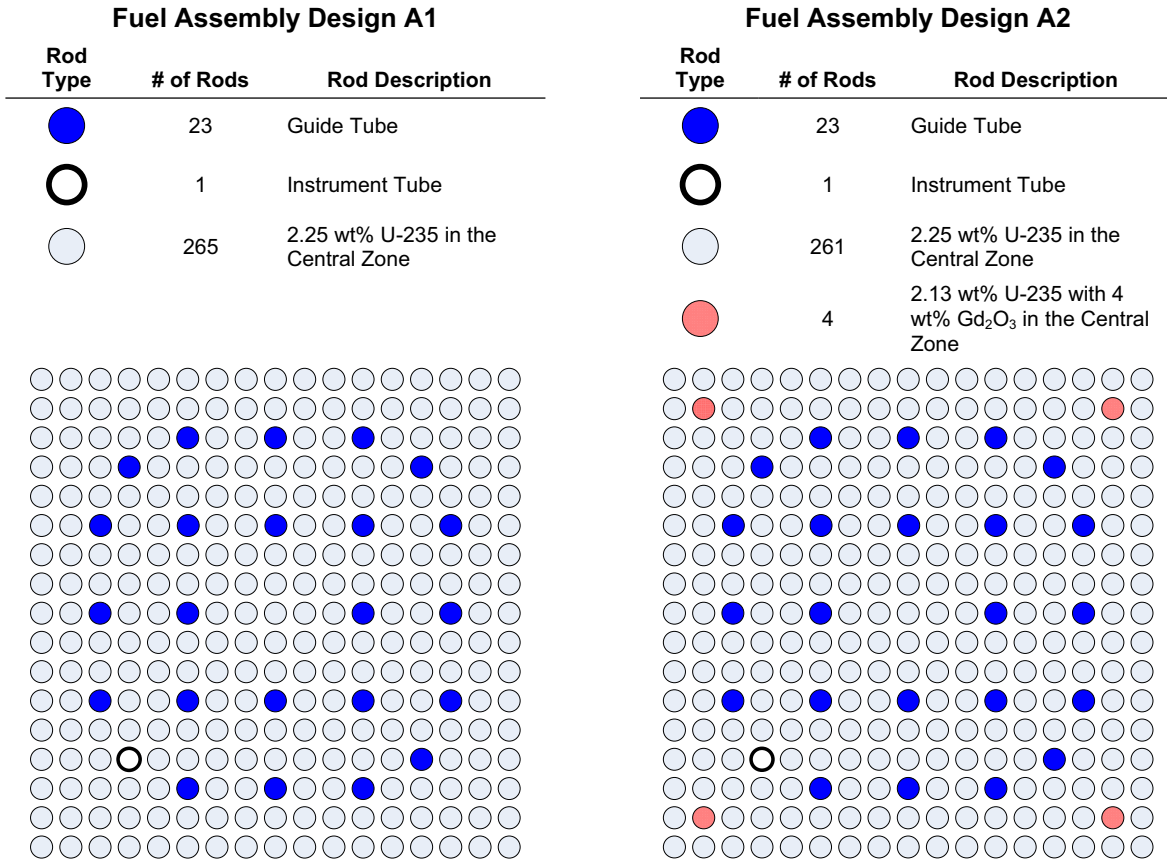
EPR2140 T2

Figure 4.3-5—Boron Concentration Versus Burnup for a First Core



EPR2145 T2

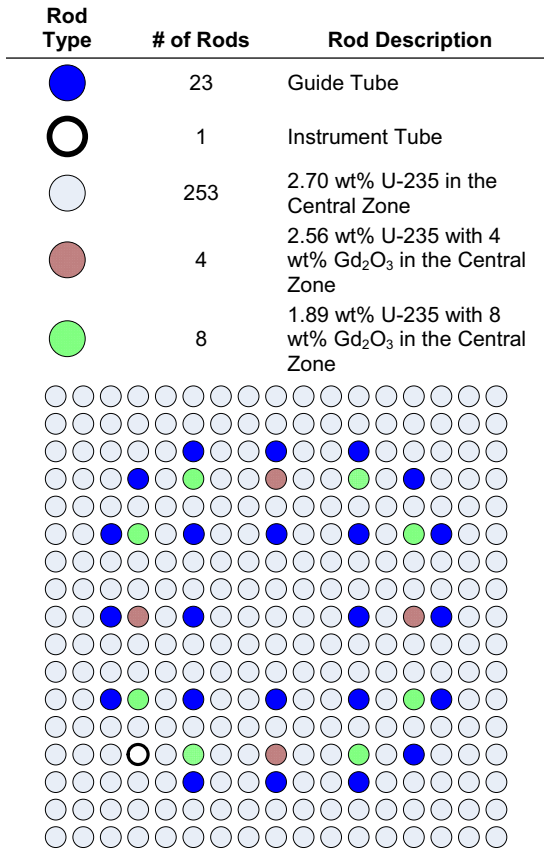
Figure 4.3-6—Fuel Assembly Designs A1 and A2



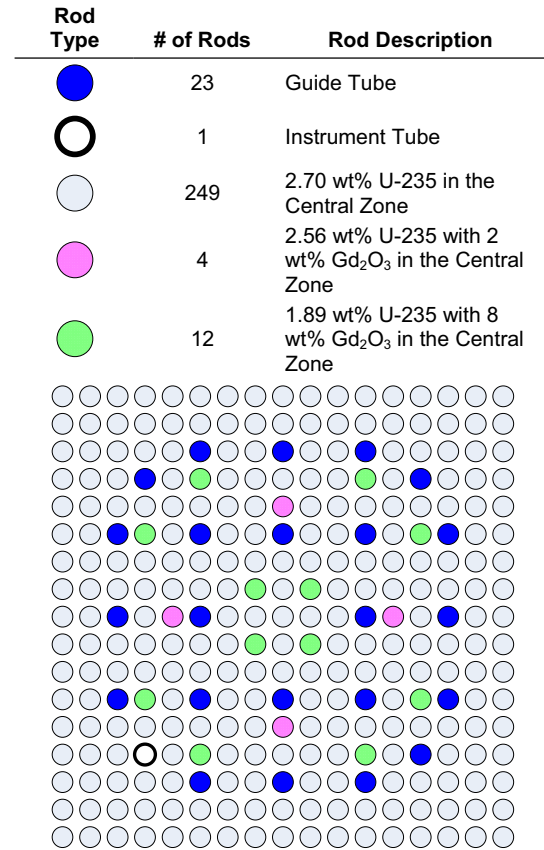
EPR2150 T2

Figure 4.3-7— Fuel Assembly Designs B1 and B2

Fuel Assembly Design B1



Fuel Assembly Design B2



Fuel Assembly Design B1

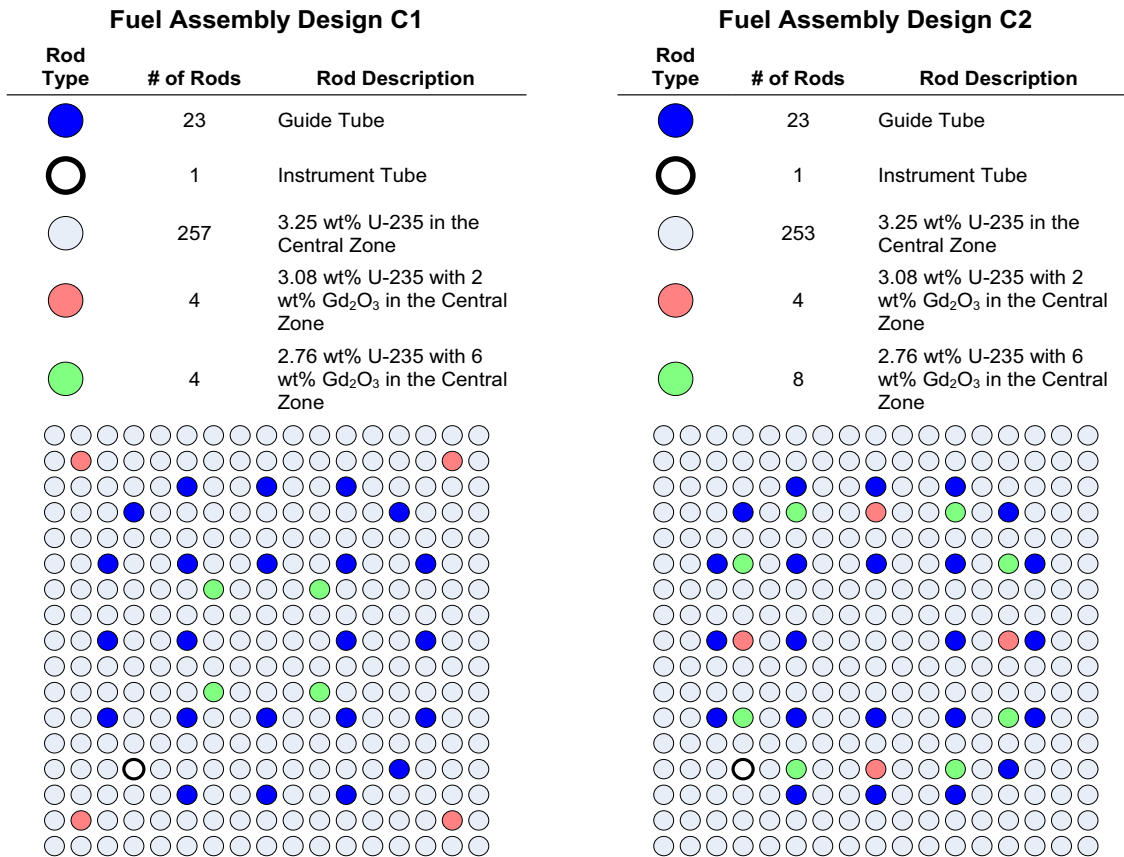
Axial Height (in)	Zone	Zone Enrichment (wt% U-235)		
165.354	Blanket	2.00	2.00	2.00
157.354	Cutback		2.70	2.70
151.354	Central	2.70	1.89 with 8 wt% Gd <sub>2</sub> O <sub>3</sub>	2.56 with 4 wt% Gd <sub>2</sub> O <sub>3</sub>
12.000	Cutback		2.70	2.70
6.000	Blanket	2.00	2.00	2.00
0.000				

Fuel Assembly Design B2

Axial Height (in)	Zone	Zone Enrichment (wt% U-235)		
165.354	Blanket	2.00	2.00	2.00
157.354	Cutback		2.70	2.70
151.354	Central	2.70	1.89 with 8 wt% Gd <sub>2</sub> O <sub>3</sub>	2.56 with 2 wt% Gd <sub>2</sub> O <sub>3</sub>
12.000	Cutback		2.70	2.70
6.000	Blanket	2.00	2.00	2.00
0.000				

EPR2155 T2

Figure 4.3-8— Fuel Assembly Designs C1 and C2



### Fuel Assembly Design C1

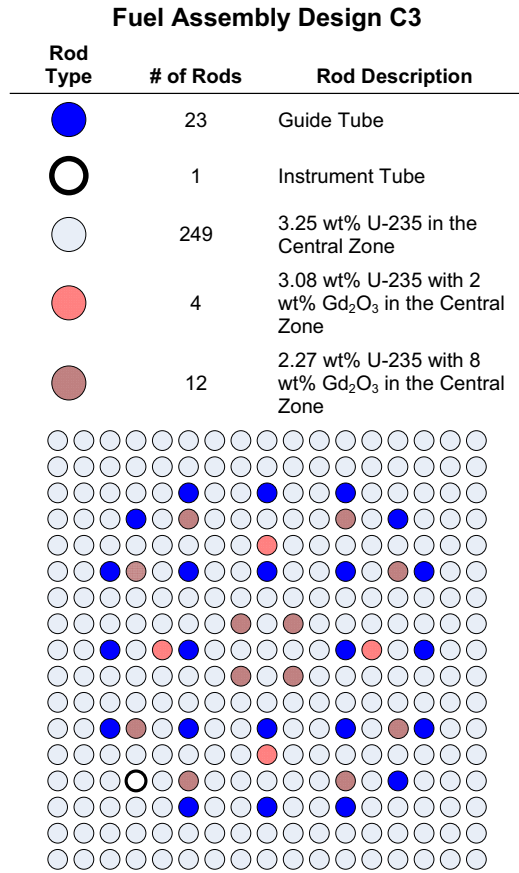
Axial Height (in)	Zone	Zone Enrichment (wt% U-235)		
165.354	Blanket	2.00	2.00	2.00
157.354	Cutback		3.25	3.25
151.354	Central	3.25	2.76 with 6 wt% Gd <sub>2</sub> O <sub>3</sub>	3.08 with 2 wt% Gd <sub>2</sub> O <sub>3</sub>
12.000	Cutback		3.25	3.25
6.000	Blanket	2.00	2.00	2.00
0.000				

### Fuel Assembly Design C2




Axial Height (in)	Zone	Zone Enrichment (wt% U-235)		
165.354	Blanket	2.00	2.00	2.00
157.354	Cutback		3.25	3.25
151.354	Central	3.25	2.76 with 6 wt% Gd <sub>2</sub> O <sub>3</sub>	3.08 with 2 wt% Gd <sub>2</sub> O <sub>3</sub>
12.000	Cutback		3.25	3.25
6.000	Blanket	2.00	2.00	2.00
0.000				

EPR2160 T2

**Figure 4.3-9—Fuel Assembly Design C3**



**Fuel Assembly Design C3**

Axial Height (in)	Zone	Zone Enrichment (wt% U-235)		
				
165.354	Blanket	2.00	2.00	2.00
157.354	Cutback	3.25	3.25	3.25
151.354	Central		2.27 with 8 wt% Gd <sub>2</sub> O <sub>3</sub>	3.08 with 2 wt% Gd <sub>2</sub> O <sub>3</sub>
12.000	Cutback		3.25	3.25
6.000	Blanket	2.00	2.00	2.00
0.000				

EPR2165 T2

**Figure 4.3-10—Quarter Core Relative Assembly Radial Power Distribution  
(HFP at BOL, ARO, No Xenon)**

	J	K	L	M	N	P	R	S	T
9	1.244	1.111	1.156	1.038	1.066	0.965	1.105	1.172	0.770
8	1.111	1.081	1.051	1.120	0.980	1.046	1.003	1.176	0.768
7	1.156	1.051	1.124	1.003	1.055	1.014	1.012	1.251	0.741
6	1.038	1.120	1.003	1.041	0.955	1.030	1.135	1.159	0.578
5	1.066	0.980	1.055	0.955	1.075	1.063	1.168	0.809	
4	0.965	1.046	1.014	1.030	1.063	1.117	1.085	0.552	
3	1.105	1.003	1.012	1.135	1.168	1.085	0.615		
2	1.172	1.176	1.251	1.159	0.809	0.552			
1	0.770	0.768	0.741	0.578					

EPR2170 T2



**Figure 4.3-11—Quarter Core Relative Assembly Radial Power Distribution  
(HFP Near BOL, ARO, Equilibrium Xenon Power Distribution)**

	<b>J</b>	<b>K</b>	<b>L</b>	<b>M</b>	<b>N</b>	<b>P</b>	<b>R</b>	<b>S</b>	<b>T</b>
<b>9</b>	1.251	1.126	1.180	1.059	1.076	0.972	1.095	1.156	0.778
<b>8</b>	1.126	1.099	1.074	1.143	0.993	1.053	0.998	1.160	0.775
<b>7</b>	1.180	1.074	1.149	1.022	1.061	1.013	1.003	1.229	0.747
<b>6</b>	1.059	1.143	1.022	1.056	0.958	1.021	1.114	1.140	0.585
<b>5</b>	1.076	0.993	1.061	0.958	1.063	1.045	1.145	0.808	
<b>4</b>	0.972	1.053	1.013	1.021	1.045	1.093	1.067	0.558	
<b>3</b>	1.095	0.998	1.003	1.114	1.145	1.067	0.617		
<b>2</b>	1.156	1.160	1.229	1.140	0.808	0.558			
<b>1</b>	0.778	0.775	0.747	0.585					

EPR2175 T2

**Figure 4.3-12—Quarter Core Relative Assembly Radial Power Distribution  
(HFP Near BOL, Bank D at PDIL, Equilibrium Xenon Power Distribution)**

	<b>J</b>	<b>K</b>	<b>L</b>	<b>M</b>	<b>N</b>	<b>P</b>	<b>R</b>	<b>S</b>	<b>T</b>
<b>9</b>	1.166	1.107	1.186	1.068	1.080	0.956	1.024	1.141	0.781
<b>8</b>	1.107	1.093	1.081	1.155	0.997	1.048	0.983	1.157	0.781
<b>7</b>	1.186	1.081	1.160	1.028	1.062	1.014	1.006	1.241	0.758
<b>6</b>	1.068	1.155	1.028	1.053	0.942	1.016	1.122	1.157	0.596
<b>5</b>	1.080	0.997	1.062	0.942	0.993	1.033	1.155	0.821	
<b>4</b>	0.956	1.048	1.014	1.016	1.033	1.092	1.080	0.568	
<b>3</b>	1.024	0.983	1.006	1.122	1.155	1.080	0.626		
<b>2</b>	1.141	1.157	1.241	1.157	0.821	0.568			
<b>1</b>	0.781	0.781	0.758	0.596					

EPR2180 T2

**Figure 4.3-13—Quarter Core Relative Assembly Radial Power Distribution  
(HFP Near MOL, ARO, Equilibrium Xenon Power Distribution)**

	<b>J</b>	<b>K</b>	<b>L</b>	<b>M</b>	<b>N</b>	<b>P</b>	<b>R</b>	<b>S</b>	<b>T</b>
<b>9</b>	1.248	1.140	1.033	1.116	1.232	1.160	1.207	1.076	0.592
<b>8</b>	1.140	1.125	1.096	1.054	1.161	1.092	1.123	1.061	0.582
<b>7</b>	1.033	1.096	1.036	1.135	1.256	1.181	1.114	1.024	0.546
<b>6</b>	1.116	1.054	1.135	1.099	1.199	1.192	1.160	0.931	0.435
<b>5</b>	1.232	1.161	1.256	1.199	1.280	1.166	1.093	0.642	
<b>4</b>	1.160	1.092	1.181	1.192	1.166	1.128	0.916	0.444	
<b>3</b>	1.207	1.123	1.114	1.160	1.093	0.916	0.505		
<b>2</b>	1.076	1.061	1.024	0.931	0.642	0.444			
<b>1</b>	0.592	0.582	0.546	0.435					

EPR2185 T2

**Figure 4.3-14—Quarter Core Relative Assembly Radial Power Distribution  
(HFP Near MOL, Bank D at PDIL, Equilibrium Xenon Power Distribution)**

	<b>J</b>	<b>K</b>	<b>L</b>	<b>M</b>	<b>N</b>	<b>P</b>	<b>R</b>	<b>S</b>	<b>T</b>
<b>9</b>	1.146	1.115	1.038	1.136	1.252	1.154	1.134	1.049	0.588
<b>8</b>	1.115	1.117	1.108	1.070	1.179	1.090	1.111	1.049	0.580
<b>7</b>	1.038	1.108	1.048	1.152	1.272	1.187	1.121	1.026	0.550
<b>6</b>	1.136	1.070	1.152	1.100	1.192	1.189	1.171	0.940	0.441
<b>5</b>	1.252	1.179	1.272	1.192	1.206	1.149	1.096	0.650	
<b>4</b>	1.154	1.090	1.187	1.189	1.149	1.128	0.922	0.450	
<b>3</b>	1.134	1.111	1.121	1.171	1.096	0.922	0.511		
<b>2</b>	1.049	1.049	1.026	0.940	0.650	0.450			
<b>1</b>	0.588	0.580	0.550	0.441					

EPR2190 T2

**Figure 4.3-15—Quarter Core Relative Assembly Radial Power Distribution  
(HFP Near EOL, ARO, Equilibrium Xenon Power Distribution)**

	<b>J</b>	<b>K</b>	<b>L</b>	<b>M</b>	<b>N</b>	<b>P</b>	<b>R</b>	<b>S</b>	<b>T</b>
<b>9</b>	1.149	1.080	1.014	1.085	1.174	1.115	1.174	1.091	0.697
<b>8</b>	1.080	1.077	1.070	1.028	1.110	1.053	1.105	1.083	0.690
<b>7</b>	1.014	1.070	1.016	1.091	1.179	1.116	1.100	1.062	0.663
<b>6</b>	1.085	1.028	1.091	1.047	1.123	1.120	1.147	0.992	0.548
<b>5</b>	1.174	1.110	1.179	1.123	1.190	1.111	1.092	0.735	
<b>4</b>	1.115	1.053	1.116	1.120	1.111	1.128	0.975	0.546	
<b>3</b>	1.174	1.105	1.100	1.147	1.092	0.975	0.602		
<b>2</b>	1.091	1.083	1.062	0.992	0.735	0.546			
<b>1</b>	0.697	0.690	0.663	0.548					

EPR2195 T2

**Figure 4.3-16—Quarter Core Relative Assembly Radial Power Distribution  
(HFP Near EOL, Bank D at PDIL, Equilibrium Xenon Power Distribution)**

	J	K	L	M	N	P	R	S	T
9	1.075	1.073	1.028	1.103	1.184	1.099	1.088	1.068	0.696
8	1.073	1.082	1.087	1.045	1.120	1.048	1.085	1.075	0.693
7	1.028	1.087	1.033	1.104	1.186	1.118	1.103	1.070	0.671
6	1.103	1.045	1.104	1.046	1.106	1.115	1.154	1.006	0.558
5	1.184	1.120	1.186	1.106	1.104	1.093	1.099	0.747	
4	1.099	1.048	1.118	1.115	1.093	1.123	0.984	0.555	
3	1.088	1.085	1.103	1.154	1.099	0.984	0.611		
2	1.068	1.075	1.070	1.006	0.747	0.555			
1	0.696	0.693	0.671	0.558					

EPR2200 T2

**Figure 4.3-17—Fuel Assembly ( $\frac{1}{2}$  Assembly Symmetry) Power Distribution  
(HFP Near BOL, ARO, Equilibrium Xenon Power Distribution)**

1.347																
1.321	1.295															
1.313	1.289	1.297														
1.313	1.290	1.325														
1.314	1.295	1.300	1.223	1.211												
1.316	1.318		0.475	1.198												
1.311	1.285	1.266	1.158	1.228	1.314	1.303										
1.310	1.284	1.271	1.175	1.240	1.322	1.309	1.297									
1.311	1.311		0.626	1.233		1.338	1.295	1.289								
1.310	1.284	1.271	1.175	1.240	1.322	1.309	1.297	1.295	1.297							
1.311	1.285	1.266	1.158	1.228	1.314	1.303	1.309	1.338	1.309	1.303						
1.316	1.318		0.475	1.198		1.314	1.322		1.322	1.314						
1.314	1.295	1.300	1.223	1.211	1.198	1.228	1.240	1.233	1.240	1.228	1.198	1.211				
1.313	1.290	1.325		1.223	0.475	1.158	1.175	0.626	1.175	1.158	0.475	1.223				
1.313	1.289	1.297	1.325	1.300		1.266	1.271		1.271	1.266		1.300	1.325	1.297		
1.321	1.295	1.289	1.290	1.295	1.318	1.285	1.284	1.311	1.284	1.285	1.318	1.295	1.290	1.289	1.295	
1.347	1.321	1.313	1.313	1.314	1.316	1.311	1.310	1.311	1.310	1.311	1.316	1.314	1.313	1.313	1.321	1.347

EPR2205 T2

**Figure 4.3-18—Fuel Assembly ( $1/2$  Assembly Symmetry) Power Distribution (HFP Near EOL, ARO, Equilibrium Xenon Power Distribution)**

1.106																
1.103	1.101															
1.109	1.110	1.135														
1.117	1.122	1.166														
1.125	1.144	1.189	1.207	1.195												
1.131	1.163		1.097	1.197												
1.132	1.149	1.178	1.175	1.172	1.181	1.160										
1.132	1.148	1.175	1.168	1.166	1.177	1.155	1.134									
1.132	1.161		1.138	1.180		1.165	1.131	1.126								
1.132	1.148	1.175	1.168	1.166	1.177	1.155	1.134	1.131	1.134							
1.132	1.149	1.178	1.175	1.172	1.181	1.160	1.155	1.165	1.155	1.160						
1.131	1.163		1.097	1.197		1.181	1.177		1.177	1.181						
1.125	1.144	1.189	1.207	1.195	1.197	1.172	1.166	1.180	1.166	1.172	1.197	1.195				
1.117	1.122	1.166		1.207	1.097	1.175	1.168	1.138	1.168	1.175	1.097	1.207				
1.109	1.110	1.135	1.166	1.189		1.178	1.175		1.175	1.178		1.189	1.166	1.135		
1.103	1.101	1.110	1.122	1.144	1.163	1.149	1.148	1.161	1.148	1.149	1.163	1.144	1.122	1.110	1.101	
1.106	1.103	1.109	1.117	1.125	1.131	1.132	1.132	1.132	1.132	1.132	1.131	1.125	1.117	1.109	1.103	1.106

EPR2210 T2



Figure 4.3-19—Typical Axial Power Shape at Beginning of Life

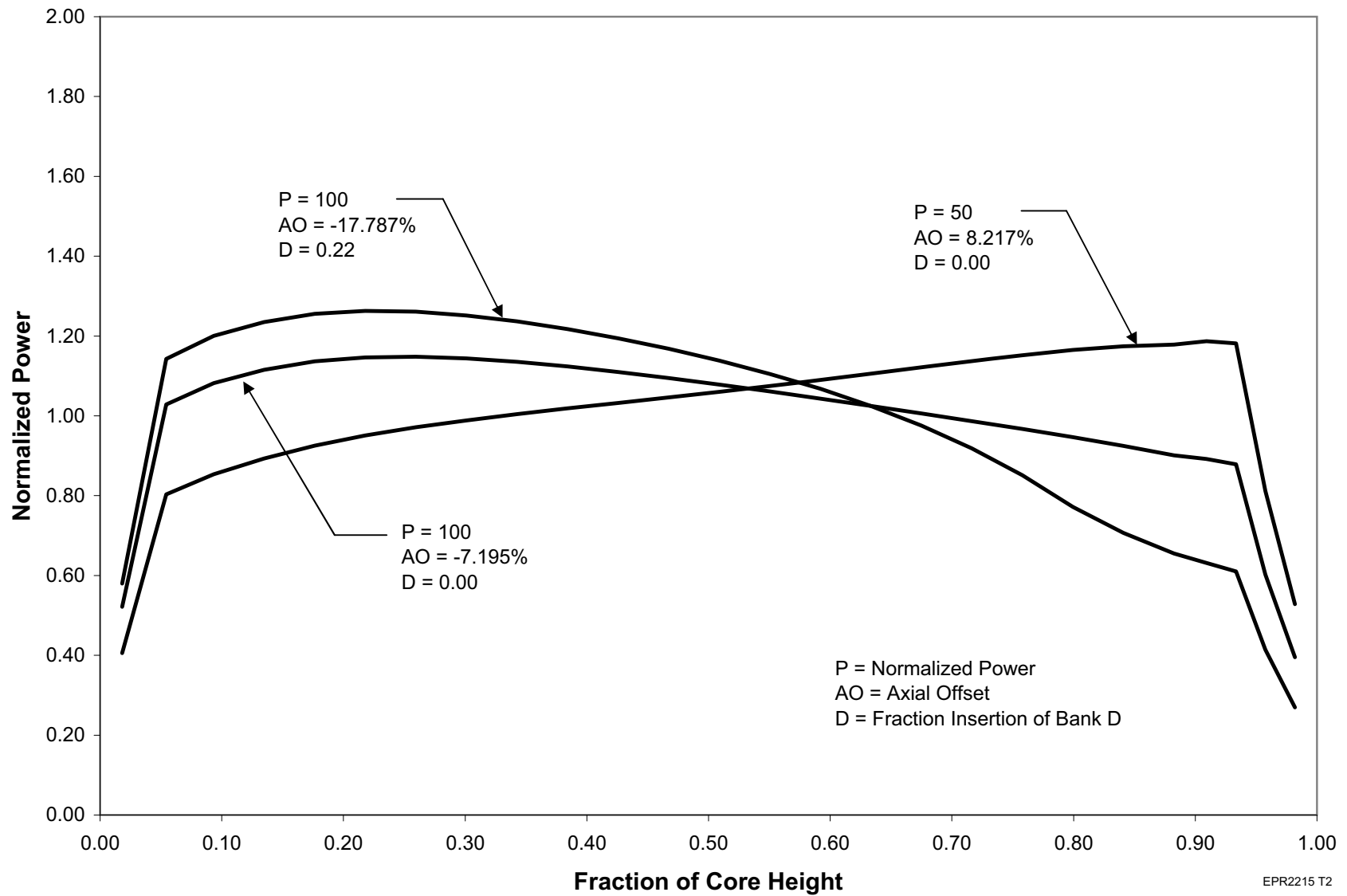


Figure 4.3-20—Typical Axial Power Shape at Middle of Life

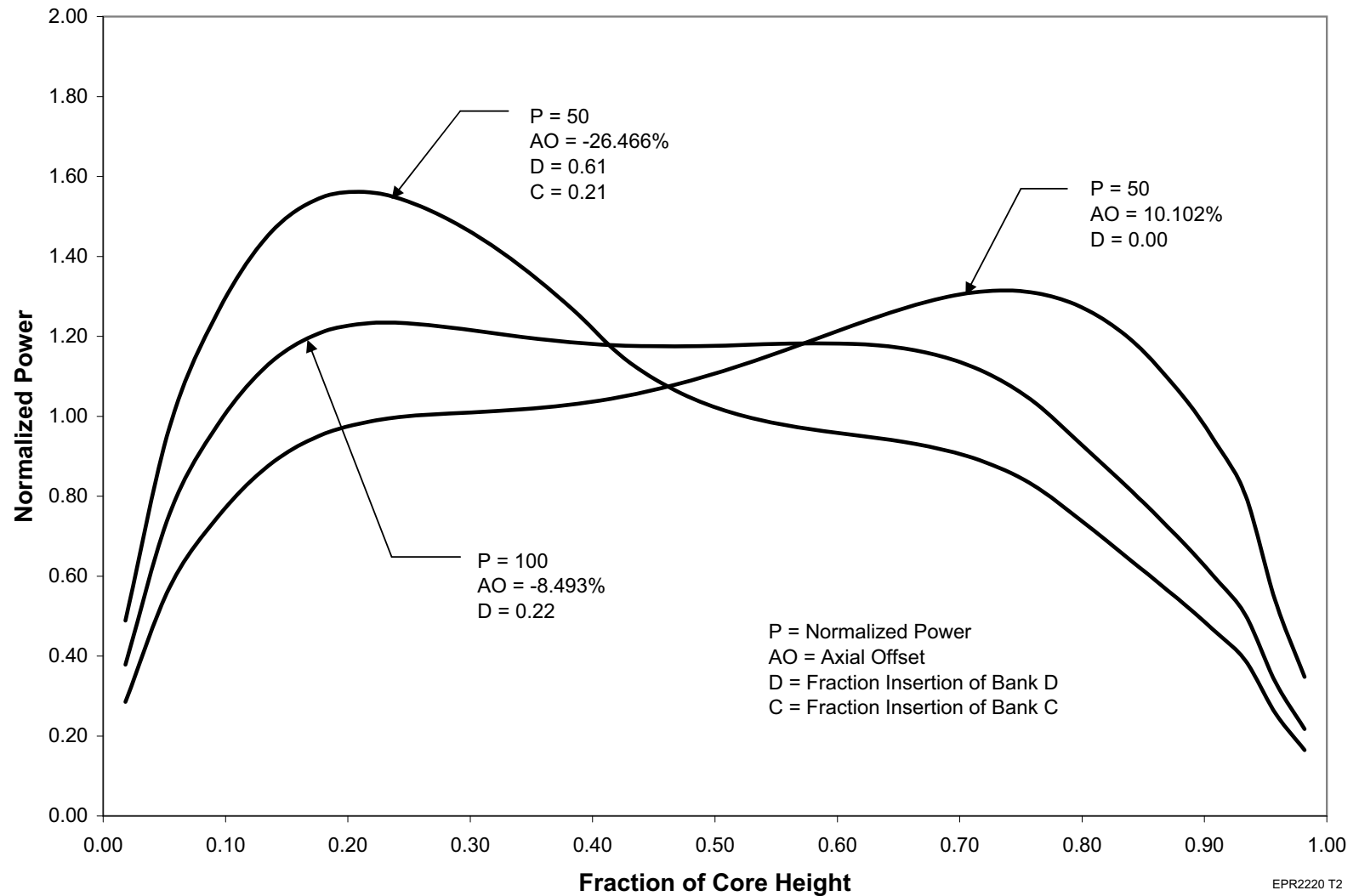


Figure 4.3-21—Typical Axial Power Shape at End of Life

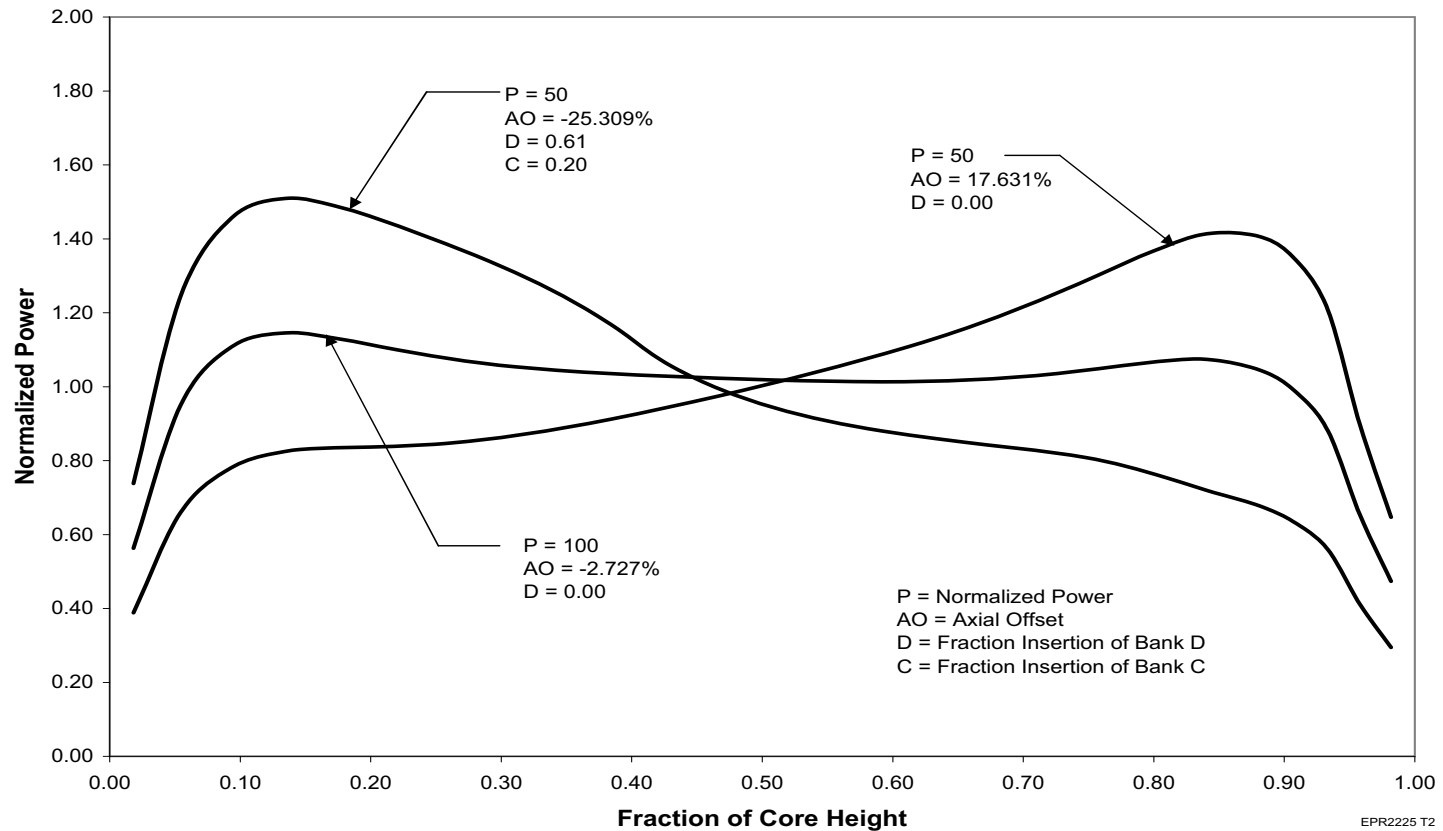


Figure 4.3-22—Comparison of Typical Fuel Assembly Axial Power Distributions with a Core Average Axial Power Distribution and Bank D Slightly Inserted

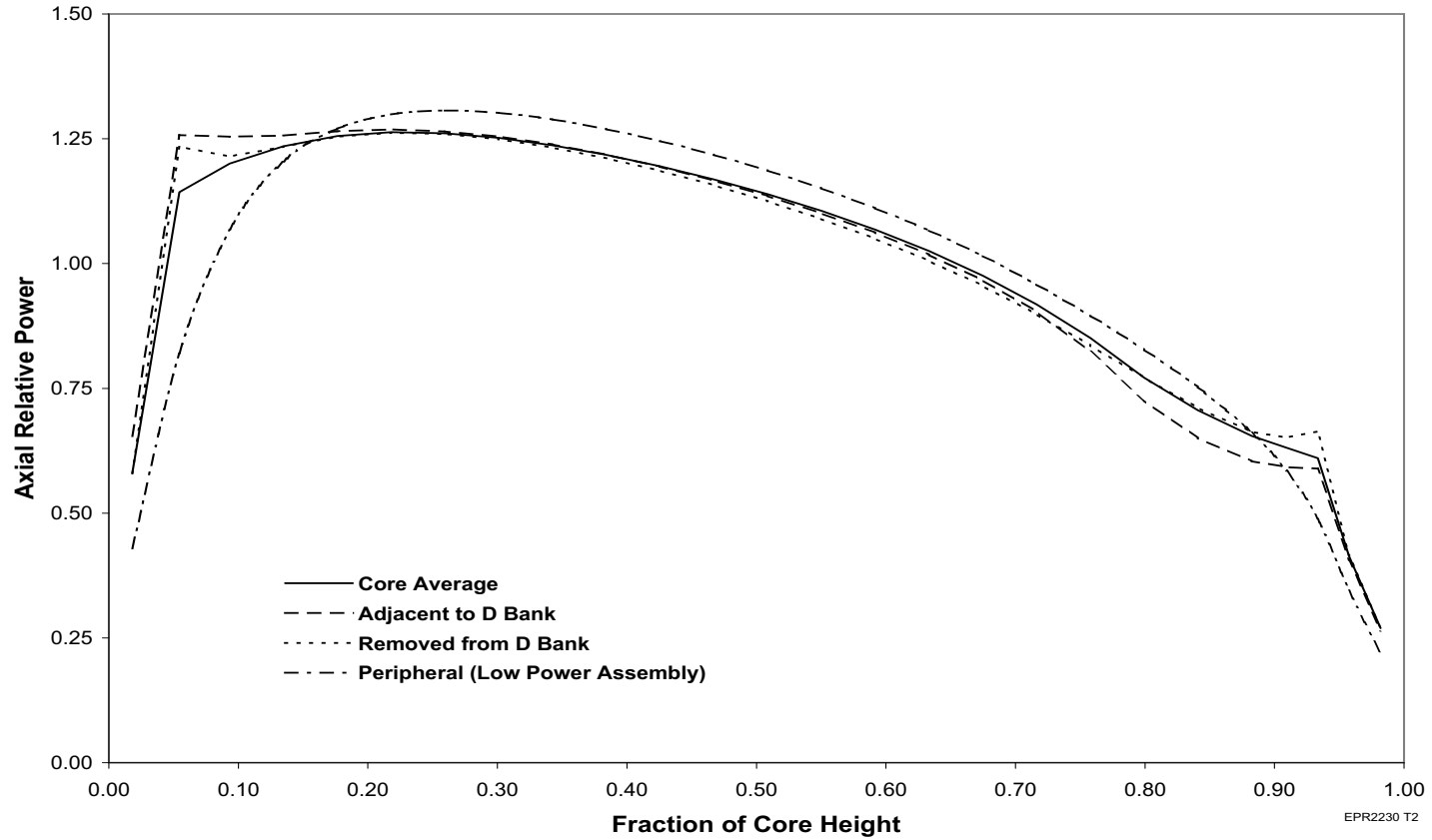


Figure 4.3-23—Maximum  $F_Q$  as a Function of Core Height

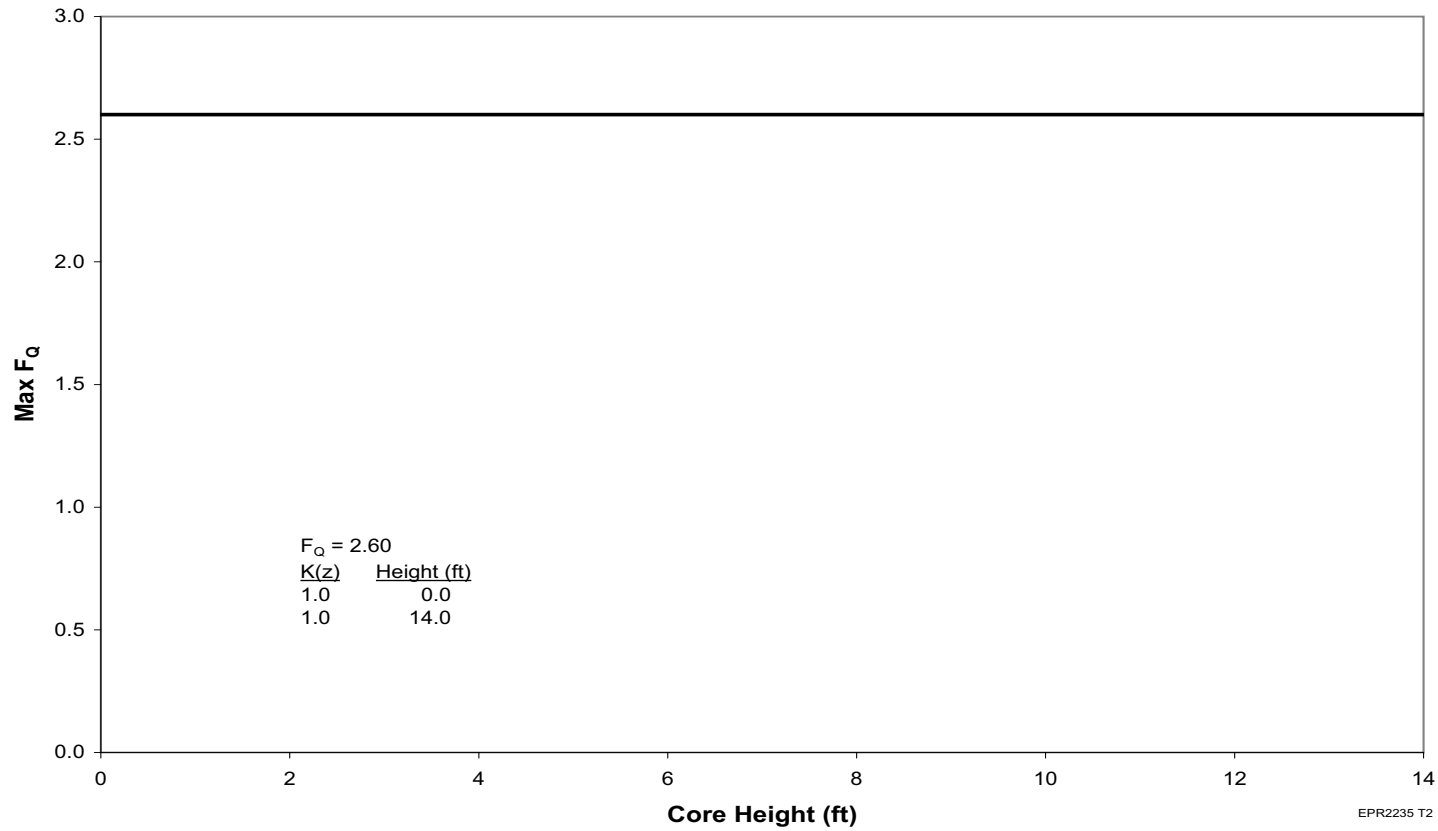


Figure 4.3-24—Measured Values of  $F_Q$  for Steady State Full Power Rod Configurations

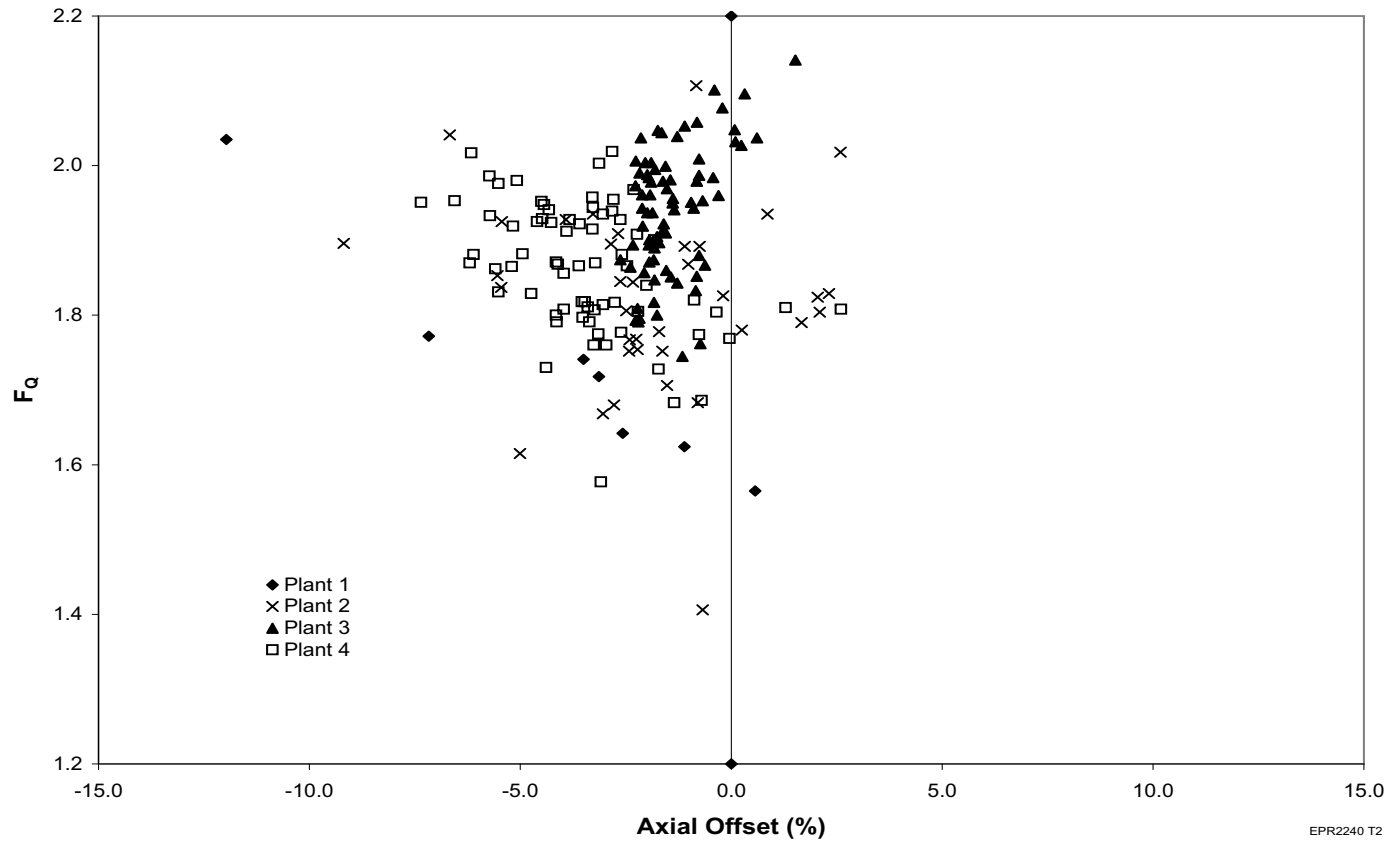


Figure 4.3-25—Typical Doppler Temperature Coefficient

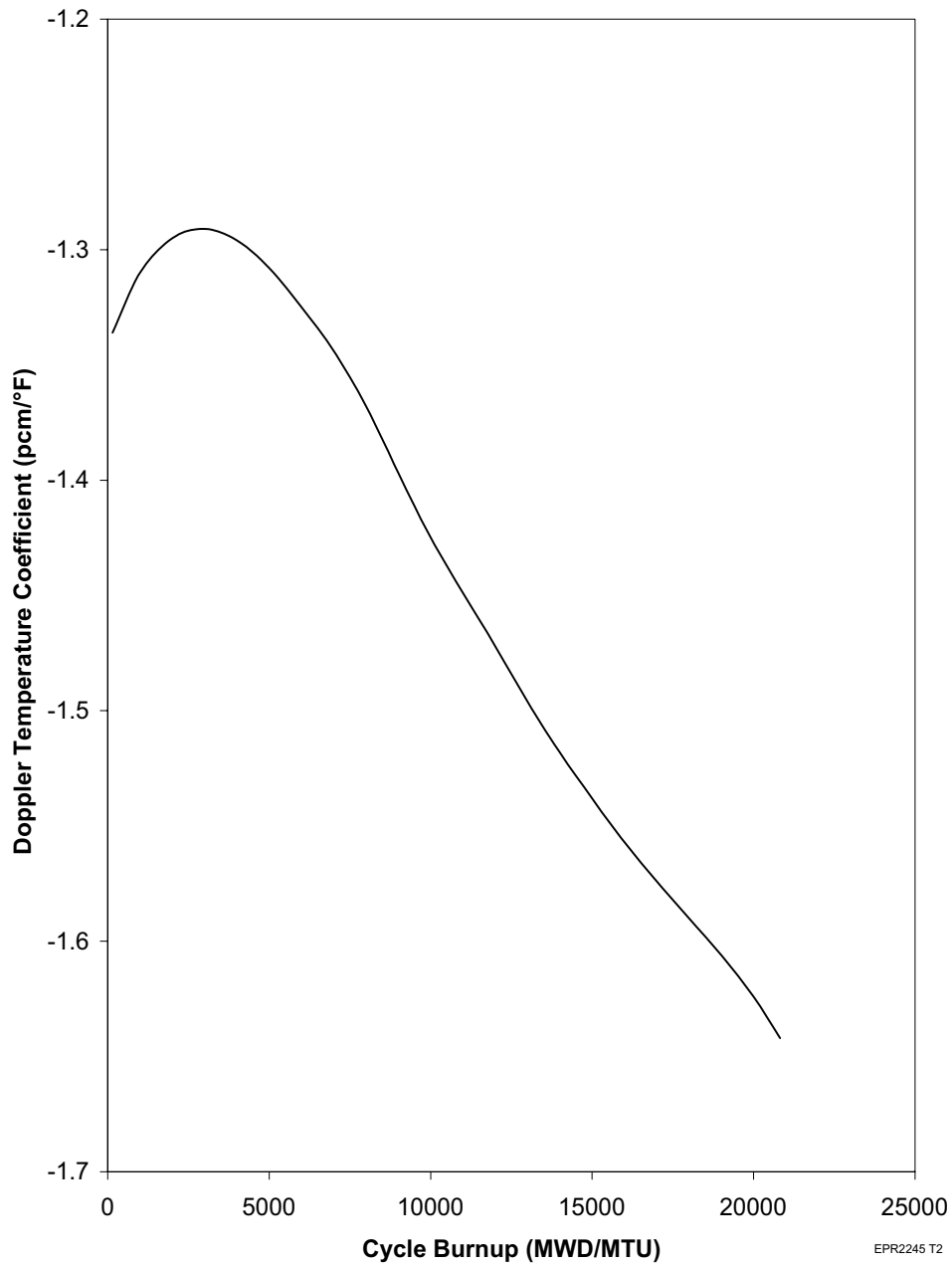


Figure 4.3-26—Typical Doppler-Only Power Coefficient at BOL and EOL

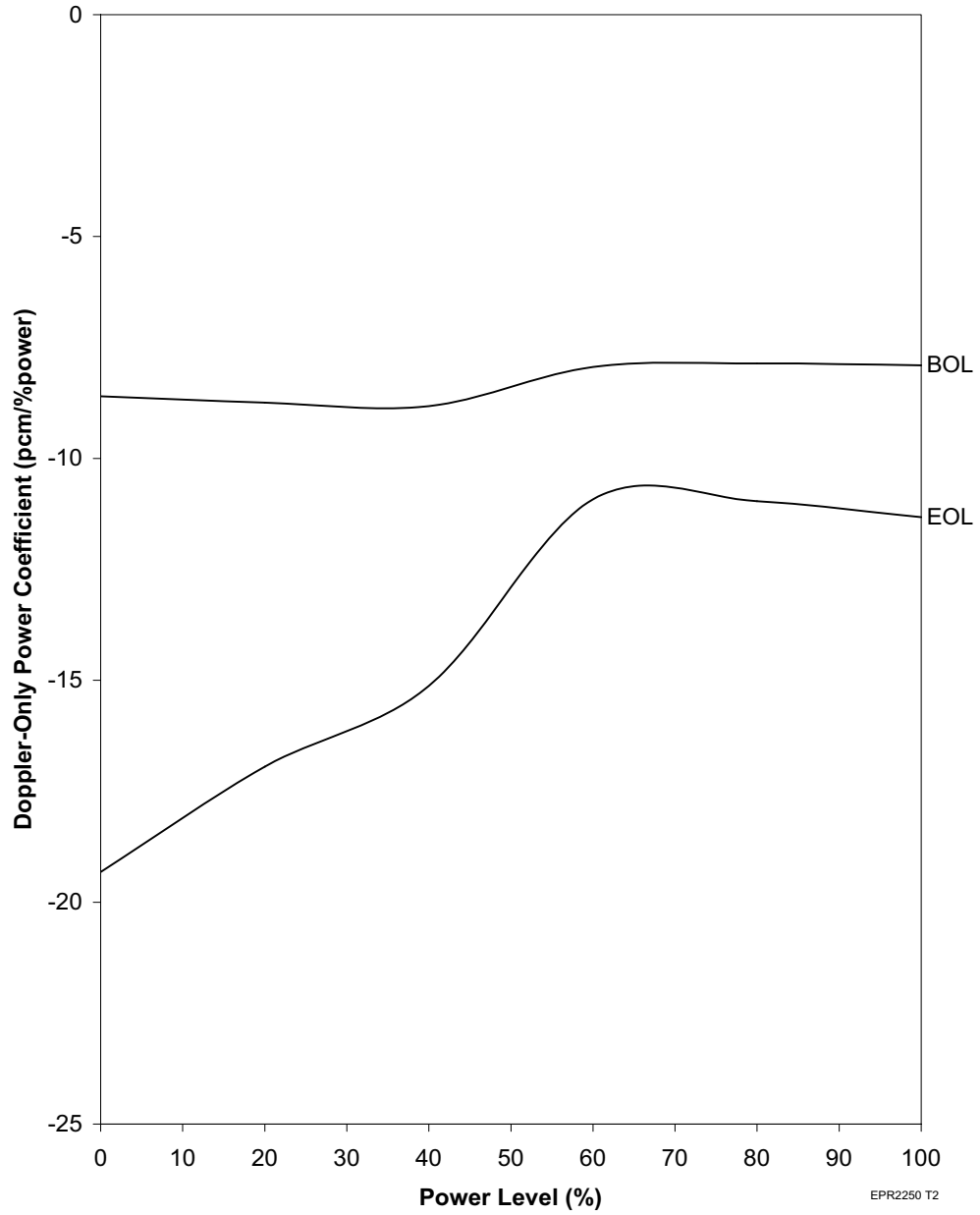




Figure 4.3-27—Typical Doppler-Only Power Defect at BOL and EOL

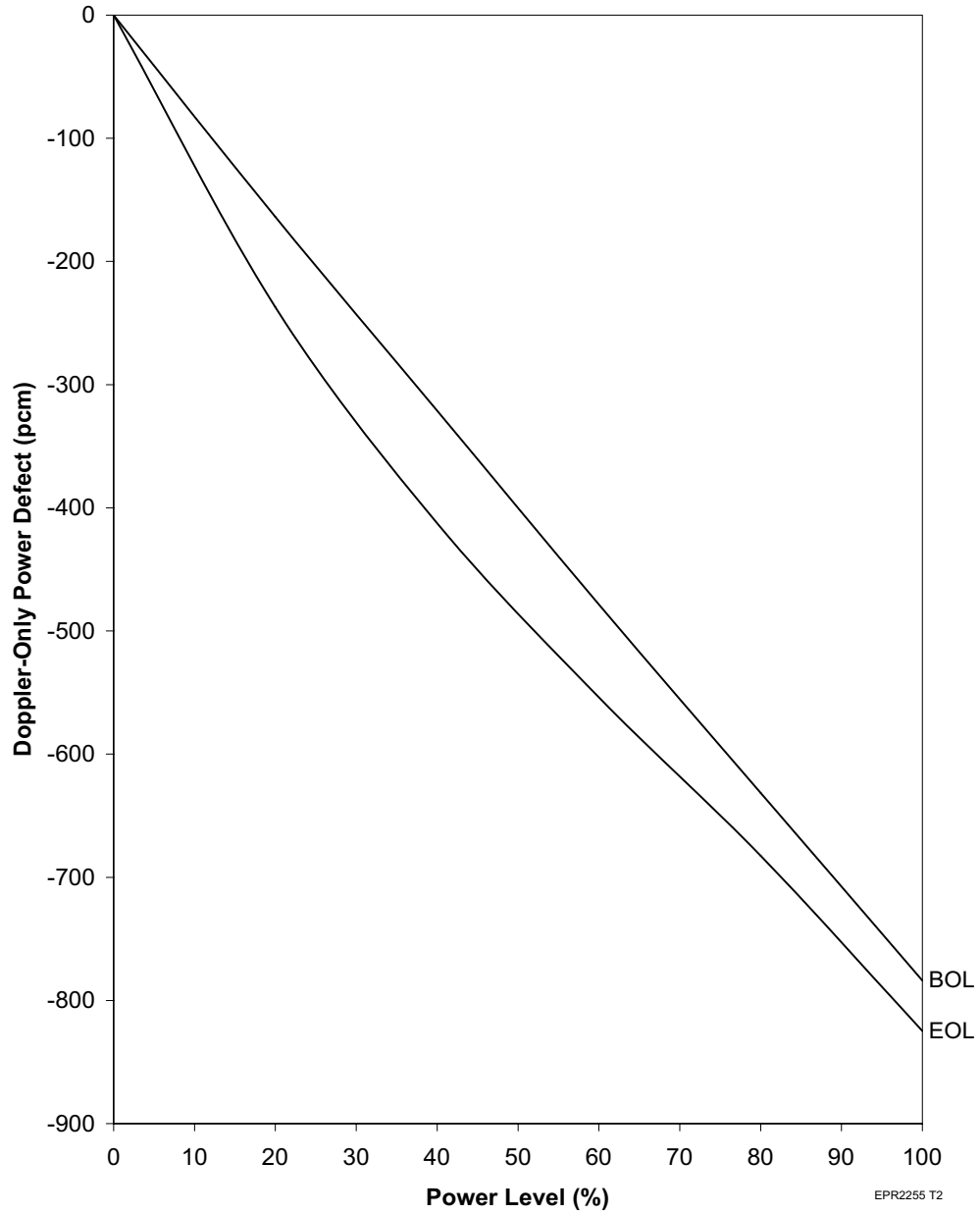
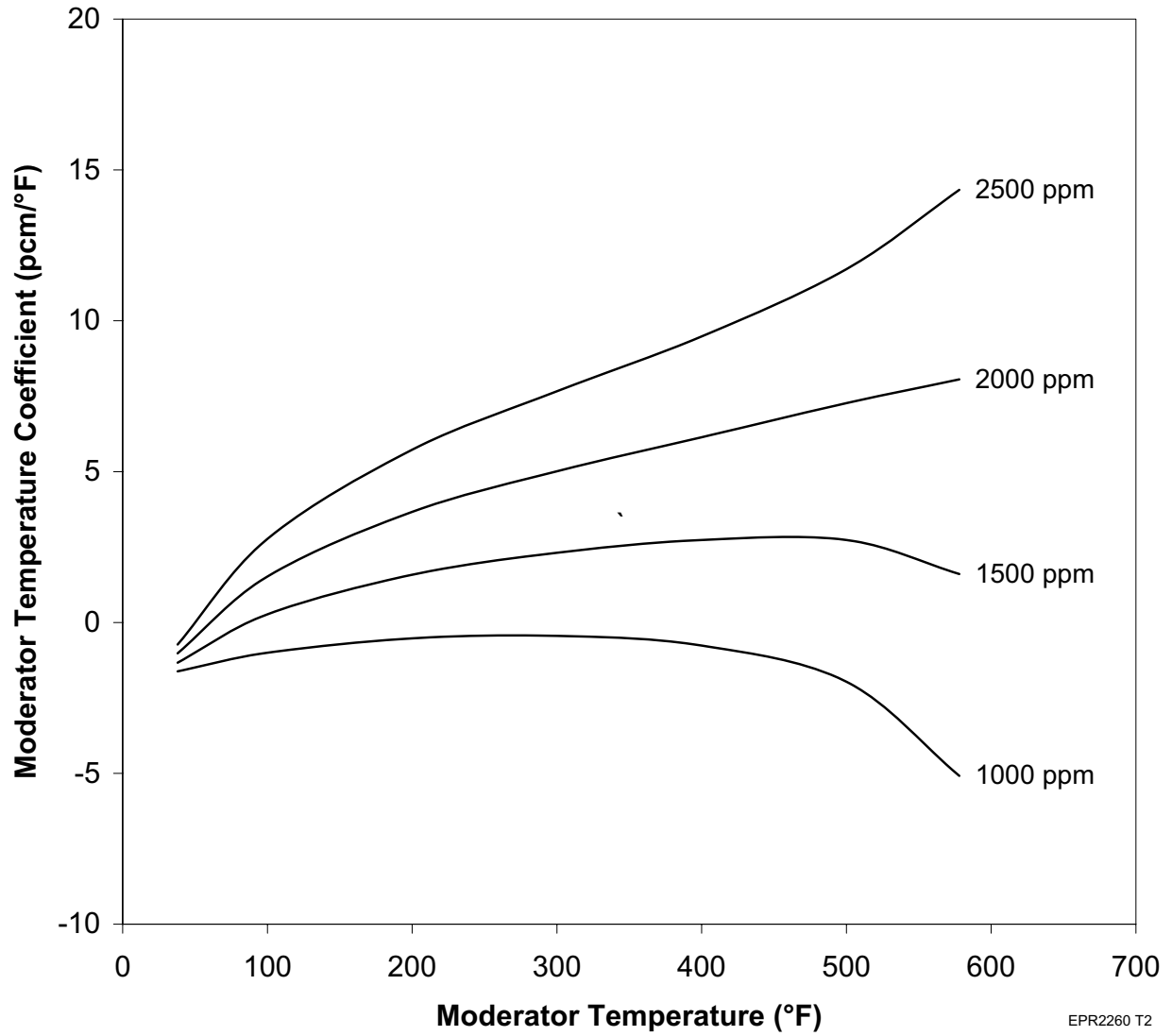
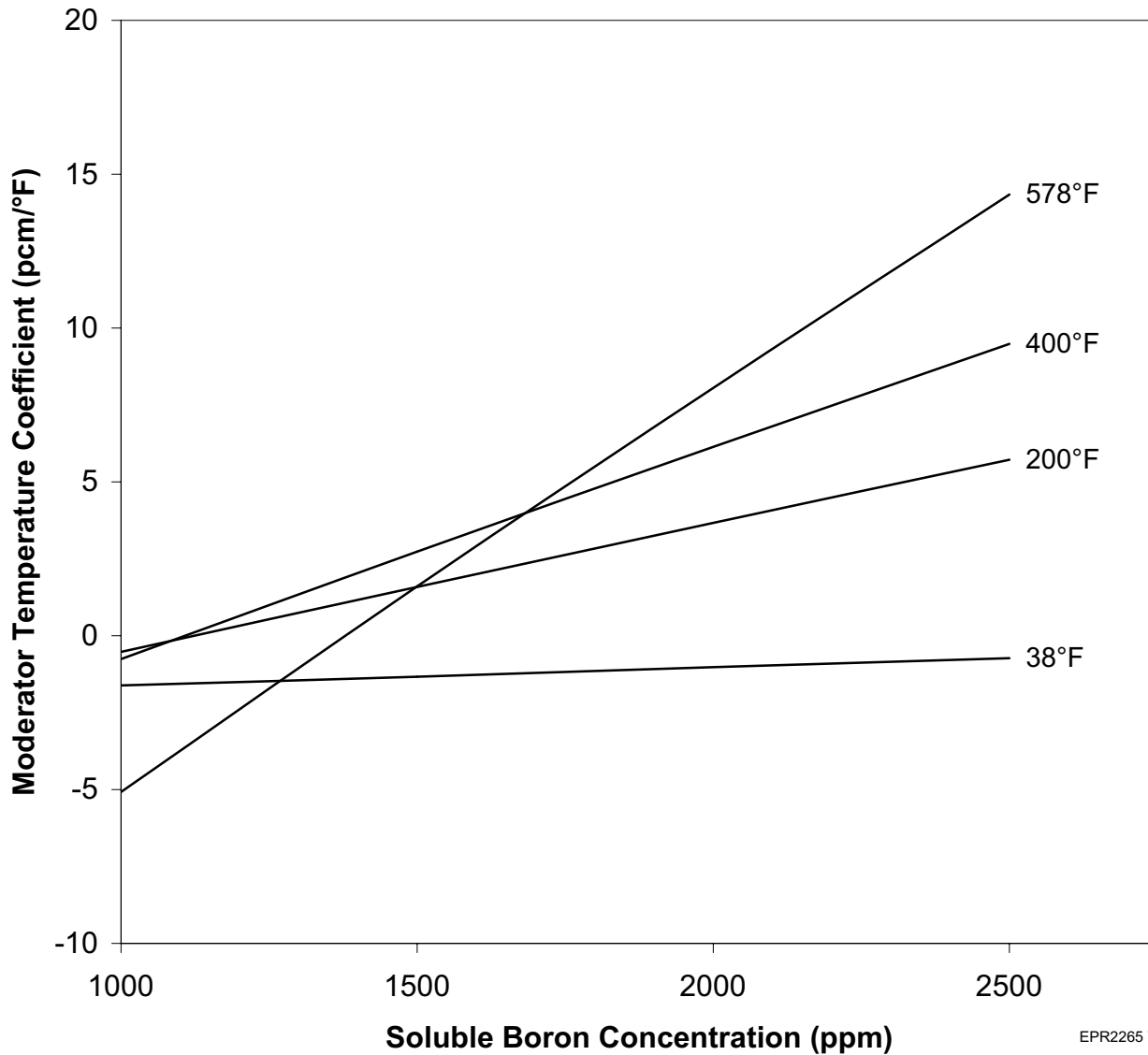


Figure 4.3-28—Typical Zero Power Moderator Temperature Coefficient at BOL



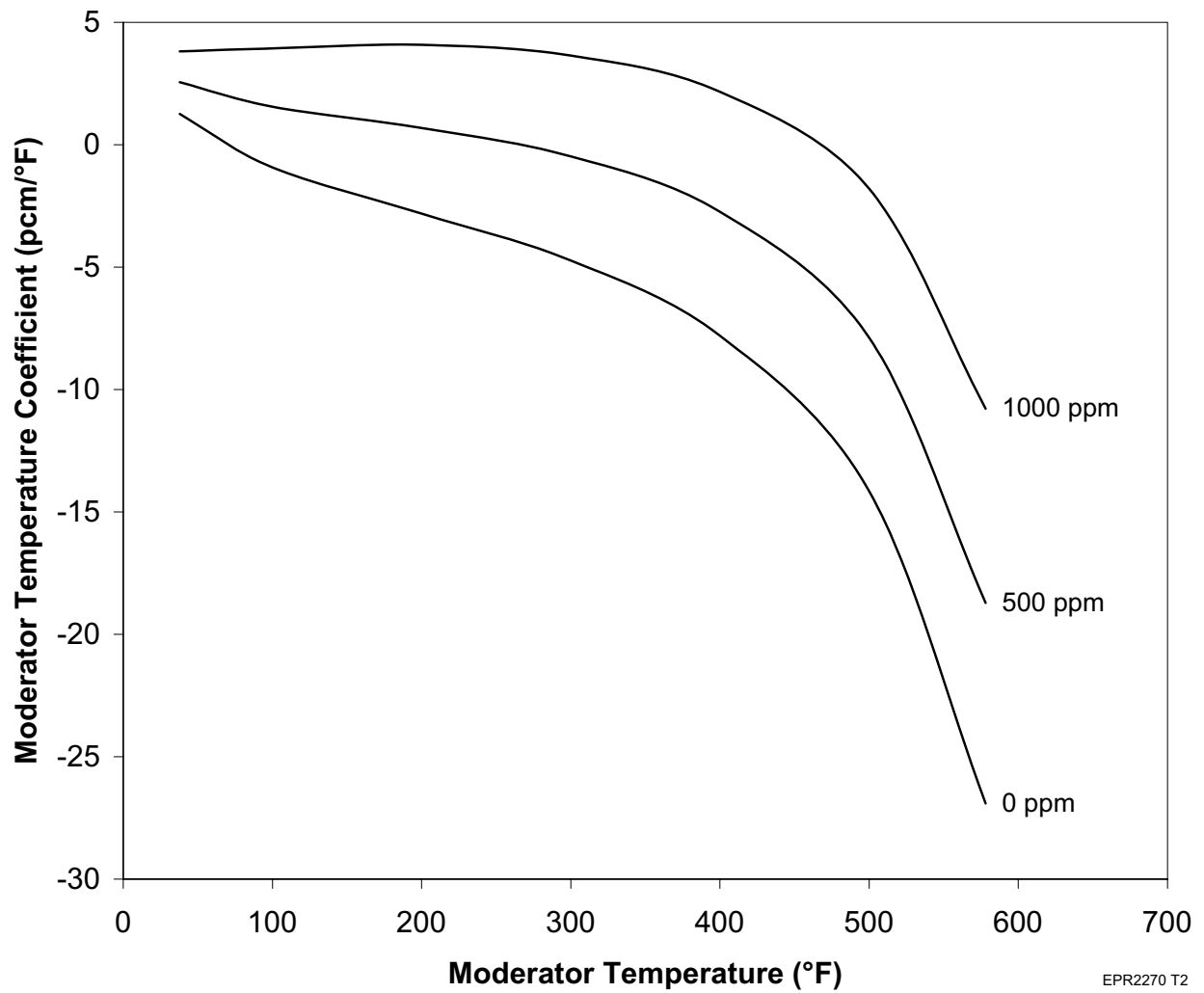
EPR2260 T2

**Figure 4.3-29—Typical Zero Power Moderator Temperature Coefficient as a Function of Boron Concentration at BOL**



EPR2265 T2

Figure 4.3-30—Typical Zero Power Moderator Temperature Coefficient at EOL



EPR2270 T2

Figure 4.3-31—Typical Hot Full Power Moderator Temperature Coefficient

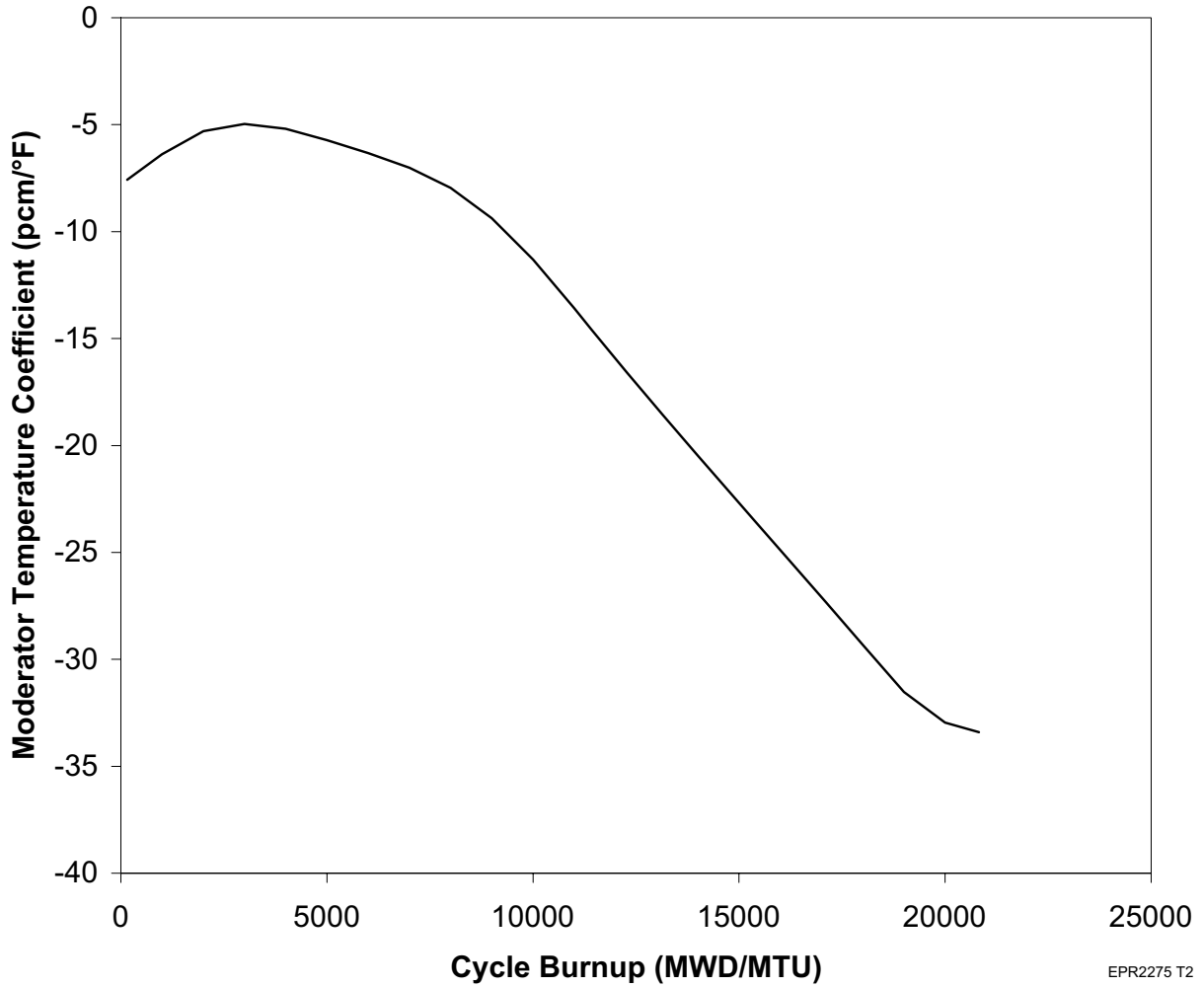


Figure 4.3-32—Typical Total Power Coefficient at BOL and EOL

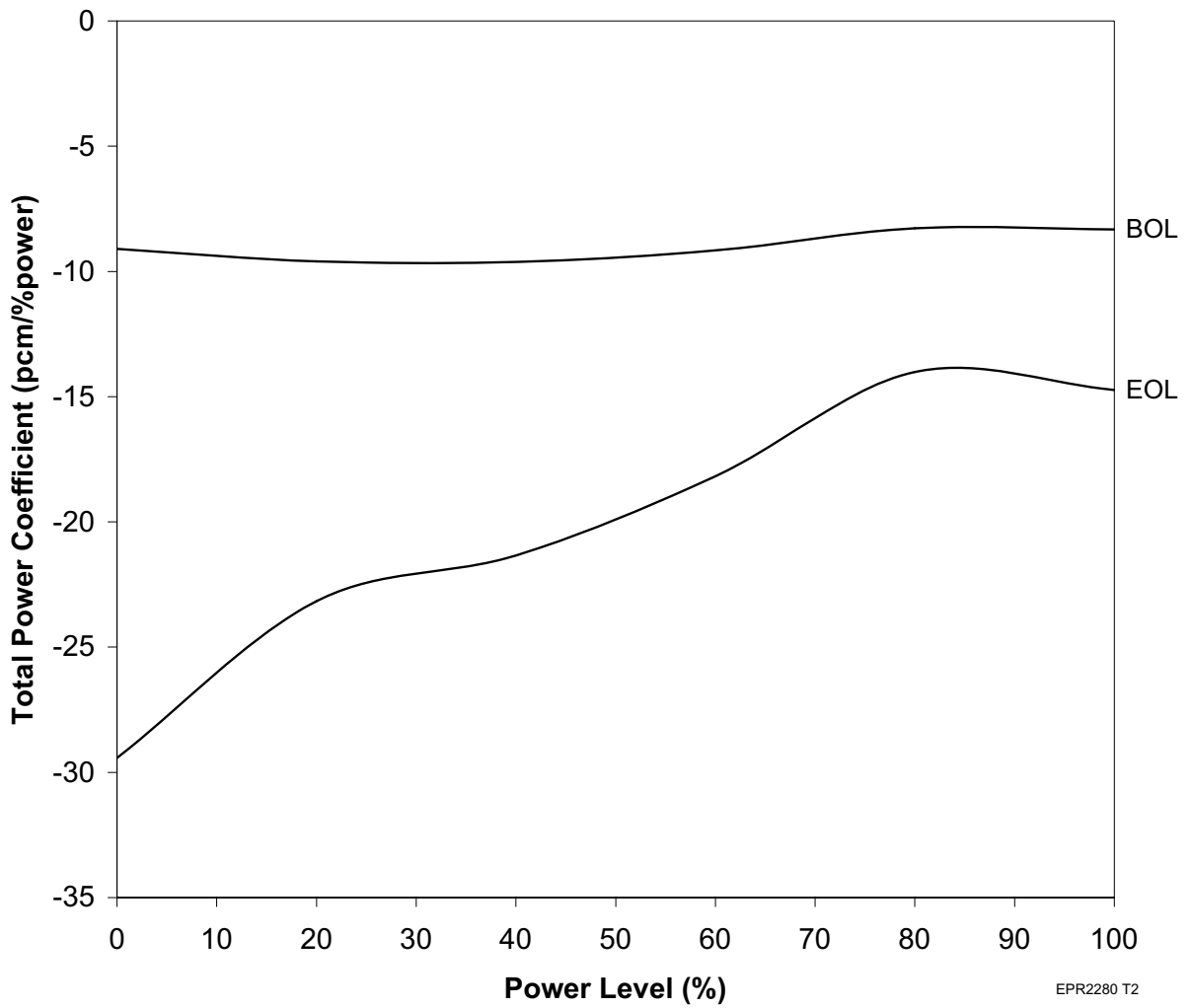


Figure 4.3-33—Typical Total Power Defect at BOL and EOL

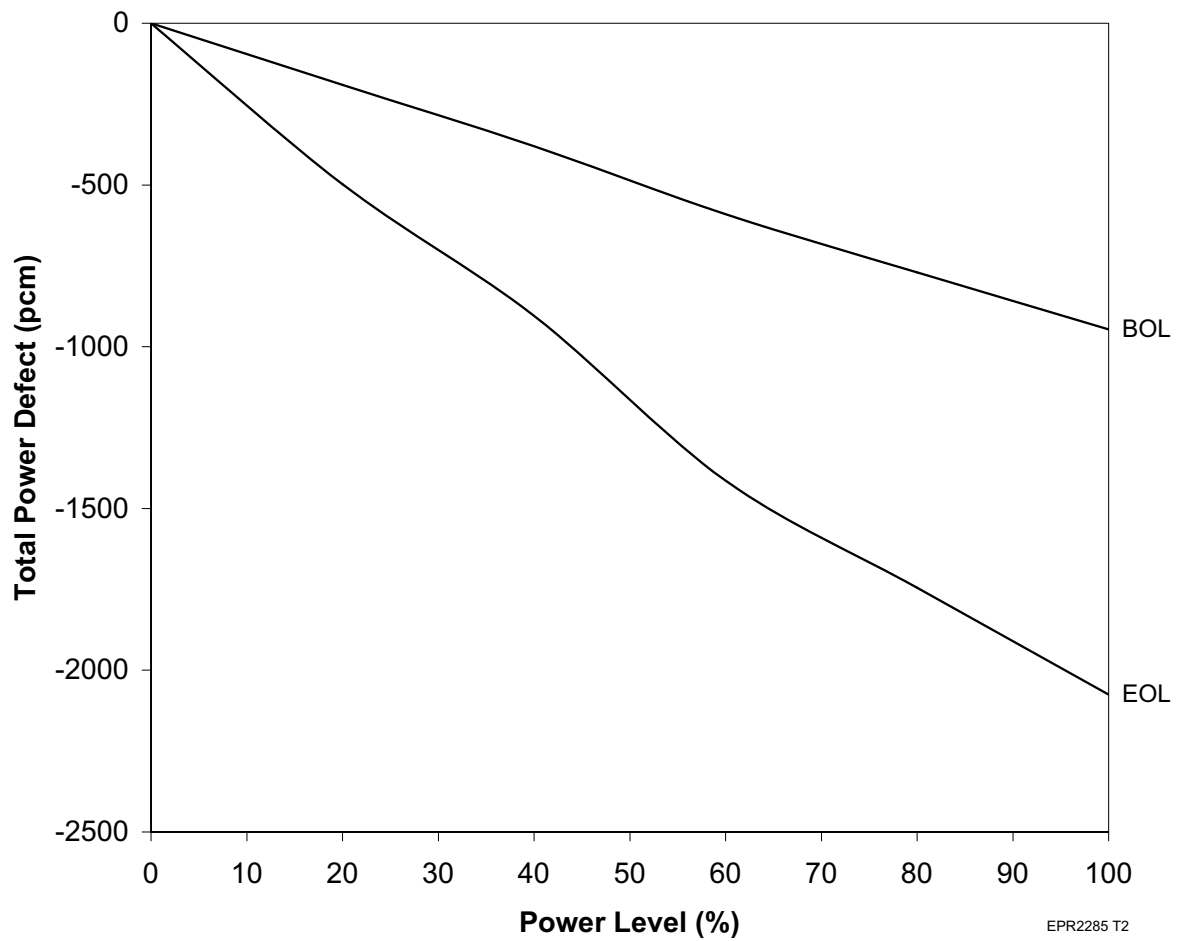
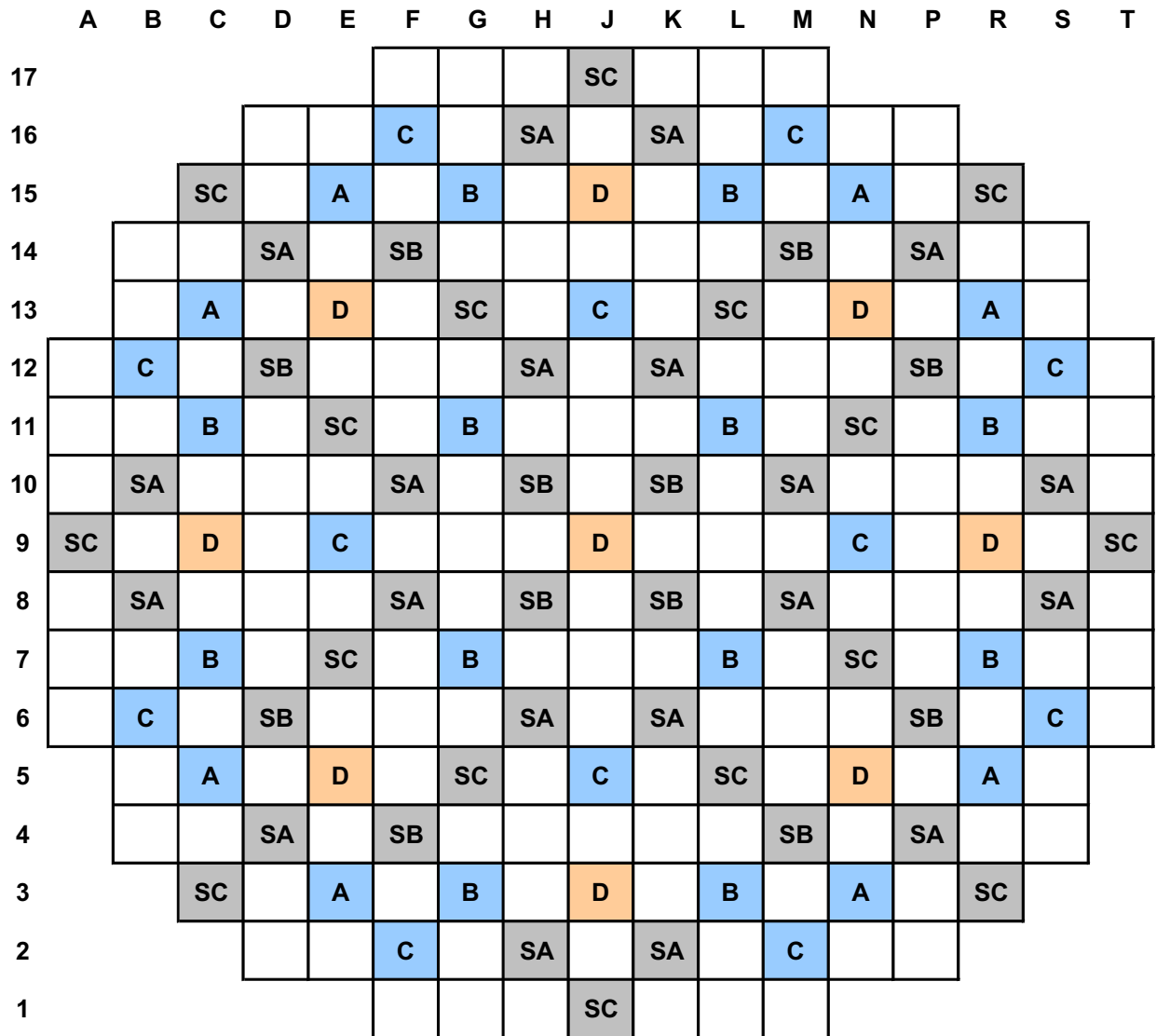


Figure 4.3-34—Rod Cluster Control Assembly Pattern



Control Banks

D	9
C	12
B	12
A	8

Shutdown Banks

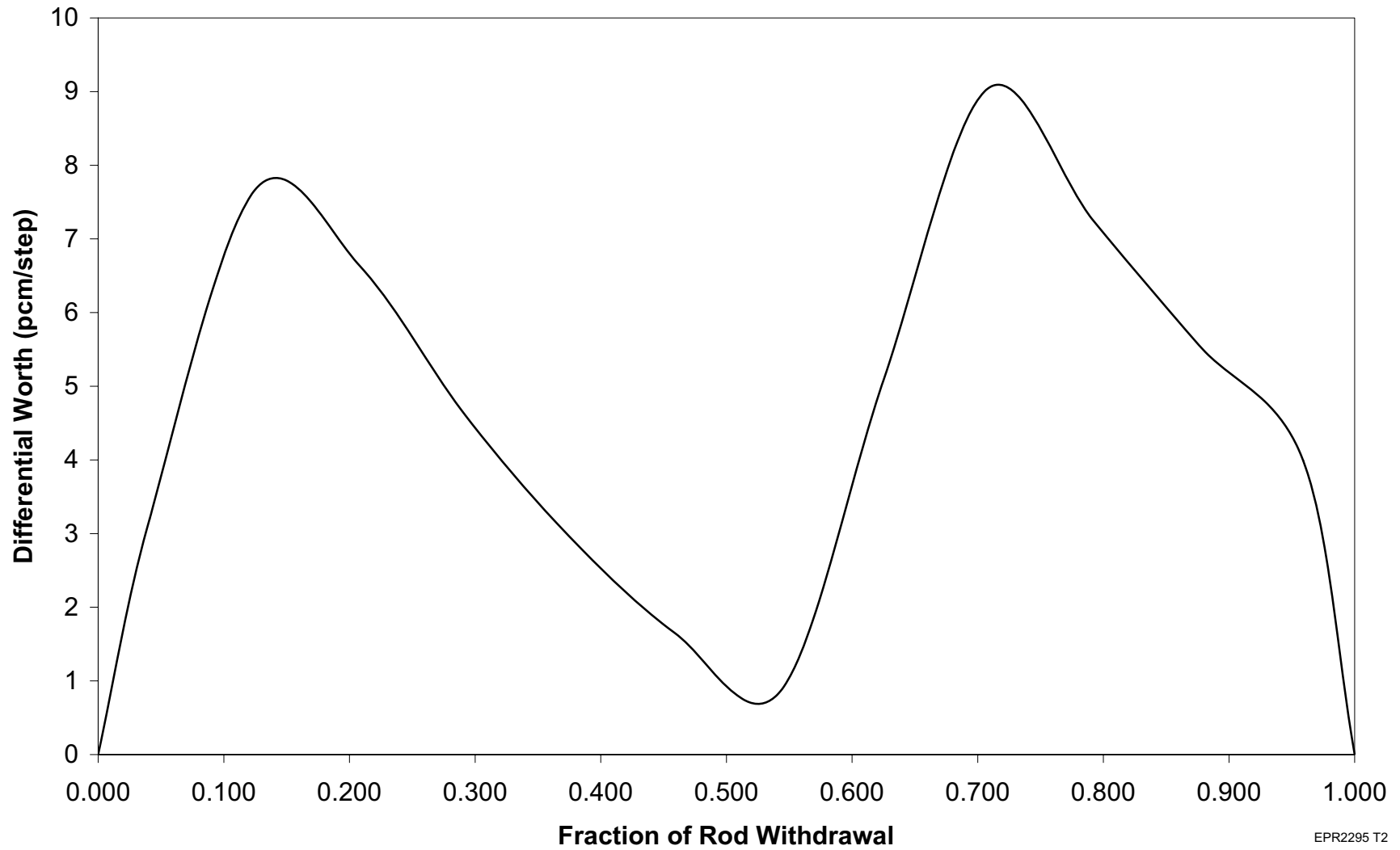
SC	16
SB	12
SA	20

Total RCCA: 89

EPR2290 T2

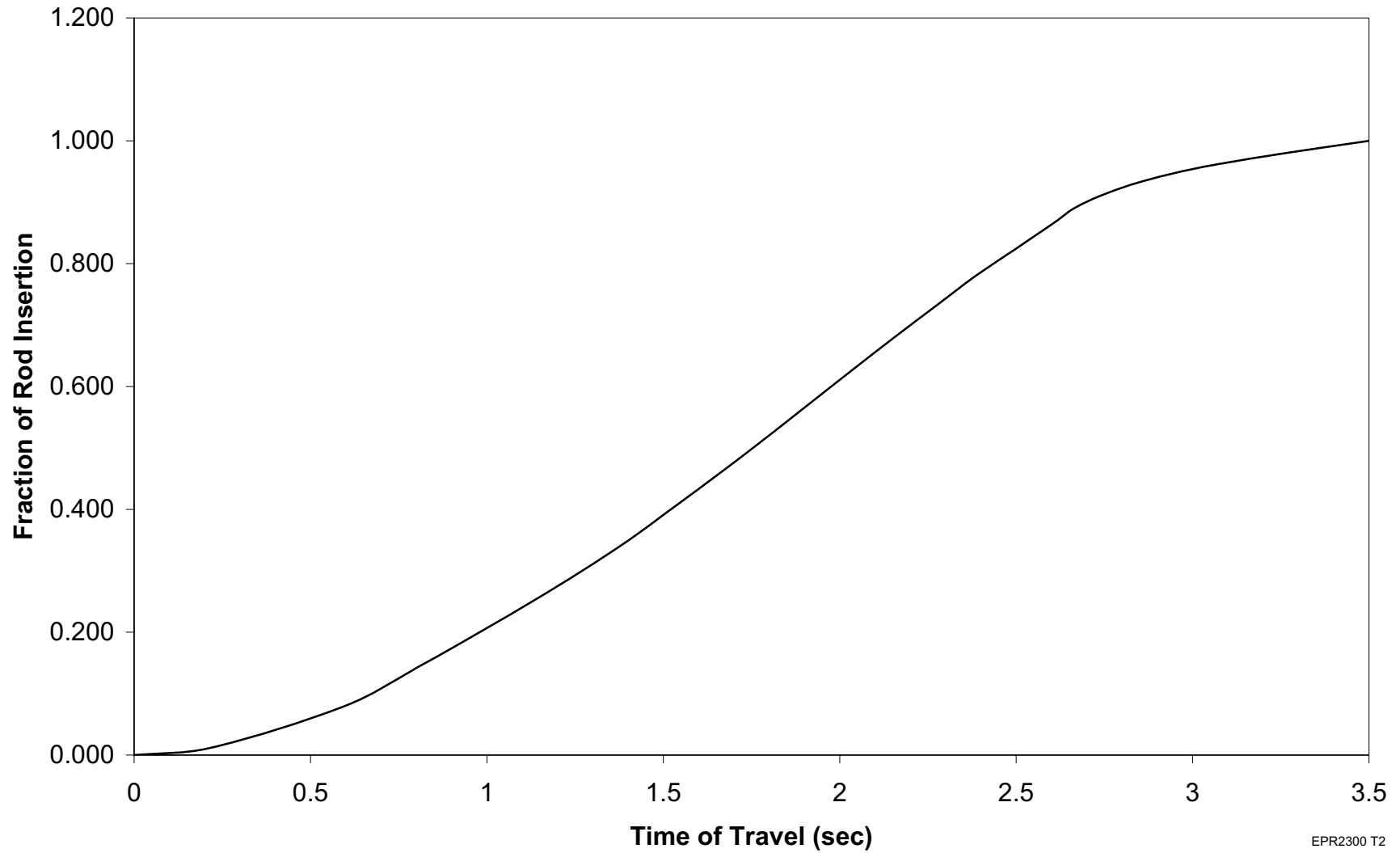


Figure 4.3-35—Differential Bank Worth with Two Banks in Overlap



EPR2295 T2

Figure 4.3-36—Rod Position versus Time of Travel after Rod Release



EPR2300 T2

Figure 4.3-37—Reactivity Worth versus Rod Position

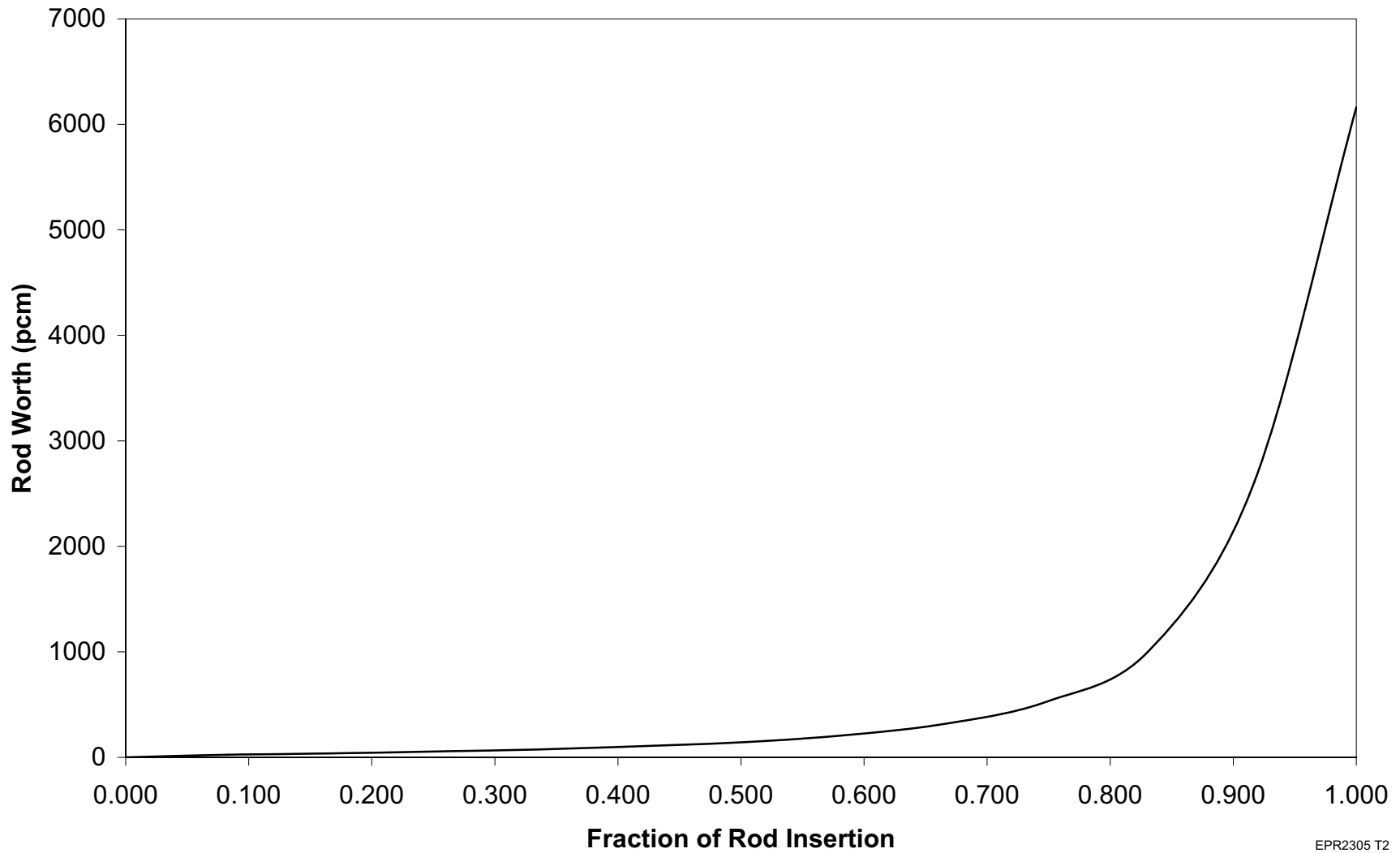
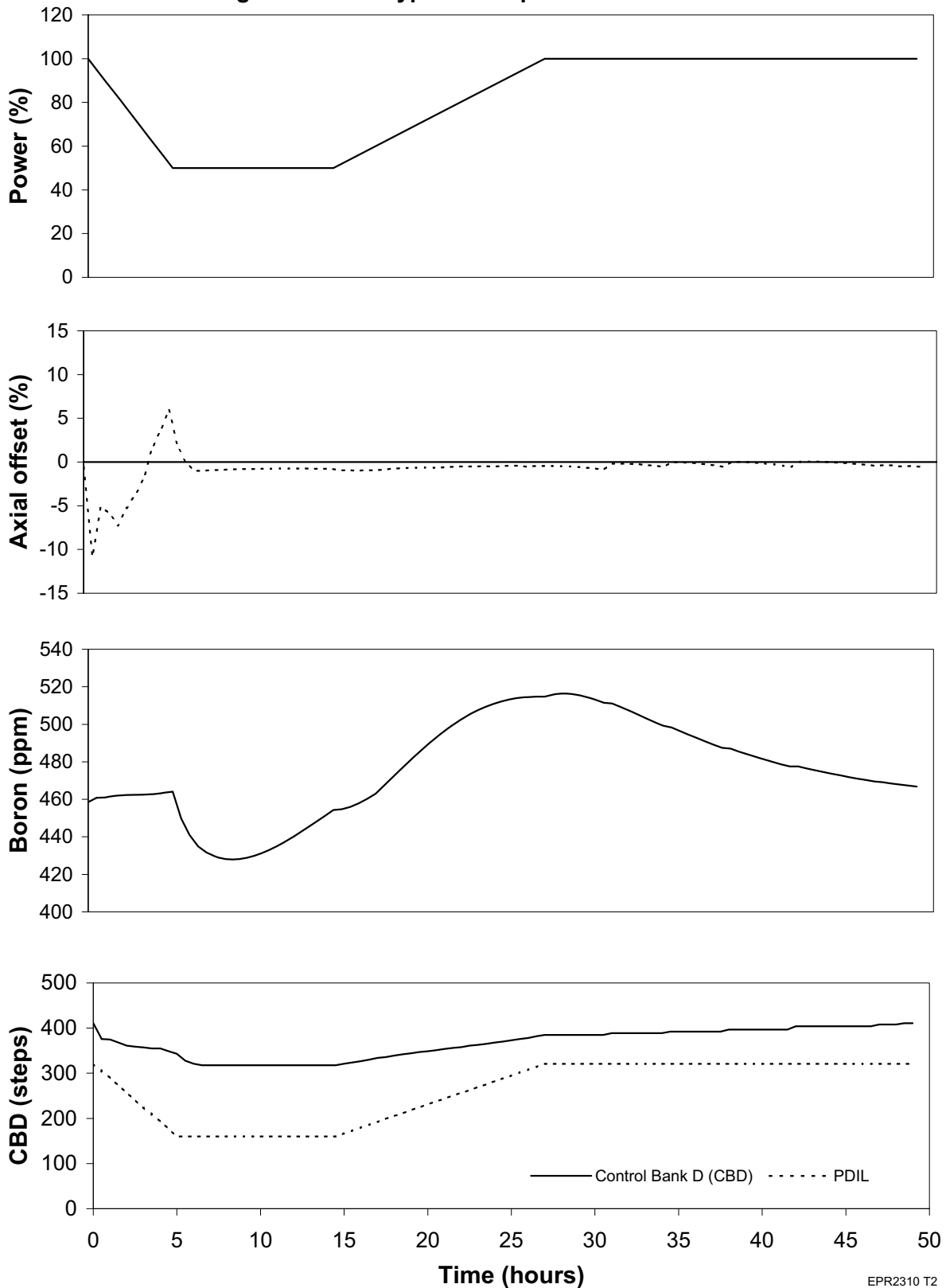
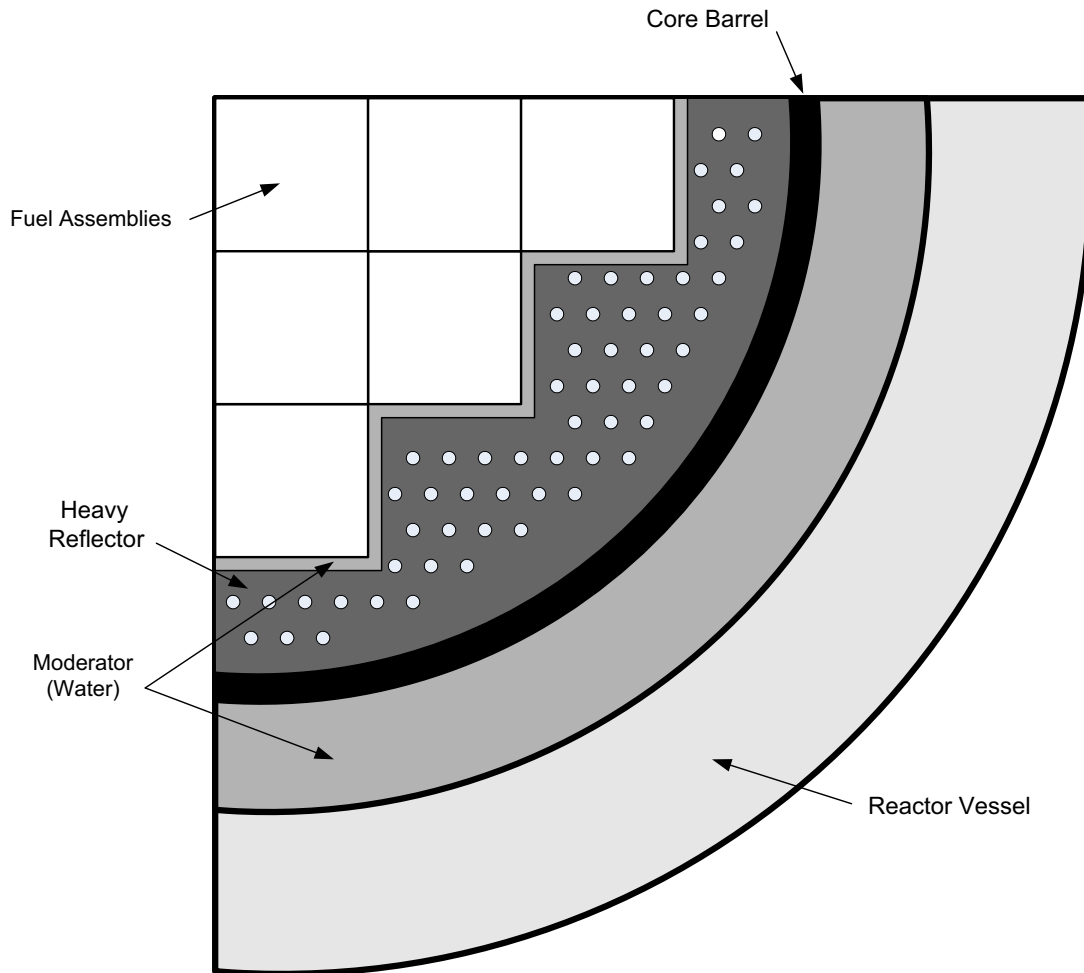


Figure 4.3-38—Typical Damped Xenon Oscillation



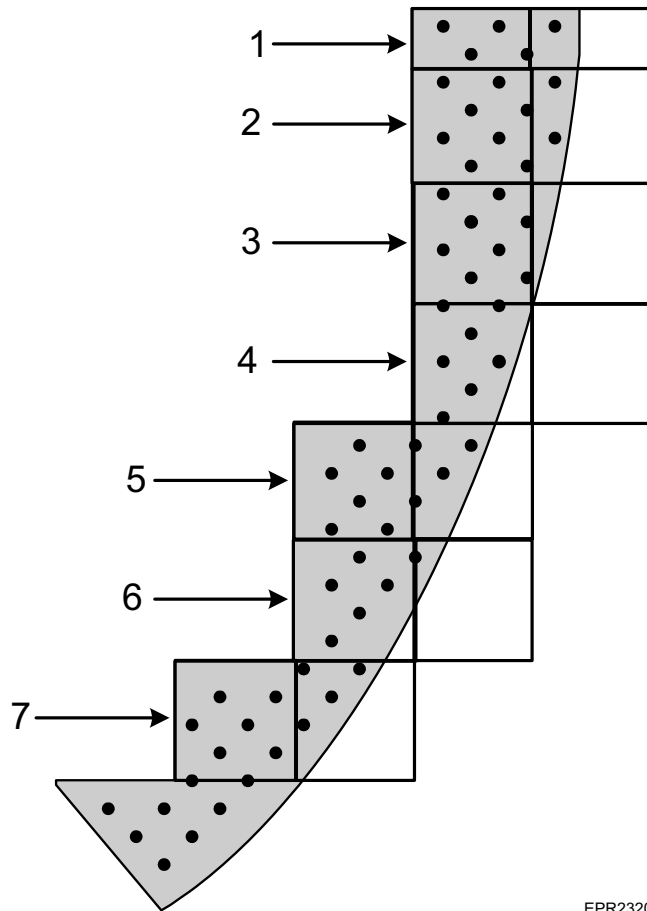
EPR2310 T2

Figure 4.3-39—Typical Layout of the Reflector



EPR2315 T2

Figure 4.3-40—U.S. EPR Reflector Geometry



EPR2320 T2